Brownout–based Power Allocation Strategies in Microgrids

Thesis submitted to the
Indian Institute of Technology Guwahati
for the award of the degree

of

Doctor of Philosophy
in
Computer Science and Engineering

Submitted by
Basina Deepak Raj

Under the guidance of
Dr. Arnab Sarkar and Prof. Diganta Goswami

Department of Computer Science and Engineering
Indian Institute of Technology Guwahati
June, 2022

Abstract

Future Smart Grids are expected to transform into hierarchically connected networks of miniaturized power systems called *Microgrids*, which are usually aimed to cater to a small geographical region. Microgrids have been envisaged to integrate heterogeneous *distributed energy resources* (DERs) including renewables (like photovoltaics, wind turbines and hydro–electricity), fossil fuel based micro–generators and batteries, along with occasional transfers of power from/to the main grid. Microgrid operations management is an important and yet a challenging problem. This is especially because, microgrids must be effectively tuned to maximize renewable energy penetration which are often volatile/intermittent, while still being able to schedule power generation, distribution and consumption in a fashion that ensures an economic and reliable operation. In order to achieve an effective balance between demand and supply, in the face of possible intermittent power shortage scenarios, Demand Response (DR) management strategies for microgrids must include mechanisms that allow adaptive urgency–prioritized control over electricity consumption. Today, with the advancements in smart metering as well as information and networking technologies, implementation of such adaptive power management schemes which require precise knowledge and finer controllability over consumer loads on the demand side, have become practical. The thesis of this dissertation is as follows:

In the presence of intermittent power deficits, efficient policies for microgrid sizing, equitable power distribution, appliance scheduling, real–time power balancing, etc., can be designed by using brownout–oriented approaches which allow selective provisioning of electricity to essential appliances while curtailing supply to less important ones, in times of power shortages.

The entire thesis work is composed of four distinct contributory chapters. In the first chapter, we deal with equitable distribution of power available with an Electricity Distribution Company (EDCo), among microgrids under its purview. We propose a comprehensive *Brownout*–framework which attempts to determine electricity pricing for a stipulated power allocation mechanism. The framework prescribes an electricity usage–urgency based appliance classification mechanism and microgrids are expected to report their demands under different urgency classes, to the EDCo. The EDCo then disburses its available power in an equitable fashion. However, untruthful microgrids may attempt to obtain higher profits by acquiring more power through deceitful projection of their demands. To prevent such unjust activities from selfish microgrids, we propose a Vickrey–Clarke–Groove based truthful pricing strategy which encourages microgrids to advertise truthfully. The second chapter deals with the problem of handling transient power deficits in real–time. We propose an efficient *Brownout*–framework which enables grid operators to equitably distribute a limited available power so that complete disruption of electricity even to critical appliances / establishments in a region, may be avoided. The third chapter deals with the scheduling of individual consumer appliances, taking into consideration their priority towards uninterrupted power supply and preferred time periods of operation. Finally in the last chapter, we focus on designing a microgrid. We take into consideration typical load profiles, solar irradiance, wind speeds, and determine appropriate selection and sizing of DERs. The objective is to minimize investment cost while ensuring reliable and economic operation. All the presented works have been validated through extensive experiments using synthetically generated microgrid scenarios. The obtained results have demonstrated the versatility and efficacy of the proposed approaches.

Declaration

I certify that:

a. The work contained in this thesis is original and has been done by me under the guidance of my supervisors.

b. The work has not been submitted to any other Institute for any degree or diploma.

c. I have followed the guidelines provided by the Institute in preparing the thesis.

d. I have conformed to the norms and guidelines given in the Ethical Code of Conduct of the Institute.

e. Whenever I have used materials (data, theoretical analysis, figures, and text) from other sources, I have given due credit to them by citing them in the text of the thesis and giving their details in the references. Further, I have taken permission from the copyright owners of the sources, whenever necessary.

Basina Deepak Raj

Copyright

Signature of Author.....

Basina Deepak Raj

Certificate

This is to certify that this thesis entitled, **"Brownout–based Power Allocation Strategies in Microgrids"**, being submitted by **Basina Deepak Raj**, to the Department of Computer Science and Engineering, Indian Institute of Technology Guwahati, for partial fulfillment of the award of the degree of Doctor of Philosophy, is a bonafide work carried out by him under our supervision and guidance. The thesis, in our opinion, is worthy of consideration for award of the degree of Doctor of Philosophy in accordance with the regulation of the institute. To the best of our knowledge, it has not been submitted elsewhere for the award of the degree.

.....

Dr. Arnab Sarkar
Associate Professor
Advanced Technology Development Center
IIT Kharagpur

.....

Prof. Diganta Goswami
Professor
Department of Computer Science and Engineering
IIT Guwahati

Dedicated to,

almighty GOD, my beloved parents and all my respected teachers *whose knowledge, blessing, love and inspiration paved my path of success.*

Acknowledgments

I wish to express my deepest gratitude to my supervisors, Prof. Arnab Sarkar and Prof. Diganta Goswami for their valuable guidance, inspiration, and advice. I feel very privileged to have had the opportunity to learn from, and work with them. Their constant guidance and support not only paved the way for my development as a research scientist but also changed my personality, ability, and nature in many ways. I have been fortunate to have such advisors who gave me the freedom to explore on my own and at the same time the guidance to recover when my steps faltered. Besides my advisors, I would like to thank the rest of my thesis committee members: Prof. G Sajith, Prof. H. K. Kapoor and Prof. T. Venkatesh for their insightful comments and encouragement. Their comments and suggestions helped me to widen my research from various perspectives.

I would like to express my heartfelt gratitude to the director, the deans and other managements of IIT Guwahati whose collective efforts has made this institute a place for world-class studies and education.

From the bottom of my heart, I would like to thank my uncle Prof. S.V.Rao and my aunt Srmt. Sailaja for their invaluable advice that guided me in taking decisions on many critical situations. I am also thankful to my grand parents S.Veerabhadra Rao and S Satyavathi Devi for their love, care and support.

A special thanks to my friends, Brijesh, Bhagat, Sanjit, Rajesh D, Satish, Bala and Hema for supporting and motivating to overcome many problems either related to work and others. The countless discussions, sharing ideas has strengthened my ability to counter problems in life. I am also grateful to all my seniors, friends and juniors especially Manoj Bhai, Saptrishi, Sukarn,

Sudha, Surajit, Chiranjivi, Debanjan, Sanjay, Shibaji, Sangeet, Prasen, Debabrath, Piyush, Ashwathy and Mohit Sir, for their unconditional help and support. You made my life at IIT Guwahati a memorable experience.

Most importantly, none of this would have been possible without the love and patience of my family. I want to thank my wife Prabha (Sowji), my daughter Manvitha, my parents Sri. Dali Raju and Srmt. Madhavi Lalitha, my brother Ravi Teja as well as my in-laws Sri. Sreenivasa Rao and Srmt. Sarvalakshmi, for being a constant source of love, concern, support, and strength all these years.

Contents

List of Figures

List of Algorithms

List of Tables

List of Acronyms

SG Smart Grid

PCC point of common coupling

HV high voltage

DOE *Department of Energy*

DERs distributed energy resources

DGs distributed generators

SEM smart energy manager

MGs Microgrids

NP-Hard non-deterministic polynomial-time hard

PVs photovoltaics

WTs wind turbines

MTs Microturbines

FCs Fuel Cells

ESSs energy storage systems

UC Unit Commitment

ED Economic Dispatch

DR Demand Respose

DSM Demand Side Management

QoSE quality-of-service in electricity

DLC Direct Load Control

EDCo Electricity Distribution Company

LA Load Aggregator

VCG *Vickrey–Clarke–Grooves*

ILP *Integer Linear Program*

DP Dynamic Programming

CSP Constraint Satisfaction Problem

ICT information and communication technologies

NIST National Institute of Standards and Technology

AMI Advanced metering infrastructure

HEMSs home energy management systems

WAMs Wide Area Monitoring Systems

PMUs Phasor Measurement Units

ToU Time-of-Usage

RTP Real-time Pricing

HVAC Heating, Ventilation and Air Conditioning

MILP mixed integer linear program

List of Symbols

N	Number of microgrids
P	Total available power
MG_i	i^{th} microgrid
M	Number of urgency classes
c_j	j^{th} urgency class
μ_j	Utility value assigned to the urgency class c_j
A_{ji}^k	k^{th} appliance in class c_j of MG_i
p_{ji}^k	Power demand of the appliance A_{ji}^k
K_{ji}	Number of appliance in class c_j of MG_i
p_{ji}	Aggregate power demand of class c_j in MG_i
u_{ji}	Aggregate utility value for p_{ji}
LA_i	Load aggregator of MG_i
θ_i^j	j^{th} cumulative choice of MG_i
P_i^j	Cumulative power demand of class c_j in MG_i
U_i^j	Cumulative utility value for P_i^j

PL	Number of discrete power allocation levels in P
pu	Discretization parameter (smallest unit of power)
a	Profile of the selected demand choices of LAs
π_i	Calculated Payoff/payment for LA_i
$\mathcal{N}$	Number of Subareas in a distribution area
S_i	i^{th} Subarea
K_i	Number of priority levels in S_i
l_i^j	j^{th} priority level in S_i
tar_i^j	Tariff corresponding to priority level l_i^j
p_i^0	Total essential demand of subarea S_i
p_i^j	Aggregate non-essential demand corresponding to priority levels l_i^1 through l_i^j.
P_R	Remaining residual power after satisfying all essential loads
ϱ	Index for upper bound on power level
L	Upper bound on the number of priority levels
res_t	Power resource available at time t of a day
pc_l	l^{th} Priority class offered by microgrid LA to its consumers
tar_i	Tariff rate associated with priority class pc_l
$\mathcal{L}$	Number of priority classes
T	Number of equal length time slots in a day
$PI\langle st, len\rangle$	A preferred interval having start timeslot st and length len
A_i	i^{th} Appliance request

pow_i	Rated power of appliance request A_i
pr_i	Subscribed tariff rate of appliance request A_i
typ_i	Type of an appliance whether *rigid* or *elastic*
PI_{ij}	j^{th} preferred interval of appliance request A_i
st_{ij}	Start time slot of preferred interval PI_{ij}
len_{ij}	Length of preferred interval PI_{ij}
$\mathcal{M}_i$	Number of preferred intervals in appliance request A_i
$Pe()$	Penalty function
$\mathcal{K}$	Number of elements (bins) in *Bin* data structure
Bin_c	c^{th} element of *Bin* data structure
N_{DG}	Number of dispatchable generators
N_{NDG}	Number of non-dispatchable generators
N_{BAT}	Number of battery units
N_{mt}	Number of microturbines
N_{fc}	Number of fuel cells
N_{pv}	Number of photovoltaic cells
N_{wt}	Number of wind turbines
C_i^{inv}	Fixed investment cost of i^{th} DG
C_j^{inv}	Fixed investment cost of j^{th} NDG
C_k^{inv}	Fixed Investment cost of k^{th} Battery Unit
OC	Total operational cost
IC	Total investment cost

Chapter 1

Introduction

1.1 Background

In traditional electricity grids, power is typically generated at centralized generation units and dispatched over long distance high voltage (HV) transmission lines in an effort to minimize power losses. The generated power is fed to distribution networks for consumption. In spite of these efforts, long established unidirectional power grids can only convert about 10% to 20% of energy into electricity without paying any attention to the waste heat generated [37]. Moreover, the centralized power plants are largely dependent on fossil fuels like coal, natural gas, oil etc, which contribute significantly to carbon emission related hazards. In addition to the core concern of global warming, several other serious issues relating to reliability, economics and sustainability of these power systems have been raised. A paradigm shift converting these decades–old power grids to "smart grids" or "intelligent grids" is being perceived as the primary approach towards addressing the above mentioned concerns. The U.S. *Department of Energy* (DOE) [90] has described smart grid as an automated, widely distributed energy delivery network, characterized by a two-way flow of electricity and real-time information that will be capable of monitoring everything from power plants to customer preferences to individual appliances and enable near-instantaneous balance of supply and demand. In addition, the smart grid will also allow seamless integration of renewable energy based distributed generators (like hydro, wind and solar energy) whose contribution in the

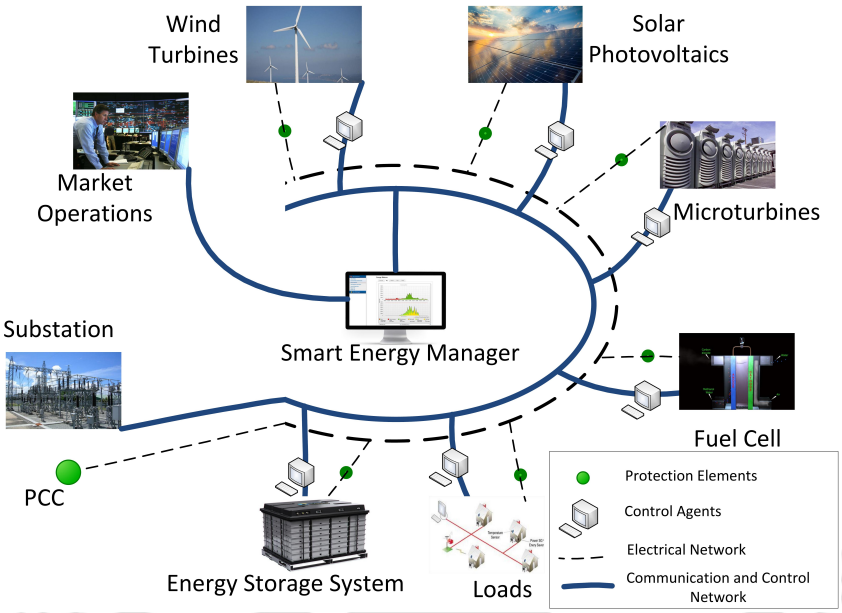

Figure 1.1: *A typical layout of microgrid power system*

world's total power generation is expected to increase by three folds between 2010 and 2035 reaching to a significant fraction of about 31% by 2035. Forecasts predict that hydro, wind and solar energy will provide 50%, 25%, and 7.5% respectively of the total renewable power generation in 2035 [119].

In addition to the centralized primary electric power backbone, smart grids of the future are expected to become an interconnected network of small-scale and self-contained Microgrids (MGs) [74]. A recent definition of microgrids given by the CIGRE Working Group C6.22 goes as: "*Microgrids are electricity distribution systems containing loads and distributed energy resources (DERs), (such as distributed generators (DGs), storage devices, and controllable loads) that can be operated in a controlled, coordinated way while connected to the main power network or while islanded*" [80]. From this definition, the architecture of a typical futuristic microgrid with multiple distributed generation sources may be envisaged as shown in figure 1.1. By integrating distributed generation units, energy storage systems and loads into a single controllable subsystem capable of operating either in grid connected or islanded mode, a microgrid can realize a low-emission, efficient system. Being designed to supply electrical and heat loads in a small

geographical area with a specific climatic pattern (including average wind speeds or solar radiation) and geographical terrain/water sources, power generation from all the three principal types of renewable energy sources may not be feasible/economical for a given microgrid. Therefore, while the distributed generators of a microgrid in a typically windy area may be powered by wind mills, the renewable energy based generators in a region with ample solar radiation may be powered by photovoltaic panels.

A microgrid is usually connected to the main grid through a circuit breaker (a point of common coupling (PCC) as represented in figure 1.1) which allows the entire microgrid to be islanded from main grid if required (for example, during a fault in the main grid). Otherwise, the microgrid remains synchronized to the main grid during normal circumstances allowing energy import/export from/to the main grid. Various sub-sections of the microgrid may similarly be isolated as required using circuit breakers (protection elements) placed within the microgrid.

The operation and control of a microgrid is carried through a central controller (represented as "smart energy manager (SEM)" in figure 1.1) [53]. It is responsible for i) controlling power and voltage of each generation/storage unit at short time granularities in response to load changes and disturbances, ii) regulating power flows through multiple feeder lines, iii) optimizing energy flow within the microgrid, iv) managing energy import (export) from (to) the main grid and finally v) handling faults by isolating sub-sections of the microgrid.

However, efficiently conducting these activities and providing reliable and demand sensitive power supply to consumers in a cost effective manner, requires intelligent adaption and scheduling strategies at the central controller. These strategies must consider a plethora of performance parameters to not only satisfy an increasingly performance-demanding consumer but also minimize a microgrid's overall carbon footprint (this is primarily achieved by minimizing power imports from the main grid which is majorly driven by fossil fuels) [66]. This calls for detailed analysis and research. *This thesis deals with the design of efficient policies for power distribution, appliance scheduling and real–time power balancing, especially in scenarios with insufficient total available power. As*

a spin-off, this thesis has also endeavored to address a few important problems relating to microgrid planning/sizing and DER scheduling.

1.2 Challenges

Power generation, distribution and allocation strategies in a microgrid must meet several challenges. A few important challenges are as follows:

- **Demand Aggregation**

  Demand may be defined as a quantitative measure of a consumer appliance's need for electricity supply. Appliances can be of different categories such as fixed, elastic, deferrable, thermostatically controllable, curtailable, preemptable, etc. Further, different consumers can have varying urgency/priority towards uninterrupted power supply for a certain type of appliance. Depending on this priority, a consumer may show his willingness to pay a certain price for electricity supply of an appliance. Considering all these aspects during the demand aggregation procedure is challenging due to variations in the above mentioned parameters.

- **Computational complexity associated with efficient power distribution**

  Power distribution strategies that are targeted to maintain real–time balance of power during transient overload scenarios must adhere to power quality standards [111] so that they can be practically realizable in real world situations. Similarly, power allocation problems involving the day-ahead scheduling of a large number of consumer appliances are computationally complex to solve as they are typically non-deterministic polynomial-time hard (NP-Hard) in nature. Thus, efficient but fast algorithms are needed to be designed so that reasonably good solution can be generated within acceptable time bounds.

- **Accurate modeling of Distributed Energy Resources**

  A typical microgrid accommodates a wide variety of DERs such as photovoltaics (PVs), wind turbines (WTs), Microturbines (MTs), Fuel Cells (FCs) as well as

energy storage systems (ESSs) such as batteries etc. These DERs have varying operational characteristics. For example, while the outputs of conventional fuel based generators are controllable (subject to ramp up/down restrictions), renewable generators such as PVs, wind turbines etc., are non-dispatchable. The above discussion suggests that in order to deliver a reliable consolidated supply to a microgrid in a cost-effective manner, effective coordination must be achieved among the different types DERs. Often, accuracy in modeling of these DERs is compromised so as to ease the underlying procedure. For example, charging and discharging characteristics of battery models have often been envisaged and modeled similar to data buffers in communication networks [73] [114]. However, batteries possess additional characteristics such as, charging and discharging efficiencies, allowed depth of discharge, number of charge/discharge cycles, etc. Similarly, the power output of microturbines is often represented as a linear cost function, although in practice, the output may have a quadratic, cubic or even more complex nature. Approximate models can lead to significantly suboptimal solutions.

1.3 Related Works: An Overview

In order to deploy a microgrid in a particular region according to a given set of specifications, effective strategies for microgrid planning/design as well as operations control must be adopted. Microgrid planning/design is a very challenging and yet important step in the implementation of a new microgrid. Designing a microgrid is the process of converging onto an optimal system configuration with respect to obtaining a suitable generation mix, sizing of DERs and their placement in a locality etc. Economic feasibility of a microgrid design is evaluated over the capital and maintenance costs (together represented as fixed cost) as well as operational costs. Therefore, typical objective of a microgrid design is the minimization of overall cost while being able to meet the load requirements of a given region. Other objective functions include, the optimization of revenue, emissions, reliability, production, life span etc. Due to the conflicting nature of many of these objectives, researchers have addressed the design problem in different

ways. Logenthiran et.at. [77] proposed a generic population based metaheuristic algorithm for obtaining optimal DER size for an islanded microgrid, with the objective of minimizing the sum total of capital operational and maintenance costs. Sizing problems not only concern suitable choice of DERs and their generation capacities but also the deployment of appropriate storage systems such as batteries. In this regard, Chen et.al. [21] formulates a battery sizing problem as a mixed integer linear program to perform a cost-benefit analysis over two different scenarios, i.e., grid connected and islanded. There also exists many commercially available software tools for obtaining optimal microgrid designs. Among them, the most popular tools are HOMER, HYBRID2, GAMS, ORIENTE etc. These tools provide an easy way for understand basic concepts related to microgrid sizing and optimization. However, they are basically *black box* code utilization approaches which provide limited configurable settings and are generally based on first order linear approximation models [33].

The usual objective of microgrid operation and control is to reduce overall costs by providing an efficient scheduling and coordination mechanism between DERs and loads. In addition, it also focuses on the reduction of carbon footprint while simultaneously maintaining a stipulated level of power quality and reliability [85]. In this context, Unit Commitment (UC) and Economic Dispatch (ED) are extensively studied in both smart grids as well as microgrids. In a microgrid environment, UC deals with the problem of judicious scheduling of DERs with minimal exchange of power from the main grid, given the estimated local loads and renewable forecasts over a day or few days, such that overall operational costs are minimized [83] [92]. On the other hand, ED takes into consideration more accurate forecast data obtained over relatively shorter duration compared to those used for UC, and determines optimal adjustments in the power generation levels of various distributed generators. With incomplete information about the future, the scheduling mechanisms apply a variety of stochastic prediction strategies. Typically, when a microgrid is operated in islanded mode, the objective of the central controller (SEM) is to economically serve the local loads. On the other hand, for grid-connected mode, the usual objective would be maximize profit. Other objectives

include renewable energy maximization and fuel or carbon emission minimization. In [43] and [64], authors have formulated stochastic optimization problems to minimize the average cost of energy over all random scenarios.

In general, microgrids procure power from the main grid to mitigate demand and supply imbalances caused by renewable generators and in order to ensure reliable operation at all times. Many-a-times, due to insufficient availability of power and other operational factors, even the main grid may not be able to supply the total demand of a microgrid. This is especially true for developing countries like India, which are presently facing severe intermittent shortages of electricity. According to the Central Electricity Authority, in India, the anticipated power deficits of certain regions range from 11%–17.8% of the total energy requirement [13]. Further, this situation is not expected to change in the near future. Thus, both the main grid as well as microgrids may have to deal with power shortages by satisfying its critical demands while not violating power quality standards [111]. Traditionally, power deficits are handled through a technique known as *Rolling Blackout*– Electricity is intentionally cut-off for non-overlapping time intervals over different subregions of a distribution region. However, blackouts cause complete disruption of electricity supply to even essential loads which may include life saving and business critical establishments as well as basic conveniences like lights and fans. There is a necessity for schemes which have comparatively benign side effects but at the same time are efficient in controlling power consumption. Today, with advancements in technologies like smart metering equipment, networking infrastructure, etc., design of improved schemes which essentially depend on more precise knowledge and finer controllability over consumer loads, have become more practical. In literature, such schemes are known as Demand Respose (DR) programs or Demand Side Management (DSM) programs. These programs include activities which aim to alter the consumers' demand profiles in time and/or in shape, so that it matches the supply at times when market prices are high or when grid reliability is jeopardized [44]. With this core idea towards managing consumer demands, Huang et.al. in [48] have introduced the concept of quality-of-service in electricity (QoSE) in a microgrid perspective. Here, res-

idential energy demands have been classified into basic and quality usage, respectively. While the basic usage is always guaranteed, the quality usage is controlled based on the state of the microgrid. The central controller schedules the renewable energy sources and energy storage devices, such that microgrid's operational costs are minimized, while satisfactory QoSE is maintained.

Researchers have proposed many approaches towards DR programs. John S. Vardakas, et al. [115] have classified these schemes into the following three categorizations based on, (i) whether the DR scheme is *centrally* controlled or *distributed* in nature, (ii) the mechanism by which customers are motivated to shape their demands; accordingly, we have *pricing or incentive* based DR programs, and (iii) the technique by which appliances are scheduled in a DR optimization problem. Based on the third classification, electricity allocation to appliances are adapted by a) selecting appropriate time slots at which an appliance can be run, and/or b) choosing appropriate energy levels for running an appliance. One of the primary objectives of the DR schemes is to cut–down peak load demands [54]. As consumption during peak periods increases, the generation cost as well as the consumers electricity bills also increasing in a proportionate manner, especially in grids which levy revenue based on peak load consumption [93].

Brownout [10, 59, 94] refers to an umbrella of DR schemes which enable operators to selectively supply electricity to critical establishments/appliances in a region, while curtailing supply to less important ones. Adopting to such schemes, consumers benefit by managing their electricity consumption and lowering their bills, while grid operators and utilities benefit by making more informed decisions on scheduling power, especially during shortages. Direct Load Control (DLC) is another such DR scheme which allows the grid operator to monitor and directly control specific appliances within households and commercial establishments, during peak and emergency periods [19, 84]. In this scheme, the consumers are often motivated by offering incentives (through monetary benefits or compensations) such as discounts on their electricity bills etc., in response to their active participation [107]. In the past few years, researches have addressed the appliance scheduling problem by considering various objectives such as maximizing

satisfaction [82], user comfort [51, 61] and thermal comfort [16] or minimizing demand peaks [14, 117], demand–supply mismatches [28], consumers' electricity bills [65, 98], inconvenience [121] etc. Most researchers have focused on appliance scheduling problems confined within a smart building/home. However, appliance scheduling from the perspective of an entire microgrid is also an important problem to consider.

It is not difficult to perceive that employment of optimization-based strategies is and will be a major handle in the design of efficient scheduling mechanisms for microgrids, as they allow effective utilization of power resource available with a microgrid. However, it is evident that such mechanisms will suffer from high overheads with respect to deterministic schemes, putting enormous computational burden at the central controller especially in microgrids, as the algorithms must adapt themselves to real-time or near real-time power shortage scenarios. Therefore, algorithms which possess low-overheads and at the same time produce acceptable quality in generating solutions demand considerable research.

1.4 Objectives

The principle aim of this dissertation has been to investigate the theoretical and practical aspects of microgrid sizing, power distribution/balancing and appliance scheduling, in the face of power deficit scenarios. In particular, the objectives of this work may be summarized as follows:

1. Detailed exploration of unit commitment, economic dispatch and sizing strategies for planning new microgrids, as well as power distribution mechanisms and demand response schemes for smooth operations control in microgrids.

2. Developing new algorithms for fair and equitable day-ahead power distribution as well as real-time power balancing in scenarios when total available power is insufficient.

3. Design of novel strategies for determining appropriate unit sizes of various heterogeneous distributed energy resources (DERs) in a microgrid. The set of DERs

may include dispatchable generators, renewables and batteries. The objective of the design is to minimize overall cost by accurately matching a given load curve for the region under consideration. Such sizing mechanisms must achieve effective coordination among DERs through optimal unit commitment and economic dispatch.

4. Devising a comprehensive framework for simulating a microgrid in operation. This framework is build upon the following modules, i) accurate system modeling given, the inputs such as consumer loads and their behaviors, available power capacities, intermittencies in renewables, charging discharging specifications, etc., ii) mathematically accurate problem formulation, ii) synthesis of efficient solution strategies (both optimal and heuristic), iii) designing data generation frameworks for generating real-world microgrid scenarios and iv) performance evaluation of the proposed strategies through extensive experiments conducted on the generated microgrid scenarios.

1.5 Summary of Contributions

As part of this thesis, four challenging problems related to microgrid sizing, power distribution, appliance scheduling and real–time power balancing, have been addressed. In the first work, we address the problem of fair and equitable distribution of a limited amount of power available with a distribution company, among microgrids under its purview. The second contributory study deals with the design of as set of optimal and heuristic brownout based real–time power distribution mechanisms for handling transient power shortages. A centralized, price–based DR-framework has been proposed in the third work, in order to enable operators to handle power deficits through priority–based appliance scheduling within islanded microgrids. In the last work, we propose a generic approach for sizing a cost-effective microgrid through an automated constraints optimization mechanism. We now provide brief overviews of the major contributions of this dissertation.

1.5.1 Equitable Electricity Distribution and Pricing for a Network of Microgrids

The first work proposes a novel comprehensive DR–framework for fair and equitable distribution of a limited amount of power available with an Electricity Distribution Company (EDCo), among microgrids under its purview. The EDCo uniformly grades appliances/establishments into a disjoint set of urgency classes, across all microgrids. Here, *urgency* refers to the criticality of an appliance's need for uninterrupted power supply. Each of these urgency classes is assigned a constant utility value such that, higher the urgency of a class, higher will be its associated utility value. Further, the EDCo designates a uniform tariff policy across all microgrids, where the tariffs levied from the consumers of the microgrids are proportional to the utility values associated with the urgency classes. Demand acquisition within a microgrid is performed by a centralized entity called Load Aggregator (LA). Given the appliance demands of different urgency classes, a microgrid LA is expected to report a discrete set of alternative cumulative power demand choices and their corresponding cumulative utilities. Based on the alternative demand choices advertised by the LAs of the microgrids under consideration, the EDCo has to decide on a policy for distributing its available power among the microgrids, such that aggregate utility of the system is maximized.

In general, the EDCos are government organizations with social welfare being a core operational motivation. Thus, it may be justified to assume that the EDCos attempt to maximize proportional fairness (or aggregate utility) in the distribution of available power, among its microgrids. In contrast, microgrid LAs may be driven by their own selfish goals. For example, an LA's policy may be to maximize profit by selling power to consumers within its microgrid or maximally satisfying the needs of its consumers. In determining this policy, an LA may be completely indifferent to and disregard the demand urgency of consumers within other microgrids. Further, a manipulative LA may attempt to acquire more power than its fair share by falsely advertising inflated power demands. We have shown that simple pricing schemes such as a fixed per–unit block pricing, will fail to prevent such untruthful reporting by LAs. In order to effectively

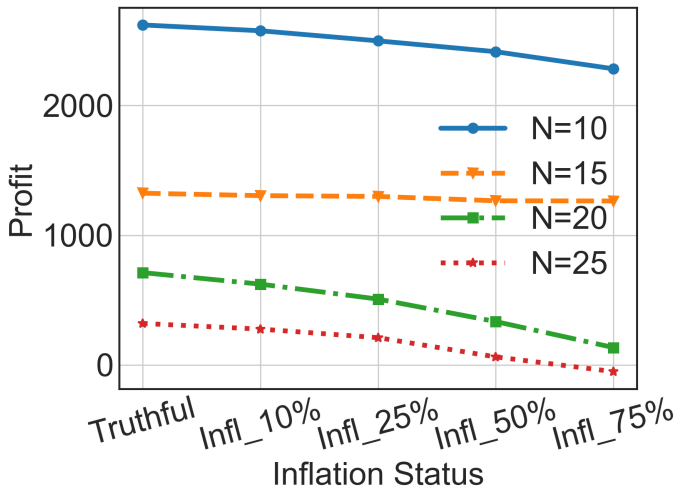

Figure 1.2: *Profits obtained by an LA, for varied inflations*

prevent such unjust activities, this work proposes a truthful payment mechanism called *Vickrey–Clarke–Grooves (VCG) based Equitable Pricing* (VCG-EP), which encourages the LAs to report their true demands. VCG-EP attempts to alleviate untruthful declaration of inflated cumulative demand choices by offering LAs a lower price when they report truthfully. Given, the declared cumulative choices of microgrids, available power and an optimal allocation algorithm, VCG-EP decides the payoff amount for each LA. The LA's payoff is determined by the aggregate reduction in the utility suffered by the other LAs due to the power that has been allocated to the LA under consideration. We validate the payment mechanism by proving that an LA's profit is maximized when it advertises a microgrid's actual demands.

Extensive experiments on various empirically generated microgrid scenarios have been conducted. The obtained results show that, profit acquired by an LA is maximum when it advertises its true demands; in comparison, the profit decreases as the degree of untruthful demand inflation becomes higher. A pictorial representation of the above finding can be seen in figure 1.2. This figure portrays the variation in average profits obtained by any given LA when it reports truthfully as well as when it is untruthful with different degrees of inflations on the actual demand choices. For this experiment,

we have generated data sets for varying number of aggregators N = 10, 15, 20, and 25, and randomly generate demand choices for all the LAs using a data generation framework. These datasets are considered as true choices. Then, we generate inflated demand choices data sets. The process of inflation is as follows. From a data set, an LA is randomly selected (uniformly) and subjected to four different degrees of inflations ("Infl_10%", "Infl_25%", "Infl_50%" and "Infl_75%",) on actual demand choices. For example, a data set for "Infl_10%" is obtained by selecting the actual demand choices of all LAs except one randomly chosen LA. The aggregate demand of a certain class (say, Cat-2) for this LA is enhanced by promoting 10% of the aggregate demand of its immediately lower urgency class (Cat-3) to Cat-2. In effect, the cumulative demand choices of Cat-3 and all higher urgency classes get transformed. Consequently, the EDCo benefits by achieving the desired system level goal (i.e., maximization of total utility) while equitably distributing its available power in the process.

1.5.2 Brownout based Blackout Avoidance Strategies in Smart Grids

Transient power shortages within a grid is a common problem in developing nations such as India. According to the Central Electricity Authority, in India, the anticipated power deficits of certain regions range from 11%–17.8% of the total energy requirement [13]. Traditionally, power shortages are handled through a mechanism called *Rolling Blackouts*. This scheme works by imposing blanket power cuts over stipulated time intervals to different subareas within a distribution grid. A severe drawback of this approach is *complete disruption of electricity* even to important establishments/appliances like schools, hospitals as well as lights and fans, within the affected subarea. With advancements in technologies which enable precise knowledge and finer controlability over consumer appliances, power distribution schemes with more benign side-effects have now become practical. In the second work, we delve towards handling mechanisms for equitably distributing electricity to different subareas within a distribution area under transient overload situations. The proposed strategy is based on a technique called *Brownout* which allows selective provisioning of power supply to support essential loads while cur-

tailing supply to less critical loads.

The system model considered in this framework is as follows. Under the purview of an electricity distribution company (/an electric utility) there are a certain number of subareas each of which consists of a collection of establishments/households. Based on their urgency towards uninterrupted power supply, appliance demands within establishments/households are classified into a fixed number of priority classes. Each of these classes is associated with a distinct tariff rate. These tariffs are modeled such that higher the priority of a class, higher is its associated tariff rate. Depending on the nature of the need for electricity, a consumer may choose to subscribe to any one of the urgency classes for his appliance. Given, a) the power available with the electric utility and b) the cumulative demands and its associated revenues of different urgency classes, the electric utility attempts to distribute its available power so that the total revenue obtained is maximized. Being an online power allocation strategy that strives to mitigate dynamic imbalances between electricity supply and demand, the framework is guided by the following soft real-time specification (governed by recommendations of IEEE standards on power quality [111]): *Brownout based mitigation of imbalances in demand-supply must be conducted quickly and within about* $\sim$0.5 *seconds (for a 50Hz power system) in order to maintain satisfactory power quality.*

We formulate the brownout based power distribution problem as an *Integer Linear Program* (ILP) and show that solution strategies such as conventional Dynamic Programming (DP) impose substantial overheads. Experimental results reveal that, given 50 subareas with 10 priority classes per subarea and with 250 MW of available power, *DP* takes $\sim$13 secs on average to generate a solution on a 3.2 GHz computing core. Clearly, this overhead is significantly high to be useful for distributing available power among subareas, in real-time. So, we propose an efficient optimal algorithm called *Streamlined DP-based Priority level Allocator (SDPA)*, which attempts to generate the overall optimal solution far quicker by memoizing a lower number of non-dominating partial DP-solutions. *SDPA* is found to be about 9 to 33 times faster than *DP*, as shown in table 1.1 and is applicable for real-time power distribution in moderate sized

Table 1.1: *Comparison of Execution Times and Speedup between DP, SDPA & PBPA*

Power (in MW)	Time in (ms)				Speed Up		
	DP	SDPA	HA	PBPA	DP vs SDPA	DP vs PBPA	SDPA vs PBPA
50	1337	151	0.013	0.013	9	1.0×10^5	1.1×10^4
100	3472	283	0.018	0.017	12	2.1×10^5	1.7×10^4
150	6208	384	0.021	0.019	16	3.2×10^5	2.0×10^4
200	9355	468	0.024	0.021	20	4.5×10^5	2.2×10^4
250	12942	539	0.026	0.022	24	5.8×10^5	2.4×10^4
300	17233	597	0.029	0.023	29	7.5×10^5	2.6×10^4
350	21387	643	0.032	0.024	33	8.8×10^5	2.6×10^4

grids. Experimental results show that, given 50 subareas with 10 priority classes per subarea and with 250 MW of available power, *SDPA* takes ∼0.5 sec, thus able to satisfy the stipulated soft real-time requirement. However, for scenarios with a higher number of subareas and larger amounts of available power, SDPA may take a few seconds to obtain optimal solutions. Thus, SDPA becomes unsuitable for real–time power distribution in very large scenarios. To cope with such situations, we have designed a fast and efficient heuristic algorithm called *Proportionally Balanced Priority level Allocator (PBPA)*. PBPA is a greedy yet poised strategy which allows power balance to be restored quickly. Experimental results show that although solutions provided by *PBPA* could be less effective by upto 12% compared to optimal dynamic programming based schemes, being about 4 orders of magnitude faster (as shown in table 1.1), it can be deployed for real–time allocations of power even to large grids.

1.5.3 An Efficient Framework for Brownout–based Appliance Scheduling in Microgrids

Islanded microgrid designs provide a mechanism for the electrification of remote geographical regions such as high altitude terrains, deserts, small islands, etc [7]. More-

over, i) to avoid loss of power due to long distance transmissions, ii) reduce emissions through enhanced penetration of renewable generation and iii) to contain the effects of faults/disturbances within small localized regions, partial or fully *islanded mode* of operation is being considered increasingly important [9]. In the face of power shortages, demand response schemes such as Brownout based appliance scheduling can be an efficient handling mechanism for such microgrids. Researchers in the past have have addressed the appliance scheduling problem by considering various objectives such as maximizing user comfort [51, 61], minimizing demand peaks [14, 117], minimizing consumers' electricity bills [65, 98] and minimizing inconvenience [121] etc. Most of these works deal with appliance scheduling problems within a smart home or a building. In this work, we address the appliance scheduling problem from the perspective of an entire microgrid. To deal with power deficit scenarios, we propose a comprehensive brownout based methodology for distributing the available electrical energy among appliances within a microgrid.

The system is modeled as follows. The microgrid utility defines a fixed number of alternative electricity tariff rates which its consumers can subscribe to, depending on their appliances' urgency towards uninterrupted power supply. In addition, an appliance request is characterized by its rated power, its type (rigid or elastic), and a set of preferred intervals for running its operation. For this setting, the proposed work attempts to address the following scheduling problem.

Given, (a) the day–ahead predicted amounts of time slot–wise power resources available with a microgrid, (b) the appliances' characteristics such as rated power, subscribed tariff rate, type (whether *rigid* or *elastic*) and preferred time intervals during which electricity service is required, and (c) the monetary penalty towards allocation of non–preferred slots to appliances, *determine a schedule of appliances for the entire day, such that the total revenue earned by the microgrid is maximized.*

We first formulate the above mentioned scheduling problem as an Integer Linear Program (ILP). This appliance scheduling problem was observed to be an NP-Hard problem. We show that optimal strategies would incur substantial overheads in terms

Table 1.2: *Average Execution times of ILP and RaAS, as #Houses and #Time slots are varied*

				No. of Households			
				2500	**5000**	**7500**	**10000**
No. of Time slots	**T=24**	**Exec. Times (in sec)**	**ILP**	236.72	1102.48	2034.86	3662.57
			RaAS	0.90	1.99	3.04	4.05
		Speedups		264.1	553.2	670.3	905.4
	T=48	**Exec. Times (in sec)**	**ILP**	294.48	1131.93	2818.95	5042.03
			RaAS	0.93	2.04	3.08	4.07
		Speedups		315.6	554.7	915.0	1239.3
	T=72	**Exec. Times (in sec)**	**ILP**	438.40	1526.62	3215.16	6057.16
			RaAS	0.95	2.09	3.18	4.19
		Speedups		459.4	731.1	1011.8	1444.3
	T=96	**Exec. Times (in sec)**	**ILP**	536.94	1862.51	4365.06	7506.27
			RaAS	0.99	2.18	3.24	4.30
		Speedups		543.3	855.7	1345.4	1745.1

of solution generation times. Therefore, we have proposed a fast yet efficient heuristic algorithm namely, *Revenue–aware Appliance Scheduler* (RaAS). *RaAS* is an iterative algorithm for scheduling a given set of appliances. At any iteration, RaAS schedules the highest priority interval of an appliance, which is currently unallocated.

RaAS is able to produce appreciably good solutions with obtained revenues only about 2% lower on average, than the optimal ILP solutions. Contrarily, *RaAS* has been found to be 2^8 to 2^{11} times lower compared to ILP, in terms of solution generation times. The execution times and speedups for different scenarios are shown in table 1.2. For example, our experimental results show that for ∼1 lakh appliance demands, the average execution time of an ILP based solution is ∼7500 seconds. In comparison, RaAs is able to generate a solution in ∼5 seconds. Furthermore, our experimental results show that for ∼5 lakh appliance requests, the average execution time of *RaAS*, taken over 30 different sample microgrid scenarios, is ∼25 seconds. Thus, *RaAS* can be applicable even in big microgrids with a large number of appliance demands.

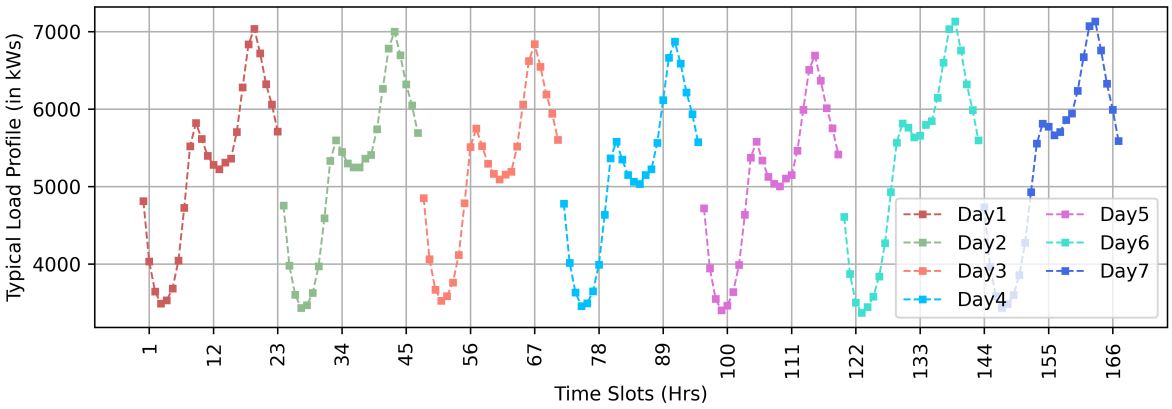

Figure 1.3: *Typical Loads during summer*

1.5.4 A Generic Framework for Designing a Cost–Optimal Microgrid

As microgrids are typically designed to supply electricity to a small geographical area with specific climatic conditions (including average wind speeds or solar radiation), geographical terrains, consumer behavior patterns etc., a plethora of design alternatives seem possible for microgrids depending on the variations in these parameters. One of the primary aspects while designing a new microgrid for a specific region is the judicious selection of a subset of DERs from available alternatives (say, Photovoltaics, Diesel Generator, Batteries etc.,) and determining the appropriate number of modules of each selected DER type. *In this work, we investigate the DER sizing problem with the objective of minimizing the total investment as well as operational cost.* The problem takes into consideration the following inputs: i) Hourly solar irradiances and wind speeds of a region, over a typical week in a season (say Summer or Winter), ii) typical load curves and iii) normalized costs for buying and installing one unit/module of Photovoltaic, Wind Turbine, Diesel/Gas Generator and Battery. Given the above inputs, we determine the appropriate number of units of each DER type, required to satisfy the considered demands, such that the sum total of investment cost and operational cost is minimized while satisfying specific operational constraints relating to DERs.

Three different case studies have been conducted. In the first scenario, renewable

generators and batteries are neglected i.e., a microgrid with only fuel based generators (microtubines and fuelcells) has been designed. In the second scenario, results for both renewable generators (solar and wind) as well as with the dispatchable fuel based generators (microturbines and fuelcells) has been obtained. In the last scenario, we add battery systems to the previous scenario and perform optimization. All the case studies are performed by taking into consideration weather data and load profile for the region Arizona, US (Lat. 34.29, Long. -111.66). The hourly data corresponding to a particular week of the month June (June 1 to June 7 of a typical meteorological year (TMY3)) has been taken as input. The load profiles for the considered region are shown in figure 1.3. Results for the last case study are discussed as follows. In the last case study we deal with the optimal selection and sizing problem of both dispatchable (microturbines and fuel cells) and non-dispatchable (renewables and wind) as well as battery system. Given the hourly load profiles over a week, the optimal sizing is obtained as follows, four microturbines, one fuel cell, seven PVs, sixteen wind turbines and five battery systems. The total cost of the system is obtained as $78870.

We formulate this optimization problem as a Constraint Satisfaction Problem (CSP)/ Integer Linear Programming (ILP). A few noteworthy important constraints include, real power balance, spinning reserves, ramp up and down limits of DG and state of charge in batteries. In this work, we perform case studies for the state region Arizona, in the US. The weather data such as typical wind speeds and solar irradiance as well as consumption profiles over the region for a particular design period, have been considered. Then, we model specific unit sizes of DERs using System Advisor Model (SAM). As example, a wind turbine system that can generate 1000 kW of power, a PV system with 1000 kW peak power and battery system with 1000 kW of power having an energy capacity of 4000kW, has been modeled and corresponding investment costs have been obtained using SAM tool. Given this data, we conduct a systematic design space exploration over all possible solutions and generate optimal sizes of DER by using an industry grade ILP solver called IBM CPLEX. The proposed methodology has been validated using a set of case studies. The first case study deals with the sizing of only microturbines for

the considered load. In the second case study, we co-optimize both the microtubines and renewable generators, and corresponding optimal sizes have been obtained. Finally, we have solved the sizing problem by including all the the four types of DERs viz, microturbines, wind turbines, solar photovoltaics and batteries. Our experimental results show that, significant cost saving can be achieved by sizing the DERs and by effective coordination among these DERs in order to satisfy a given demand curve in a reliable and economic manner.

1.6 Organization of the Thesis

The thesis is organized into seven chapters. A summary of the contents in each chapter is presented as follows:

- **Chapter 2: Literature Survey**

  In this chapter, we present the necessary background and current related works on microgrid planning, power distribution and appliance scheduling problems. In particular, we present the vocabulary needed to understand the subsequent chapters.

- **Chapter 3: Equitable Electricity Pricing for a Network of Microgrids**

  Accounting the fact that untruthful microgrid LAs may attempt to acquire higher profits through deceitful projection of their demands, this work presents a truthful pricing mechanism to ensure fair electricity distribution among microgrids.

- **Chapter 4: Brownout–based Real–Time Power Distribution Strategies**

  In this chapter, we propose an efficient DR framework which enables an EDCo to distribute a limited amount of power among different subareas under its purview, in an equitable fashion. Based on an urgency based appliance classification mechanism, demands of a subarea are represented by a set of cumulative demands choices (each having a demand and associated revenue). Given this demand information,

an EDCo then attempts to distribute its available power so that total revenue obtained is maximized.

- **Chapter 5: A Centralized Appliance Scheduling Mechanism for Microgrids**

  In Chapter 5, we address the problem of power deficits in islanded microgrids which are usually caused due to intermittent power outputs from renewable sources. Sometimes, instantaneous procurement of power from an external source can be difficult or infeasible. Therefore, we propose an efficient brownout–framework which attempts to schedule critical appliances at their preferred time intervals, as far as possible while possibly cutting down supply to a few less important appliances.

- **Chapter 6: Sizing and Unit Commitment for Cost-Optimal Microgrid Designs**

  This chapter first presents a comprehensive methodology for modeling various types of DERs including Photovoltaics, Wind Turbines, Microturbines and Batteries. Based on these mathematical models, location specific inputs and the load curve of a region, we propose a generic methodology for obtaining an appropriate selection and sizing of DERs.

- **Chapter 7: Conclusion and Future Perspectives**

  The thesis concludes with this chapter. We also present a list of possible extensions and future works that can be done in this area.

Chapter 2

Literature Survey

This dissertation focuses towards developing efficient strategies for equitable power allocation, real–time power balancing and appliance scheduling in microgrids, especially in the face of power shortages. In addition, this thesis also addresses a few problems related to microgrid sizing. In the previous chapter, a brief discussion on a few critical challenges that are posed by the existing power grids, has been provided. This chapter describes in detail the basics of smart grids, microgrids, distributed energy resources and demand size management. Then, a brief survey on power scheduling and microgrid sizing is provided.

2.1 Smart Grids

Although dated, our traditional power grids are an engineering marvel, being able to satisfy even the electricity needs of the modern era. They have evolved over time as enormous distributed systems and consist of highly complex subsystems. For more than a century, demand is supplied almost instantaneously through the transmission and distribution of electricity that is generated at centralized power plants, typically by burning fossil fuels like coal, oil, gas, etc. However, catastrophic outage events such as The Northeast blackout 2003, Java-Bali blackout 2005, India blackout 2012 etc., have raised serious challenges to the entire traditional power system. Primary reasons for the occurrence of such events are observed to be the lack of efficient sensing, monitoring and

controlling capabilities, out of bounds peak load consumption, power losses in the transmission and distribution networks, etc. For this reason, key players such as generation companies, transmission and distribution companies as well as Governments and policy makers, have pitched for significant advancements to the existing power system so as to improve its efficiency and reliability. Moreover, issues related to global warming, fossil fuel depletion, enhanced electricity demands, aging technology etc, should be addressed to ensure sustainability of the system. In short, the power system must not only be secure, manageable and cost effective, but need to be more reliable, highly scalable and eco-friendly. These goals have led to the concept of *Smart Grid*.

The Smart Grid (SG), also often referred to as Intelligent Grid, is the pathway to addressing most of the concerns that traditional power systems face. Although, there does not exist any concrete definition of SG, many reputed organizations have attempted to define SG in their own way. Some of the definitions are listed as follows:

1. National Smart Grid Mission, Ministry of Power, Government of India, describes SG as, "*electrical grids with automation, communication and IT systems that can monitor power flows from points of generation to points of consumption and control the power flow or curtail the load to match generation in real-time or near real-time*".

2. The U.S. Department of Energy describes SG as follows. "*SG is an automated, widely distributed energy delivery network, characterized by a two-way flow of electricity and information, and capable of monitoring everything from power plants to customer preferences to appliances. SG incorporates into the grid the benefits of distributed computing and communications to deliver real-time information and enable the near instantaneous balance of supply and demand at the device level*".

3. The Canadian Electricity Association says, "*SG is a suite of information based applications made possible by increased automation of the electricity grid, as well as the underlying automation itself; this suite of technologies integrates the behavior and actions of all connected supplies and loads through dispersed communication*

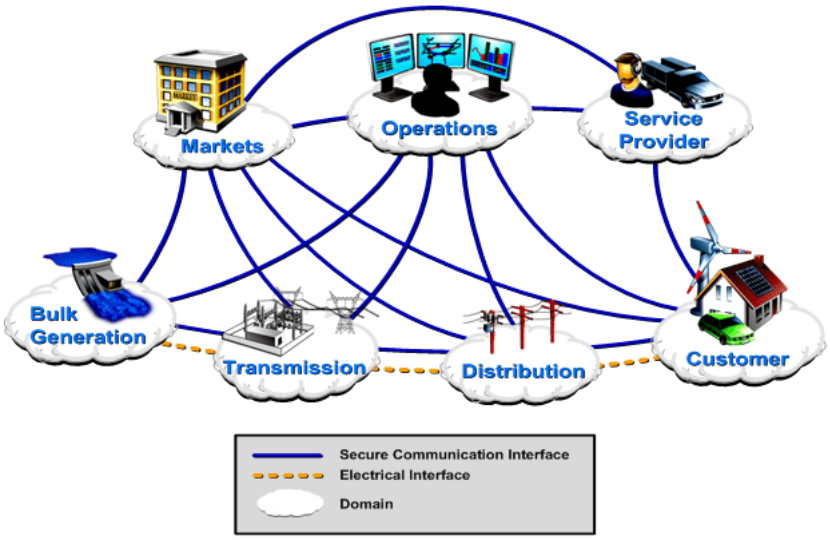

Figure 2.1: *A conceptual smart grid model, NIST Framework, Release 4.0, 2020*

capabilities to deliver sustainable, economic and secure power supplies".

From the definitions above, main characteristics of a smart grid and their benefits can be summarized as follows.

i) Two-way flow of power and information: With the help of advanced information and communication technologies (ICT), an SG enables bidirectional flow of power and information. A conceptual layout of such an SG framework, as given by National Institute of Standards and Technology (NIST), can be seen in figure 2.1. As shown in the figure, an SG is composed of various domains, actors and applications. Each domain is represented by one or more actors which may include devices, systems, or programs that exchange necessary information and take appropriate decisions for performing tasks. A brief summary of domains and actors is given in table 2.1. With this feature, consumers can install renewable energy resources such as wind turbines, solar photovoltaics etc., at their own premises and the generation from these sources can be fed back to grid. SG also enables information sharing among various parties such as markets, grid operators, service providers and consumers etc., which can help them take efficient decisions in their respective domains.

ii) Seamless integration of multiple generation and storage options: SG

Table 2.1: *Actions performed under different domains, according to NIST SG framework*

Domain	**Actors and applications**
Customers	End users who generate, store, manage and consumer energy.
Markets	Operators that participant in electricity markets.
Service Providers	Provide electricity services to customers and utilities.
Bulk Generation	Companies that generate and store electricity in bulk quantities.
Transmission	Companies that schedule transmission of bulk electricity.
Distribution	Distributors of electricity to and from customers.

allows distributed generation sources such as photovoltaics, wind turbines, diesel generators as well as storage devices like batteries to be easily integrated into the system in a plug-and-play manner. These resources can be of small generation capacities from an individual prosumer (one who consumes as well as produces) or be large grid-scale systems. Nevertheless, these diverse options can help in addressing the problems of depleting fossil fuels and growing demand. In addition, they enable SG to be more eco-friendly and sustainable.

iii) Active consumer participation: Advanced metering infrastructure (AMI) enables real-time information exchange between consumers and electric utilities. With the advent of AMI, consumers can now contribute to grid management through the use of intelligent devices such as home energy management systems (HEMSs) using which their demands can be controlled. In addition to reducing peaks, these flexible devices can contribute by compensating fluctuations in system outputs from renewable generators. Prompt access to information on electricity usage can also influence power generation and purchasing decisions. Automated meter readings can potentially reduce the operational costs of distribution system operators.

iv) Attack resistance and self-healing: Continuous assessments of grid health is now practical with the advanced communication, monitoring and measuring technologies such as Wide Area Monitoring Systems (WAMs), Phasor Measurement Units (PMUs), Smart Meters, etc. Detecting, analyzing, responding, and restoring capabilities of these advanced grid components can effectively resist attacks and promote self-healing abili-

ties.

2.2 Microgrids

Microgrid is a miniaturized smart grid targeted to provide electricity service to a small geographical region, by employing a wide variety of distributed energy resources, storage devices and controllable loads, which are operated in a coordinated manner. These micro-power grids can function autonomously, if the generation from its internal resources is sufficient to manage loads while satisfying power quality standards. Otherwise, in general, they procure the deficit power from an external grid such as a conventional utility or main grid to maintain balance between supply and demand.

A few important characteristics of a microgrids are, improved reliability with distributed generation, increased efficiency with reduced long distance transmission and easier integration of alternative energy sources. In contrast, a smart grid refers to the modernization and automation of traditional grid with the help of information and communications technology in a way that improves efficiency, reliability, economics and grid sustainability. In summary, a microgrid can be thought of as a local power provider for a confined geographical region with limited advanced control tools, where as a smart grid is a wide area provider with more sophisticated monitoring, controlling and operational capabilities.

2.2.1 Distributed Energy Resources

One of the main components of a microgrid are distributed energy resources (DERs) which include distributed generators (DG) and energy storage systems (ESS). DERs can be of large capacities which are typically invested by the microgrid utility or be smaller generation sources which are equipped by a consumer at her premises such as a household or an establishment. Based on the operational characteristics of DGs, they can be categorized into two types namely, dispatchable and non-dispathable. Dispatchable DGs are generally combustion based systems which run on fuels such as gas, oil, etc. The power output from these DGs can be controlled by varying the amount of fuel input.

However, they are subject to various operational constraints such as power capacity limits, bounds on ramping up and down, minimum time to on/off, time required to cold start and emission limits. A few popular dispatchable DGs are microturbines, fuel cells and diesel generators. Microturbines are small scaled combustion based generators which are typically capable of producing both electrical and heat energy by using fossil fuels like oil and gas. They are approximately the size of a refrigerator and are rated to generate power from 25 kW upto 500 kW. Fuel cells also produce both electricity and heat, but are based on converting chemical energy of hydrogen or other fuels, like batteries. Unlike batteries, fuel cells do not discharge or need any recharging, but produce electricity and heat as long as fuel is supplied. Comparatively, fuel cells are more efficient than conventional combustion systems such as diesel generators, in terms of toxic emissions.

In contrast to controllable DGs, the power generation from non-dispatchable DGs cannot be modified as they primarily dependent on uncontrollable sources such as sun's radiance, availability of wind, amount of water stored at an elevation etc. Because these sources are renewable in nature and the fact that power generation from these sources is emission-free, the are growing in popularity. Among the most popular renewable DGs are solar photovoltaics (PVs) and wind turbines (WTs). A PV panel is an assembly of PV cells that convert sunlight into electrical energy. PV arrays are composed of a large number of PV panels that are laid in specific series-parallel configurations to obtain a desired power output (voltage and current capacities). PV systems are a collection of PV arrays. A wind turbine converts the kinetic energy of wind into electrical energy by using the rotational force from rotor blades. Therefore, the power output is highly dependent on the availability of wind. Because of these operational dependencies on climatic conditions, renewable generators produce volatile and intermittent outputs. While, intermittency refers to the generation that may not be available at all times, volatility indicates to fluctuations in the generation at different time periods. Accurate forecasting of weather information becomes critical in the prediction of power output from renewable generators, so that mitigation of demand and supply imbalances are

maintained with appropriate planning and operation of dispatchable DGs. In general, these units are reinforced with energy storage systems (ESS). ESS is primarily used to maintain coordination among the DGs so that adequate generation is guaranteed at different times. ESS can also be used in electricity trading applications, where excess energy from renewable DGs or energy bought at low price hours can be sold back to external grids when the market prices are high (especially during peak hours). Yet another versatile application of ESS can be in microgrid islanding capabilities by exploiting demand side management.

2.3 Demand Side Management and Demand Response Programs

Integrated with advanced information, communication and control technologies, smart grids as well as microgrids can employ various intelligent techniques to minimize cost and wastage of generated energy. As an effect, the grid may realize reduced operating costs, minimized carbon foot prints, and slashed consumers' electricity bills. Demand Side Management (DSM) is a technique whose objective is to reshape consumption from the consumer's end in order to obtain smooth load patterns. Both parties viz., utilities/grid operators and consumers can benefit from DSM, as it is expected to bring improved efficiency in managing the generation as well as loads. The concept of DSM includes all activities which target to the alteration of a consumer's demand profile, in time and/or shape, to make it match the supply, while aiming at the efficient incorporation of renewable energy resources [115]. Following the definition, the principal activities of DSM can be classified into three categories, i) peak clipping, ii) valley filling and iii) load shifting. While peak clipping aims to reduce consumption during peak hours, valley filling focuses on increasing the consumption so as to mitigate the difference between peak and off-peak load levels. However, load shifting attempts to alter time of usage of appliances in a power system in order to simultaneously obtain the benefits of both peak clipping as well as valley filling. DSM can also be employed to facilitate the integration of distributed generation (typically in microgrids) that can yield significant savings both

in energy generation and transmission. Other applications of DSM include blackout elimination, operational cost reduction and minimization of CO_2 emissions. Among the many DSM techniques, Demand Response (DR) is an important body of schemes which is growing in popularity. We now discuss DR in detail.

2.3.1 Demand Response

According to the US Department of Energy (DoE) DR is defined as, "a tariff or program established to motivate changes in electricity use by end-use customers, in response to changes in the price of electricity over time, or to give incentive payments designed to induce lower electricity use at times of high market prices or when grid reliability is jeopardized". Federal Energy Regulatory Commission defines DR as, "changes in electric usage by end-use customers from their normal consumption patterns in response, to changes in the price of electricity over time, or, to incentive payments designed to induce lower electricity use at times of high wholesale market prices or when system reliability is jeopardized". It may be noted from these definitions that, DR is the broad classification of the following two activities conducted by utilities to economically maintain demand-supply balance: i) induce changes in the electricity usage by consumers from their normal consumption patterns by offering time varying price tariffs/rates and ii) providing incentive payments for deliberately lowering electricity usage of end-use consumers at times when market prices are high or system reliability is compromised. Three distinct responses from consumers may seem possible as an outcome of implementing these activities. Firstly, a consumer may volunteer in reducing the electricity usage during peak time periods (typically when prices are high) by possibly suffering certain discomfort and enjoying profits/cost-cuts. For example, switching-off of an AC or room heater. Secondly, customers may respond to high electricity prices by rescheduling certain operations to off-peak periods. As example, filling water in a pool when the electricity price is low (typically during the night). In this case, a consumer will bear no loss and will incur minimal inconvenience. The third kind of response is that, a consumer may choose to invest and rely on onsite generation (such as distributed gen-

eration) to minimize electricity bills. In this case, consumer's usage pattern may have minimal change but the utility may realize reduced demands.

Demand response typically involves a customer's behavioral changes and is regarded as the outcome of an action performed by the consumers in response to a stimulus. However, benefits of DR to the society may be derived from its cumulative impacts on the entire power system. Understanding these benefits is the key to characterizing and valuing DR. A few benefits of DR are listed below.

- Relieves undesirable network stress caused during critical time periods
- Reduces electricity bills and/or provides monetary incentives for consumers
- Introduces new and competitive electricity markets
- Increases penetration from distributed generation and storage devices
- Mitigates environmental impacts by reducing consumption during peak hours

2.4 DR-aided Power Scheduling

Power scheduling is a vast subject in smart grids and microgrids. It deals with numerous optimization problems related to generation, transmission, distribution and consumption, in a power grid system. However, in this thesis, we only focus on specific sets of these problems which are primarily related to power distribution (Chapter 3), real-time power balancing (Chapter 4) and appliance scheduling (Chapter 5) within DR enabled smart grids and microgrids.

Many developing countries like India suffer from significant power deficits [3] and the situation is not expected to change in the near future. According to Central Electricity Authority, India, the anticipated power deficits of certain regions range from 11%–17.8% of the total energy requirement [13]. Currently, power deficits are typically handled through a mechanism known as *Rolling Blackout* which may be defined as *intentionally engineered electricity shutdown, where electricity distribution is fully stopped for non-overlapping time intervals over different subareas within a distribution region.* A major

side effect of a blackout is the complete disruption of electricity supply to even essential loads which may include life saving and business critical establishments as well as basic conveniences like lights, fan and TVs in residences. Since blackout causes such an indiscriminate service disruption over a given distribution region, there is a necessity for schemes which have comparatively benign side effects but at the same time are effective in lowering and controlling power consumption during contingent events such as transient overloads, intermittent power generation, power deficits, generator outage, severe weathers, etc.

With the advent of Smart Grids and especially Microgrids, design of such improved schemes which essentially depend on more precise knowledge and finer controllability over consumer loads on the demand side, have now become practically realizable [22]. Contrary to traditional grids which only support unidirectional flow of electricity, Smart Grids enable two-way flow of both electricity and information. Smart Meters and home energy management devices (HEMS) installed at households in these modern grids are capable of monitoring and controlling the electricity usage of smart appliances based on scheduling strategies chosen by the consumer and/or the utility provider. While the consumer may choose such strategies in order to manage his consumption behavior and cut-down costs, the utility provider may set them to make more informed choices on scheduling power during peak load situations, power deficits and other contingent scenarios that affect grid's reliability. A key objective of a Smart Grid is to control consumer power requirements through appropriate *Demand Response* (DR) programs. These programs involve all activities which aim to alter the consumer's demand profile, in time and/or in shape, so that it matches the supply at times when market prices are high or when grid reliability is jeopardized [115].

In this thesis, we consider a practical alternative to rolling blackouts called *brownouts*. As opposed to rolling blackouts, which impose total disruption or outage of electricity, brownout refers to the controlled distribution of a limited amount of power during demand overloads, such that uninterrupted power supply to essential appliances / establishments may be selectively maintained while cutting down supply to less critical

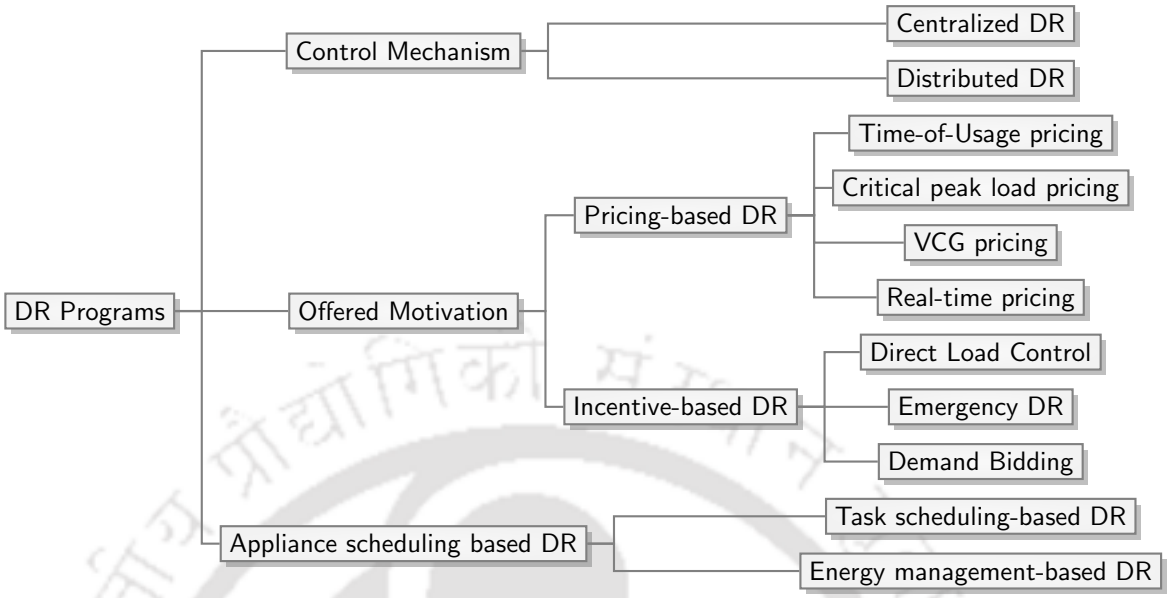

Figure 2.2: *Taxonomy of Demand Response Programs*

loads. Thus, brownout based electricity distribution can be effective in handling power deficits and allow blackout mitigation. In [59], authors introduced the brownout based energy management scheme and presented a customer-end hardware prototype system to support the scheme. Given a bound on the amount of power that a consumer can use at a certain point in time, the hardware ensures that the user will never exceed that bound. After satisfying the essential loads of all the consumers, a set of selective non-essential loads are allowed to run, provided that the aggregate demand is less than the specified limit. We now discuss in brief a few other important DR programs proposed by researchers in recent years.

DR programs may be broadly classified into the following three categorizations (shown in figure 2.2) based on, (i) whether the DR scheme is *centrally* controlled or *distributed* in nature, (ii) the mechanism by which customers are motivated to shape their demands; accordingly, we have *pricing or incentive* based DR programs, and (iii) the technique by which appliances are scheduled in a DR optimization problem [24].

Centralized vs Distributed DR: In centralized DR schemes, there is a dedicated

central controller often called a smart energy manager (SEM) which is responsible for equitably distributing power with a microgrid by taking into consideration consumer's demand profiles, possible distributed generation as well as unforeseen disturbances . In addition these managers may also perform buying and selling of power from external grids [78]. SEMs lend improved stability to the system and encourage increased penetration of renewable based distributed energy generation [95]. However, such centralized scheme may not be feasible in larger geographically distributed power grids. Here, instead of a single controller, there may be multiple distributed controllers which coordinate among themselves through the exchange of messages as well as electricity [46].

Price/Time-based DR: In these programs, consumers are offered time-varying prices which may directly reflect the cost of electricity at different time periods [6, 29]. Given these price information, consumers may be encouraged to shift their electricity usage at low prices or reduce consumption in time periods when prices are high. A few DR programs under this category are discussed as follows.

- *Time-of-Usage (ToU)*: In ToU scheme, tariff is not constant but varies temporally according to the load on the grid over a given interval of time. This scheme encourages consumers to reduce energy consumption under peak load conditions, thus reducing demand. As example, ToU pricing in Ontario, Canada, consists of three price levels for three different time periods (peak, off-peak and mid-peak) and these price levels vary in summer and winter. Similar to traditional flat pricing, in ToU schemes, prices are remained fixed within stipulated time intervals, which can be hours in a day or days within a week.

- *Critical Peak Load Pricing*: Due to occasional system/network stresses, utilities may set high fixed prices for the affected time periods [124]. In some cases, based on the average power consumption of consumers at various time periods, prices are determined and forwarded to them [47]. These prices are designed such that the payoff to the energy provider is maximized and consumers are encouraged to shift loads away from peak periods [75].

- *Vickrey-Clarke-Groves (VCG) Pricing*: VCG is an important game theoretic approach which is usually used to extract truthful information from rational self-motivated entities. VCG takes as input a set of entities, with each such entity self-reporting its individual resource demand and known associated revenue return. The VCG mechanism guarantees that when there is atmost one untruthful entity who presents an inflated demand, the entity cannot make a profit by procuring the unjustly acquired additional resource. Many researchers have applied VCG pricing to different power distribution problems within DR enabled power systems [104]. We discuss a few important works as follows. A VCG-based smart pricing mechanism has been proposed in [103] to determine optimal power consumption levels of a set of users, given the generation cost and the users' utility functions. The social objective endeavoured is the maximization of aggregate utility while also attempting to minimize generation cost. The authors in [87] propose a VCG mechanism for a load curtailment problem where a DR aggregator aims to minimize aggregate inconvenience of consumers while satisfying targeted load reduction requests from generation companies. In [105], authors develop a VCG mechanism for *control–reserves* electricity markets where the transmission system operator attempts to minimize the total cost of power acquired from control reserve entities. The authors also derive necessary conditions that prevent collusion i.e., the outcome cannot be improved by forming coalitions of entities. The authors in [120] applied VCG to wholesale markets, for preventing strategic misreporting of cost prices associated with generation companies. Authors in [86] propose a novel self-reported baseline mechanism to determine a subset of agents from a pool of recruited agents who are obligated to reduce their consumption, and in return are paid a VCG-based reward.

- *Real-time Pricing (RTP)*: In an RTP scheme, the energy provider determines and announces electricity prices at real-time (say 15 minutes ahead) [18]. Day-ahead RTP is another type of RTP, where the next day's predicted real-time prices are announced to customers a day-ahead [29].

Incentive-Based DR: These set of DR programs offer monetary incentives (fixed or time-varying payments) to customers that volunteer to reduce their electricity consumption during critical periods. Some of these programs may involve penalization for failing to contribute under established contracts. There are a few important sub-categories of schemes under this program which we discuss as follows.

- *Direct Load Control (DLC):* In this scheme, consumers voluntarily allow certain loads to be remotely controlled by the utility. Based on a load reduction target, utilities may select a subset of these loads to cycle them or turn-off whenever needed. In return, the consumers are paid monetary incentives for their sacrifice [91, 102]. As example, typical residential loads such as ACs and water heaters can be directly dispatched by the utility and the participating consumers receive payments in advance. A few works related to DLC based DR are discussed as follows. Authors in [97] developed a new stochastic optimization framework for the design and assessment of DLC programs, with the objective of minimizing consumer discomfort. In [34], authors propose a DLC scheme for residences in Norway, where water heaters are shutdown whenever peak load crosses the supply. The key idea is to reduce load during peak hours. Under DLC based DR, there are some *Emergency DR* programs which provide incentive payments to consumers for reducing their power consumption during reliability triggered events [4]. In such DR schemes, consumers are given the liberty to choose whether or not to curtail specific loads. Certain DR programs in *capacity markets* ask for predefined load reductions to replace conventional generation or transmission resources. In such planned reductions, consumers may have to deal with penalties for disobeying curtailment [60].

- *Demand Bidding:* This DR approach is usually applied to large consumers who offer curtailment capacity bids in electricity wholesale markets [4]. Similarly, bids on load reductions are allowed in *Ancillary Service Markets* for applications such as frequency regulation, voltage control and maintenance of generation reserves.

Appliance Scheduling based DR: In this categorization of DR, power supply to consumer appliances is scheduled. Such scheduling decisions may be based on, a) selection of appropriate time slots at which an appliance can be run, and/or b) choosing appropriate energy levels for running an appliance. Schemes under the former category are called task scheduling-based DR mechanisms and the schemes under the later category are called energy management-based DR approaches.

- *Task scheduling-based DR mechanisms:* These mechanisms involve determining the activation time of requested loads. A load can be of two types: *rigid* or *elastic*. Rigid loads cannot tolerate any activation delay (e.g., basic conveniences like fans, lights, TVs, refrigerators). On the other hand, elastic loads are considered to be flexible and can be shifted to other time slots [98]. Depending on the availability of power and other factors such as operation time and deadlines, these appliances are scheduled by the utilities [69]. Further, loads can be preemptive and non-preemptive [17]. The objective of these set of DR programs is to reduce the power consumption in peak hours by either curtailing rigid appliances or shifting elastic loads to off-peak hours.

- *Energy management-based DR approaches:* The main objective of these DR programs is to reduce total energy consumption of specific loads such as Heating, Ventilation and Air Conditioning (HVAC) devices, so that the consumption during peak-demand hours is minimized. This is realized by controlling the appliance's operation so that they may consume lower power during system stress [15]. For example, in a summer day, an air conditioner could be adjusted to 25°C instead of 22°C.

2.4.1 DR Programs–Typical Objectives

In general, optimization is the process of finding appropriate decisions for a given problem that maximizes a profit function or minimizes some cost function. More formally, an optimization problem consists of, a) a set of decision variables, b) constraints and

c) an objective function; the target is to determine values for the variables that maximize (/minimize) the objective function while satisfying the constraints. With respect to optimization in DR programs, the usual objective is to minimize total power consumption and/or maximize some reward function. From the perspective of an electric utility, maximizing a reward function may sometimes refer to the maximization of its own profit i.e, *revenue obtained (consumers' willingness to pay) minus total cost*, for the amount of power distributed to consumers under its purview. In the past few years, researches have considered various other objectives such as maximizing satisfaction [82], user comfort [51,61], thermal comfort [16] or minimizing demand peaks [14,117], demand and supply mismatches [28], consumers' electricity bills [65, 98], inconvenience [121] etc. Chakroborty et. al. in [14] address the problem of scheduling appliances in a smart building by formulating it as a two–dimensional Strip Packing (SP) problem. The objective is to minimize peak load. As two–dimensional SP problem is known to be NP–Hard, they propose a greedy strategy named *MinPeak* to solve it. In fact, many researchers have shown that the appliances scheduling problem is NP–Hard in general, and therefore have resorted to either approximate or heuristic solutions [25, 56, 122]. Given a day–ahead dynamic pricing scheme, the authors in [65] provide a solution to optimally schedule a set of household appliances, such that the consumer's electricity bill is minimized. In [98], the authors also attempt to minimize the consumer's bill where, in addition to household responsive loads, the set of appliances to be scheduled also includes storage devices and plug–in hybrid electric vehicles. In [121], authors have addressed the appliance scheduling problem with three minimization objectives namely, electricity cost, minimize consumer inconvenience and minimize peak loads. The appliance scheduling problem considered by Javaid et.al. [52] aim to obtain a balance between two conflicting objectives, namely, *minimizing energy consumption cost* and *maximizing user comfort*, while limiting the total consumption per timeslot to a maximum allowable bound. A cost minimization approach has be employed by the authors in [38] to solve the problem of scheduling appliances within a single smart building. The authors in [42] presented the design of a home energy management system (HEMS), which takes as input day–ahead

electricity pricing information (such as Time of usage (ToU)/real–time pricing (RTP), and schedules controllable loads like electric vehicles and water heaters in the presence of other rigid loads, such that the total daily energy consumption cost is minimized. In [31], Fadi Elghitani et. al. present a methodology to consolidate residential appliances into a set of disjoint demand blocks/clusters, where each such block/cluster of appliances share common DR capabilities like consumption profile, rated power and allowable delay. Electrical appliances from these blocks/clusters are then scheduled by a grid–level LA while maintaining a trade–off balance between scheduling accuracy and computational complexity. Here, the LA performs grid–level scheduling/optimization and sends signals to individual *Home Energy Management Systems* (HEMSs) for controlling appliances within households/establishments. Fanitabasi et al. in [36], emphasized the importance of allowing appliances to be shifted to non-preferred time slots for obtaining better reductions in demand peaks, although this flexibility may negatively impact user comfort. The authors in [71] consider a set LAs under the purview of a Distribution System Operator (DSO). Depending on the energy available with a DSO and estimated demands of LAs, the DSO can request an LA to adjust its electricity consumption by a stipulated amount against designated financial compensation. The LA in return attempts to satisfy the request by appropriately scheduling the curtailable and shiftable consumer appliances under its jurisdiction.

2.5 Selection and Sizing of DERs

Many a time, electricity supply to small isolated regions can be difficult and infeasible due to various economical and geographical challenges in expanding the traditional centralized grid [118]. Such remote areas are typically electrified using localized fuel powered generators. Due to increasing fuel prices, fast depleting fossil fuels and emission concerns, continuous operation of diesel generators becomes prohibitively expensive. An efficient alternative to this problem is to harness the rich abundance of renewable energy such as solar and wind, available within such remote areas. However, volatile and intermittent generation from renewable generators such as solar photovoltaics and wind

turbines, must be reinforced with energy storage systems. Efficient coordination among different distributed energy resources (DERs) such as conventional fuel generators, renewable generators and energy storage systems, is generally realized by establishing a cost-effective microgrid [58, 76].

While planning for a new microgrid, the design process is considered to be an important step towards successful deployment of the microgrid. As microgrids are typically designed to supply electrical and heat loads to a small geographical area with specific climatic conditions (including average wind speeds or solar radiation), geographical terrain / water sources, consumer behavior patterns etc., a plethora of design alternatives seem possible for microgrids depending on the variations in these parameters [32]. For example, the DGs of a microgrid in a typically windy area may be powered by WTs, the renewable energy based generators in a region with ample solar radiation may be powered by PV panels etc. Designing a microgrid is an optimization problem that attempts to determine optimal system configuration with respect to obtaining a suitable generation mix, sizing of DERs and their placement in a locality, such that a desired objective is attained while respecting a set of required system constraints and operational limitations of DERs.

Microgrid sizing is considered as a subproblem to the planning/designing problem which focuses towards finding appropriate sizes/units of suitable DERs for a region which include renewable generators, fuel based conventional generators and storage devices [40]. The primary objective of a microgrid sizing problem is to minimize the total cost of generation such that stipulated loads within a region are reliably satisfied. The total cost of generation is typically calculated as the sum of total capital/investment cost of DERs as well as their operational costs. Researchers in the past have dealt with different microgrid sizing problems targeted to other cost functions which include life cycle cost, net present cost, annual system cost and normalized cost of energy [32].

In general, microgrid sizing problems may be considered a generalization of unit commitment (UC) and Economic Dispatch (ED) problems. We first discuss some of the works related to UC and ED, and then present a few microgrid sizing problems. Unit

Commitment is an extensively studied topic in the context of traditional grids, smart grids and also microgrids. UC in a microgrid environment is defined as the problem of judiciously scheduling DER operations with minimal exchange of power from the utility (if grid-connected), given the forecast of local loads, typically over a day or few days of a week, such that overall implementation costs are minimized. These scheduling problems are typically solved by a smart energy manager in a microgrid. Economic Dispatch (ED) is a subproblem of UC dealing with the determination of real power outputs from DERs, (especially, dispatchable DERs like microturbines and fuel cells) so that the total fuel cost is minimized. A few related works in the context to UC and ED problems are discussed as follows. The authors in [12] present a UC based optimization method to economically schedule battery storage and hydrogen storage systems in isolated microgrids. Authors in [45] studied UC of thermal power plants and large capacity energy storage systems for smoothing load curves. In [26], authors propose a power balance mechanism for microgrids in which UC is performed by taking into consideration the adjusted load curve that is obtained after rescheduling consumer loads through a load management strategy. The problem of optimally scheduling DERs in an islanded microgrid has been investigated in [83]. Optimal operation of as set of DERs which include wind turbines, solar units, a fuel cell and a storage unit, has been formulated as a mixed integer linear program (MILP) and solutions are computed using a General Algebraic Modeling System (GAMS). Considering the presence of a single prosumer equipped with PVs, battery units and a gas turbine within a small building microgrid, the authors in [55] propose an optimal energy management strategy that works through effective coordination of two principal modules viz, a utility-end central energy management unit and a consumer-end local energy management unit. The problem of economic generation scheduling in grid connected microgrids is studied in [92]. The objective of the problem is to minimize operational costs of DERs as well as external imports from the utility, while fulfilling time-varying energy demands under various operational constraints. The authors in [100] propose a cost optimal scheduling problem for the operation of energy storage enabled wind-diesel power systems, using a knowledge based expert system (KBES). In [81],

authors propose a model predictive control based solution to solve the multi-objective power scheduling problem for a microgrid empowered with wind generation, diesel generation and storage devices. The objectives considered include, minimization of fuel costs and changes in the power outputs from diesel generators, minimizing costs associated with low battery life of energy storage and maximizing the ability to maintain real-time power balance. Khodaei in [62] and [63] presents a model for optimal scheduling under two different scenarios, one with multi-period microgrid islanding constraints and the other with the aim to improve the microgrid resiliency.

We now discuss a few microgrid sizing solutions which simultaneously incorporate both UC and ED within them and often achieve significantly higher cost savings. Logenthiran et.at. [77] proposed a generic population based metaheuristic algorithm for obtaining optimal DER size for an islanded microgrid, with the objective of minimizing the sum total of capital, operational and maintenance costs. Sizing problems not only concern suitable choice of DERs and their generation capacities but also the deployment of appropriate storage systems such as batteries. In this regard, Chen et.al. [21] formulates a battery sizing problem as a mixed integer linear program to perform a cost-benefit analysis over two different scenarios, that is, grid connected and islanded. Authors in [72] have proposed a genetic algorithm based solution strategy for the combined sizing and unit commitment problem which is formulated as a leader-follower problem. An optimal sizing methodology integrated with energy management has been proposed in [39] for designing a hybrid power system consisting of energy storage systems, wind turbines and solar photovoltaics in addition to hydrogen powered fuel cells. An optimal model for obtaining size of energy storage systems is proposed in [8], where the system consists of a set of conventional gas powered generators and a wind turbine. The objective of the proposed model is to minimize the sum total of investment and operational costs under the constraint that certain reliability criterion is met. Researchers have modeled the microgrid sizing problem with other objective functions such as minimization of cost per unit of energy generated, pollution emissions, loss of power supply probability etc., and maximization of total power generation, reliability, profit, revenue, life span,

etc [50]. However, certain objective functions may conflict with each other when considered together. For example, minimization of emissions may conflict with the objective of minimizing operational cost or fuel cost. Similarly, maximization of revenue may conflict with emission minimization objectives.

2.6 Summary

This chapter started with a brief overview of smart grids and microgrids. Core objectives related to demand side management and demand response programs have been discussed. Subsequently, a detailed survey on DR-aided power scheduling problems and microgrid sizing strategies have been conducted. These concepts and definitions will be either referred or reproduced appropriately later in this thesis, to enhance readability. In the next chapter, we present a brownout based electricity pricing scheme that allows utilities to equitably distribute its available power among a set of microgrids under its purview.

Chapter 3

Equitable Electricity Pricing for a Network of Microgrids

Future Smart Grids are evolving into interconnected networks of independent, small–scale power systems, called Microgrids, which provide electricity service to a small geographical region. Network architectures consisting of multiple microgrids radially connected to an electricity distribution company (EDCo) (also known as *distribution system operator*) are simple yet capable of lending improved electricity distribution and stability to an overall system in a cost-effective way [99]. A microgrid is typically equipped with a Load Aggregator (LA) (an integral part of *smart energy manager*) for performing various activities like demand acquisition from consumers, balancing supply with loads, participating in wholesale energy markets, implementing Demand Response (DR) based schemes, etc [20]. Contrarily, the EDCo usually deals with the distribution of a certain amount of power among multiple microgrids under its distribution purview. In this chapter, we present a novel DR–framework that allows an EDCo to distribute its available power among associated microgrids, in an equitable fashion. In this framework, the EDCo uniformly grades appliances/establishments into a disjoint set of urgency classes, across all microgrids that are radially connected to itself. Here, *urgency* refers to the criticality of an appliance's need for uninterrupted power supply. The EDCo prescribes each of the microgrid LAs to advertise its consolidated demands for different classes. Based on the urgency based cumulative utilities of demand classes as advertised by the

LAs, the EDCo optimizes and distributes its available power such that, the utility of the overall system is maximized. Given a limited amount of available power, maximizing utility achieves the social welfare objective of maximally satisfying the aggregate urgency–proportionate demand across all microgrids under an EDCo's jurisdiction. An optimal algorithm called, *Dynamic Programming based Power Allocator* (DPA) has been proposed to this problem.

The LAs who act as individual microgrid agents, may be driven by self–centered motivations which are orthogonal to the EDCo's objective of fair and equitable distribution of power among microgrids. It may be noted that, the information related to consolidated urgency based power demands are local to individual microgrids. So an EDCo must conduct electricity distribution by relying only on the power demand information as reported by the microgrids. That is, the EDCo does not have any mechanism to validate truthfulness of the reported information when the distribution decisions are made. Hence, an LA may exploit the system by falsely reporting inflated demand utilities for its microgrid in an attempt to unjustly acquire more power than what it should have received in a fair scenario. Such an unjust activity can significantly affect the EDCo's social welfare objective. In order to effectively prevent such unjust activities, we proposes a payment mechanism called *Vickrey–Clarke–Grove based Equitable Pricing* (VCG-EP), which encourages the LAs to report truthfully.

As discussed in the previous chapter (Chapter 2, Section 2.4), the VCG mechanism has been applied as an integral part of many DSM schemes. Motivated by this, we have perceived that our work which has a similar subject of concern, can also be solved through a VCG mechanism. Most of the works discussed in the literature (refer, Chapter 2, Section 2.4, VCG Pricing under Price-based DR Schemes) consider individual consumer preferences as inputs. This can often make the solution prone to unacceptably high computational complexities, especially when the desired social welfare must be imposed on an entire microgrid system or even larger systems constituted of multiple microgrids. In this work, we consider a simplified yet realistic system model where the preferences of all consumers across a set of microgrids can be aligned to a common set of discrete

choices while respecting the individual appliance usage preferences of consumers. This novel system model significantly reduces complexity and thus enhances its practical applicability.

3.1 System Model and Formulation

The system consists of an Electricity Distribution Company (EDCo), whose main objective is to equitably distribute its pool of available power P to a set of N microgrids MG_1, MG_2 ... MG_N, located within a geographical region under its purview. Each microgrid caters to the electricity demands of consumers within a logically disjoint subarea of the mentioned geographical region. A consumer demand which may refer to an individual appliance or an establishment, can have varying *urgency* towards uninterrupted power supply. For example, establishments like hospitals, laboratories, server rooms, etc., and basic conveniences such as fans and lights, are considered the most urgent. In comparison, commercial buildings, activity centers and residential appliances like washing machines, TVs, ACs, etc., can be considered to be less urgent. The EDCo provides a uniform policy for grading the appliances into M disjoint urgency classes c_1, $c_2 \dots c_M$, across all microgrids such that, lower the class–id j (of c_j), higher is its urgency. Thus, hospitals, server rooms are assigned higher urgency classes (lower class ids) compared to commercial buildings, activity centers, and residential appliances.

Each of these urgency classes say c_j, is assigned a constant utility value μ_j such that, higher the urgency of a class (lower class ids), the higher will be its associated utility value. Thus, $\mu_1 > \mu_2 > \cdots > \mu_M$. Further, the EDCo designates a uniform tariff policy across all microgrids in which the tariffs levied from the consumers of the microgrids are proportional to the utility values associated with the urgency classes. We denote the proportionality constant by ρ. Let, p_{ji}^k denote the power demand (in no. of units) of each appliance A_{ji}^k in class c_j of microgrid MG_i. Then, the aggregate demand p_{ji} of class c_j in MG_i is calculated as $p_{ji} = \sum_{k=1}^{K_{ji}} p_{ji}^k$ where, K_{ji} denotes the number of appliances in class c_j of MG_i. The utility value u_{ji} for the aggregate demand p_{ji} of a class c_j in microgrid MG_i can be calculated as, $u_{ji} = p_{ji} * \mu_j$. Therefore, the revenue obtained by

MG_i for distributing p_{ji} to its consumers can be calculated as, $u_{ji} * \rho$.

In order to equitably distribute a limited amount of power (P) among the microgrids, the EDCo expects/queries the consolidated class–based power demand values from all microgrids. If the EDCo decides to deliver power to a particular urgency class of a certain microgrid, it must supply the total power with respect to that urgency class and all higher classes. As example, when the appliances are classified into three urgency classes c_1 (highest urgent), c_2 (second highest urgent) and c_3 (least urgent), if the EDCo chooses to fulfil the demands of class c_3, it must also satisfy the demands of class c_2 and c_1. Acquisition/distribution of power and aggregation of demands within a microgrid MG_i is performed by an entity called the Load Aggregator LA_i. In order to provide information as required by the EDCo, the LA_i consolidates MG_i's power demands into M distinct cumulative choices. The j^{th} choice (where $j \in \{1..M\}$) of LA_i is comprised of, a) the cumulative power demand P_i^j and b) its corresponding utility value U_i^j. The cumulative power demand P_i^j and its associated utility value U_i^j are computed using the following equations: $P_i^j = \sum_{j'=1}^{j} p_{j'i}$ and $U_i^j = \sum_{j'=1}^{j} u_{j'i}$. Here, we denote the j^{th} cumulative demand choice of LA_i as $\theta_i^j \langle P_i^j, U_i^j \rangle$. Due to the cumulative property of the demand choices, each choice of an LA is considered as an alternative demand choice.

The EDCo distributes the available power P among microgrids based on the alternative demand choices advertised by the load aggregators, such that the aggregate utility of the system is maximized. It may be noted that, this objective attempts to maximize proportional fairness in the distribution of power based on the urgency sensitive demand choices produced by the LAs. Such an objective may be considered reasonable as EDCos are typically government controlled/supported centralized power distribution agencies, with social welfare being a core operational motivation.

Let x_i^j denote a set of decision variables; $x_i^j = 1$, if EDCo selects θ_i^j and $x_i^j = 0$,

otherwise. The power distribution problem can therefore be represented as:

$$\begin{aligned} \text{Maximize} \quad & \sum_{i=1}^{N}\sum_{j=1}^{M} U_i^j \cdot x_i^j \\ \text{subject to} \quad & \sum_{i=1}^{N} P_i^j \cdot x_i^j \leq P \\ & \textstyle\sum_{j=1}^{M} x_i^j \leq 1 \quad \forall i \in \{1...N\} \\ & x_i^j \in \{0,1\}, \quad \forall i,j \end{aligned} \tag{3.1}$$

In contrast to EDCo's social welfare motivation, individual microgrid LAs are typically concerned about and influenced by the interests of consumers under its own purview. It is also not unreasonable to assume that a selfish rationally acting LA may want to maximally satisfy the demands of its consumers, even if this results in more deserving consumers within other microgrids being deprived of power supply. A manipulative LA (say, LA_i) may thus falsely advertise inflated power demands for higher urgency classes in the endeavor to acquire higher amounts power than what it actually deserves. Inflating the demands for higher urgency classes inflates their corresponding utility values. As the EDCo attempts to maximize overall utility, such deceitful inflation may increase LA_i's chance to unfairly acquire power corresponding to higher demand choices. Thus, LA_i indirectly deprives electricity to more deserving consumers within other microgrids. Traditionally, fixed per–unit pricing is a very common pricing scheme extensively used in power grids. With its goal being equitable power distribution in a sustainable manner, such a fixed pricing scheme (with low per–unit prices) could be a simple obvious choice for the EDCo. However, as we illustrate through the hypothetical example below, this simple pricing scheme will fail to prevent untruthful reporting by LAs.

3.1.1 Example

Assume that there are two microgrid load aggregators LA_1 and LA_2 under the jurisdiction of an EDCo. Based on the nature of their need for uninterrupted power supply, the EDCo categorizes all appliances/establishments into one of three (M=3) urgency classes (c_1, c_2 and c_3). Let, the utility values corresponding to the urgency classes be,

μ_1=3, μ_2=2 and μ_3=1. The amount of power available with the EDCo is P=15 units. For LA_1 (LA_2), let the aggregate demands of classes c_1, c_2 and c_3 be p_{11}=3, p_{21}=5 and p_{31}=7 (p_{12}=2, p_{22}=5 and p_{32}=8), respectively. Given these demands, LA_1's (LA_2's) aggregate utility values for classes c_1, c_2 and c_3 becomes, u_{11}=3*3= 9, u_{12}=5*2=10 and u_{13}=7*1=7 (u_{21}=2*3=6, u_{22}=5*2= 10 and u_{23}=8*1=8). Therefore, the choices ($\theta_i^j\langle P_i^j, U_i^j\rangle$) consisting of cumulative demand and utility pairs of LA_1 and LA_2 can be obtained as follows.

$$LA_1 : \theta_1^1\langle 3, 9\rangle, \theta_1^2\langle 8, 19\rangle, \theta_1^3\langle 15, 26\rangle$$
$$LA_2 : \theta_2^1\langle 2, 6\rangle, \theta_2^2\langle 7, 16\rangle, \theta_2^3\langle 15, 24\rangle$$

The above mentioned choices are considered true/actual choices of the LAs. Given the demand choices of the LAs and the EDCo's available power P as 15 units, the maximum utility of the system can be computed by optimally solving the equation 3.1 (refer, Section 3.1, Chapter 3). An optimal solution is obtained by selecting $\theta_1^2\langle 8, 19\rangle$ for LA_1 and $\theta_2^2\langle 7, 16\rangle$ for LA_2. That is, 8 and 7 units of power will be distributed and this results in the total system's utility as $19 + 16 = 35$. Now, let's assume that the LAs are charged by using a simple block pricing mechanism, where the first 10 units of power are charged \$0.5 and the units 11 onwards are charged at \$1. Following this pricing strategy, LA_1 pays $8 * 0.5 = 4\$$ for the 8 units of allocated power and LA_2 pays $7 * .5 = 3.5\$$ for 7 units. However, consider a situation in which LA_2 falsely promotes a few less urgent appliances say, 5 units of power in class c_3's demand, to the next higher urgency class c_2. As a result, the total demand p_{22} corresponding to only class c_2 is inflated from 5 units to 10 units (note that, cumulative demand P_2^2 now increases from 7 to 12). Consequently, the total demand p_{23} of class c_3 is now 3 units but not 8 units (as reported in the true scenario). Therefore, LA_2's cumulative demand choices ($\hat{\theta}_i^j\langle \hat{P}_i^j, \hat{U}_i^j\rangle$) for the three classes now change to, $\hat{\theta}_2^1\langle 2, 6\rangle, \hat{\theta}_2^2\langle 12, 26\rangle, \hat{\theta}_2^3\langle 15, 29\rangle$, from the original choices $\theta_2^1\langle 2, 6\rangle, \theta_2^2\langle 7, 16\rangle, \theta_2^3\langle 15, 24\rangle$. Note that, the total demand of LA_2 before and after inflation remains the same (i.e., 15). However, the total utility for the demand is seen to be inflated from 24 to 29. Now, consider a scenario where, LA_2 reports these

inflated choices but LA_1 reports truthfully. As a result, the EDCo receives the following demand choice alternatives.

$$LA_1 : \hat{\theta}_1^1\langle 3, 9\rangle, \hat{\theta}_1^2\langle 8, 19\rangle, \hat{\theta}_1^3\langle 15, 26\rangle$$
$$LA_2 : \hat{\theta}_2^1\langle 2, 6\rangle, \hat{\theta}_2^2\langle 12, 26\rangle, \hat{\theta}_2^3\langle 15, 29\rangle$$

For this setting, the solution delivered by equation 3.1 (refer, Section 3.1, Chapter 3) becomes, $\theta_1^1\langle 3, 9\rangle$ for LA_1 & $\theta_2^3\langle 12, 26\rangle$ for LA_2, are selected. In this scenario, 3 and 12 units of power will be distributed respectively to LA_1 and LA_2. This results in the total system's utility as $9 + 26 = 35$. Following the same block pricing mechanism as presented above, the payments made by LA_1 and LA_2 are calculated as $3 * 0.5 = \$1.5$ and $10 * 0.5 + 2 * 1 = \$7$, respectively. It may be observed from these example scenarios that, LA_2 exploits the system by unfairly extracting a higher share of power (a part of which actually belongs to LA_1) from the EDCo. It may also be noted that, the utility value for the additional 5 units of power (actually belonging to class c_3) deceitfully acquired by LA_2 is only 5 i.e., $5^*\mu_3$ where $\mu_3 = 1$, but not 10 (inflated to $5^*\mu_2$, where $\mu_2 = 2$). In that case, the actual overall utility is observed to be reduced from 35 to 30. This reduction can be comprehended by carefully examining the inflated demand choice for LA_2 i.e., $\hat{\theta}_2^2\langle 12, 26\rangle$. Here, 5 units among the 12 units actually belong to class c_3. Therefore, the actual utility for these 12 units is only 21 (i.e., $2^*\mu_3$+$5^*\mu_2$+$5^*\mu_3$). This observation justifies the mentioned reduction, as observed in the above scenarios. This example motivates the need for an efficient pricing scheme which is able to proportionally penalize an LA for untruthfully inflating its demand, while also ensuring an equitable price for reporting truthfully.

3.1.2 Problem Definition

The EDCo's power distribution problem is formally stated as follows. Given the cumulative demand choices (demand and utility pairs) of LAs, the overall objective of this work is to determine an equitable distribution of a limited amount of power available with the EDCo, among peer microgrids such that aggregate utility of the system is

maximized (refer equation 3.1). In a scenario where the LAs may deceitfully advertise inflated demands (untruthfully increasing the demand of higher urgency classes), the objective is to determine an equitable pricing mechanism which ensures that an LA is always levied minimum payment if it advertises its true demand choices. This equitable payment mechanism ensures that truthful reporting of cumulative demand and utility values become the recommended/dominant choice for an LA. The EDCo's equitable power distribution objective can thus be achieved even in the presence of rationally acting LAs with selfish motivations.

In order to deal with challenging problems as the one discussed above, researchers especially in fields like Algorithmic Game Theory and Economics have often resorted to the mechanism design approach [89]. In general, mechanism design focuses on achieving specific properties like *truthfulness* (also called, *incentive–compatibility*) and *efficiency* for resource allocation problems in a competitive environment. The truthfulness property ensures that the competing entities do not exploit the system by lying, while the efficiency property ensures that a system wide objective is achieved. In the next section, we present the design of such a truthful mechanism which appropriately addresses the EDCo's power distribution problem.

3.2 Truthful Mechanism Design

In this section, we present the proposed solution methodology for the overall power distribution problem as described in Section 3.1.2. In subsection 3.2.1, we first discuss the design of a power distribution strategy (for the problem formulated in equation 3.1) called, *Dynamic Programming based Power Allocator* (DPA), in a scenario where the LAs report their actual demand choices. This problem essentially boils down to the well known *Multiple Choice Knapsack Problem* (MCKP) which is known to be NP–hard. In subsection 3.2.2, we propose a novel payment mechanism called *VCG based Equitable Pricing* (VCG-EP) which enforce LAs to report truthfully in a scenario where they may be selfishly motivated and even deceitful.

Algorithm 1 DP based Power Allocator (DPA)

Input:
a) The M cumulative demand choices of the N LAs,
$\theta = \{\theta_i^j \langle P_i^j, U_i^j \rangle | \ \forall i \in \{1..N\} \ \& \ j \in \{1..M\}\}$
b) The number of power allocation levels $PL = \frac{P}{pu}$,
where, P denotes the available power and pu is the discretization parameter
Output:
a) The obtained maximum total utility max_util.
b) The allocation $a = \{a_i | \ \forall i \in \{1..N\}\}$, where $a_i = j$ if j^{th} demand choice of LA_i is selected; otherwise $a_i = -1$.

1: **for** k from 0 to PL **do** ▷ Initializing base results
2: $U(0,k) = 0$
3: **for** c from 1 to N **do** $A(0,k,c) =$ '-'
4: **for** i from 1 to N **do** ▷ Iterate over all N LAs
5: **for** k from 0 to PL **do** ▷ Iterate over all PL levels
6: mj = -1 & mu = $U(i-1,k)$
7: **for** j from 1 to M **do** ▷ Iterate over all M choices
8: **if** k > P_i^j **then break**
9: **if** mu < $U(i-1,k-P_i^j) + U_i^j$ **then**
10: mu = $U(i-1,k-P_i^j) + U_i^j$ & mj = j
11: $U(i,k)$ = mu ▷ sub-problem's max total utility
12: **if** mj = -1 **then**
13: **for** $c \in \{1..N\} - \{i\}$ **do**
14: $A(i,k,c) = A(i-1,k,c)$
15: $A(i,k,i) = -1$
16: **else**
17: **for** $c \in \{1..N\} - \{i\}$ **do**
18: $A(i,k,c) = A(i-1,k-P_i^{\text{mj}},c)$
19: $A(i,k,i)$ = mj
20: Output: **i)** the obtained maximum utility $max\_util = U(N,PL)$ and **ii)** the allocation a=$\{a_i \mid a_i = A(N,PL,i) \ \& \ i \in \{1..N\}\}$

3.2.1 DP based Equitable Power Allocator (DPA)

A closer look at the maximization problem as formulated in equation 3.1 reveals that it has an optimal substructure i.e., an optimal solution may be obtained as a composition of the optimal solutions to the set of its sub-problems. Therefore, *Dynamic Programming*

(DP) provides a natural solution mechanism. The DP based algorithm finds an optimal solution in pseudo-polynomial time in terms of available number of power allocation levels, denoted by PL. Given the total available power P, number of power allocation levels PL is defined as the number of discretely quantified units of power denoted as pu. Here, pu is referred to as the power resolution and is a discretization parameter which denotes the smallest unit of power that can be distributed to any microgrid. The total number of power allocation levels (PL) is calculated as: PL/pu. As example, let the available power P be $20MW$ and the power resolution pu be $10kW$, the number of power levels can be calculated as PL=20,000kW/10kW=2000. This feature restricts the power allocation to be only in multiples of 10kW. Given, a) the total number of power allocation levels (PL) and b) the LAs' demand choices $\theta = \{\theta_i^j \langle P_i^j, U_i^j \rangle \mid \forall i \in \{1..N\} \ \& \ j \in \{1..M\}\}$, the power allocation procedure namely, *Dynamic Programming based Power Allocator* (DPA), is given in Algorithm 1.

Before we delve into the detailed description of DPA, we present two important notations: **a)** $U(i,k)$, which represents the maximum total utility obtained for the sub–problem considering load aggregators LA_1 to LA_i for a distinct number k ($\leq PL$), of available power levels, and **b)** $A(i,k,c)$, which represents the selected demand choice of the load aggregator LA_c for the above mentioned sub–problem. It may be noted that at any intermediate state of the algorithm, i) if the j^{th} demand choice (θ_i^j) has been selected then, $A(i,k,c)$ = j, ii) if LA_c is not part of the sub–problem under consideration ($i < c$), then $A(i,k,c)$ is marked with '-', and iii) if LA_c is part of the present sub–problem but not allocated any power, then $A(i,k,c)$ is assigned '-1'. A step–wise working principle of DPA is described as follows. From steps 1 to 20, DPA finds an optimal allocation $a = \{a_i \mid i \in \{1..N\}\}$, where a_i=j if the j^{th} demand choice of LA_i is selected; otherwise, a_i=-1. The obtained maximum total utility is represented by max_util. DPA follows a tabulation approach, through which it iterates over all N LAs and over all power levels (PL) and solves efficiently all sub–problems (i.e., for all possible tuples (i,k), $\forall i \in \{1..N\}$, $\forall k \in \{1..PL\}$) by caching intermediate results.

3.2.1.1 Complexity Analysis for DPA Algorithm

Given, N LAs, M demand choices for each load aggregator, and PL power levels, the computational complexity of the proposed algorithm DPA is analyzed as follows. Steps 1 to 3 involve a two-level nested looping structure. While the outer loop iterated from 1 to PL Inner loop iterates from 1 to N. Assuming the statements within these loops can be processed within a constant time i.e., $\mathcal{O}(1)$, the time complexity for the above mentioned steps is determined as $\mathcal{O}(PL * N)$. Steps 4 to 19 consists of three levels of nested loops. The outermost loop (Step 4) runs for each of the N LAs, inner loop (Step 5) runs for every power allocation level PL and finally the innermost loop (Step 7) iterates for each of the M demand choices. Considering all the intermediate steps within these loops to be computed within a constant time, the time complexity for these steps can be summarized as $\mathcal{O}(N * PL * M)$. Therefore, the total worst case complexity of the DPA may be derived as $\mathcal{O}(N * PL * M)$. Our experimental results show that for $N = 25$ load aggregators, each having $M = 5$ demand choices and for $PL = 2000$ power levels (i.e., $20MW$ at power resolution $pu = 10kW$), the execution time taken by DPA is $\sim$1 sec.

3.2.2 VCG-based Equitable Pricing (VCG-EP)

In this section, we present our proposed pricing scheme namely, *VCG-based Equitable Pricing* (VCG-EP). VCG-EP attempts to alleviate untruthful declaration of inflated cumulative demand choices by offering LAs a lower price when they report truthfully. Our approach employs the *Vikrey Clarke Groves* (VCG) mechanism design strategy [101] (a generalization of Vickrey's *Second Price Auction*), which ensures that the participating entities only benefit by advertising their true valuations for the allocated resources.

Let, $\hat{\theta}$ denote the set of declared demand choices of the LAs: $\hat{\theta} = \{\hat{\theta}_i^j \langle \hat{P}_i^j, \hat{U}_i^j \rangle | \ \forall i \in \{1..N\} \ \& \ j \in \{1..M\}\}$, where $\hat{\theta}_i^j$ represents the j^{th} cumulative demand choice of the i^{th} aggregator LA_i. Additionally, $\hat{\theta}_{-i}$ is used to denote the set of cumulative demand choices of all LAs except LA_i. Given, i) the $\hat{\theta}$ values, ii) the available power levels PL, and iii) the DPA algorithm, VCG-EP proposes the following payoff amount (denoted by

π_i) for each load aggregator LA_i:

$$\pi_i\big(\text{DPA}(\hat{\theta}, PL)\big) = \rho * (h_i - g_i) \tag{3.2}$$

where,

$$h_i = \sum_{\substack{\forall a_j \in a, \\ a \leftarrow \text{DPA}(\hat{\theta}_{-i}, PL)}} \hat{U}_j^{a_j} \tag{3.3}$$

$$g_i = \sum_{\substack{\forall a_j \in a \ \& \ j \neq i, \\ a \leftarrow \text{DPA}(\hat{\theta}, PL)}} \hat{U}_j^{a_j} \tag{3.4}$$

In equation 3.2, ρ is the proportionality constant designated by the EDCo; ρ is the same constant used to define the tariff rates associated with the urgency classes (refer Section 3.1). In equations 3.2 and 3.3, the term h_i refers to the maximum aggregate utility (max_util) returned by DPA (refer algorithm 1) in a scenario where LA_i is not considered as part of the system. Hence in equation 3.3, $\hat{\theta}_{-i}$ has been used to denote the list of declared choices at the input of algorithm DPA. Given the set $a = \{a_1 \dots a_{i-1}, a_{i+1} \dots a_N\}$ of chosen power allocation levels by DPA, $\hat{U}_j^{a_j}$ represents the utility value for LA_j, corresponding to a selected choice a_j ($\in a$). Unlike h_i, the term g_i (in equations 3.2 and 3.4) refers to the maximum aggregate utility acquired by the system when LA_i is included as part of the system but its utility contribution is ignored. Hence in equation 3.4, $\hat{\theta}$ is used as input to algorithm DPA and $\hat{U}_i^{a_i}$ is not included in the summation. Referring algorithm 1, g_i can also be expressed as: $g_i = max\_util - \hat{U}_i^{a_i}$. Intuitively, π_i represents the aggregate reduction in utility suffered by all LAs (except LA_i) due to the power allocated to LA_i.

The procedure *VCG-based Equitable Pricing (VCG-EP)* for calculating the payments (π_1, $\pi_2 \dots$ π_N) of all load aggregators is given in algorithm 2. The algorithm iterates over all N LAs and determines the appropriate payment to be made to the EDCo by the LAs using equation 3.2.

Algorithm 2 VCG based Equitable Pricing (VCG-EP)

Input:
a) The declared choices $\hat{\theta}\langle \hat{P}_i^j, \hat{U}_i^j \rangle$, $\forall i, j$
b) The power allocation levels PL
c) The optimal algorithm DPA.
Output:
a) The payments $\pi_1, \pi_2 \ldots \pi_N$

1: Obtain max_util, $\{a_1 ... a_N\} \leftarrow$ DPA($\hat{\theta}$, PL)
2: **for** i from 1 to N **do**
3: Obtain $h_i \leftarrow$ DPA($\hat{\theta}_{-i}$, PL)
4: Compute $g_i = max\_util - \hat{U}_i^{a_i}$
5: **if** a_i = -1 **then** $\pi_i = 0$ **else** $\pi_i = h_i$ - g_i

3.2.2.1 Complexity Analysis of VCG-EP

Given, N LAs, M demand choices for each load aggregator, and PL power levels, the computational complexity of the proposed algorithm VCG-EP is analysed as follows. Step 1 involves invoking Algorithm 1 (DPA), whose complexity is given as $\mathcal{O}(N*M*PL)$. Steps 2 to 5 computes the payments for each of the N LAs. For each LA, steps 3 to 5 are executed. Although, steps 4 and 5 can be considered as operations with constant computation times ($\mathcal{O}(1)$), step 3 involves invoking algorithm DPA, whose worst case complexity is given as $\mathcal{O}(N * M * PL)$. With the above analysis, the overall worst case complexity can be determined as $\mathcal{O}(N^2 * M * PL)$. Our experimental results show that for $N = 25$ load aggregators, each having $M = 5$ demand choices and for $PL = 2000$ power levels (i.e., $20MW$ at power resolution $pu = 10kW$), the execution time taken by VCG-EP is about ∼30 secs.

Theorem *Given DPA the optimal demand choice allocation strategy, the payoff function π_i (equation 3.2) ensures that an aggregator LA_i can never earn a profit through deceitful inflation of its demand choices, for a stipulated set of demand choices of all other aggregators.*

Proof: Let us assume that DPA selects the j^{th} choice ($\theta_i^j \langle P_i^j, U_i^j \rangle$) for LA_i, when all LAs (including LA_i) report their choices truthfully. Similarly, let $\hat{\theta}_i^k \langle \hat{P}_i^k, \hat{U}_i^k \rangle$ denote the

k^{th} demand choice for LA_i, selected in the scenario when LA_i reports deceitfully inflated demand choices. Without loss of generality, let $\hat{P}_i^k = P_i^j + \Delta P$ and $\hat{U}_i^k = U_i^j + \Delta U$, where ΔP and ΔU are appropriate real positive quantities. That is, LA_i attempts to acquire ΔP additional power by inflating the actual utility for ΔP and declaring it to be ΔU. Let, VCG-EP declare the payment $\pi_i' = \rho * (h_i - g_i')$ for P_i^j and $\pi_i = \rho * (h_i - g_i)$ for $P_i^j + \Delta P$.

It may be noted from equation 3.3 that, the term h_i (in π_i' and π_i) represents the maximum aggregate utility obtained by not considering LA_i as part of the system. As the demand choices of the other LAs do not change irrespective of whether LA_i is truthful or deceitful, h_i remains same in the expressions of both π_i and π_i'. LA_i pays $\Delta\pi_i = \rho * (\pi_i - \pi_i') = \rho * (g_i' - g_i)$ for the additional power ΔP. Following equation 3.4 it may be noted that, g_i' (g_i) denotes the maximum total utility of all the LAs barring LA_i, in the scenario when LA_i is truthful (deceitful). Hence, g_i' is strictly greater than g_i. Additionally, as $\Delta\pi_i$ is derived through our optimal allocation strategy DPA, $\Delta\pi_i$ may be considered to be the actual payoff for ΔP.

Therefore, the actual revenue that LA_i may possibly earn by distributing the unjustly obtained power ΔP among its consumers, can never be greater than its payoff $\Delta\pi_i$. Thus, LA_i can never earn a profit through deceitful inflation of its demands, and this enforces truthfulness in the system.

3.2.3 Example (continued...)

Following the example scenario as presented in Subsection 3.1.1, we analyse the power allocations suggested by DPA and the payments computed by VCG-EP, under Scenario I (both LA_1 and LA_2 report truthfully) and Scenario II (LA_2 reports its inflates demand choices), as shown in Table 3.1. The LAs' cumulative demand choices are given in rows 1 and 2 of this table (refer, demand choice calculations in Subsection 3.1.1). The available power P (= 15 units) remain the same for both the scenarios. Without loss of generality, the proportionality constant ρ is considered as unity. Thus, the utility values associated with the power demands represent the revenues earned by the LAs and the

Table 3.1: *LA_2 deceitfully reports its demand choices*

	Scenario I	**Scenario II**
LA_1	$\theta_1^1\langle 3,9\rangle$, $\theta_1^2\langle 8,19\rangle$, $\theta_1^3\langle 15,26\rangle$	$\theta_1^1\langle 3,9\rangle$, $\theta_1^2\langle 8,19\rangle$, $\theta_1^3\langle 15,26\rangle$
LA_2	$\theta_2^1\langle 2,6\rangle$, $\theta_2^2\langle 7,16\rangle$, $\theta_2^3\langle 15,24\rangle$	$\hat{\theta}_2^1\langle 2,6\rangle$, $\hat{\theta}_2^2\langle 12,26\rangle$, $\hat{\theta}_2^3\langle 15,29\rangle$
DPA	Obtains $max\_util = 35$, selects $\theta_1^2\langle 8,19\rangle$ & $\theta_2^2\langle 7,16\rangle$	Obtains $max\_util = 35$, selects $\theta_1^1\langle 3,9\rangle$ & $\hat{\theta}_2^2\langle 12,26\rangle$
VCG-EP	$\pi_1 = \$8$, $\pi_2 = \$7$	$\pi_1 = \$3$, $\pi_2 = \$17$

payoffs determined by VCG-EP are directly derived from these advertised utilities. Row 3 of the table shows the obtained allocations (the demand choices selected by DPA) and the maximum total utility (max_util obtained by DPA) obtained by the system. Row 4 of this table shows the the payoffs (π_1 and π_2) computed by VCG-EP, for both the scenarios.

It may be noted from Scenario II that, LA_2 deceitfully inflates its second demand choice ($\theta_2^2\langle 7,16\rangle$) to $\hat{\theta}_2^2\langle 12,26\rangle$, by promoting 5 units of power from the lower urgency class c_3 (whose actual utility/tariff is $\mu_3 = 1$) to urgency class c_2 (whose utility/tariff is $\mu_2 = 2$). As a result, the choices selected by our optimal strategy DPA, change from $\theta_1^2\langle 8,19\rangle$ (in Scenario I) to $\theta_1^1\langle 3,9\rangle$ (in Scenario II) for LA_1 and, $\theta_2^2\langle 7,16\rangle$ (in Scenario I) to $\hat{\theta}_2^2\langle 12,26\rangle$ (in Scenario II) for LA_2. Correspondingly, the payoffs for the selected demand choices as computed by VCG-EP, change from \$8 (in Scenario I) to \$3 (in Scenario II) for LA_1 and, \$7 (in Scenario I) to \$17 (in Scenario II) for LA_2. It may be observed that, LA_2 pays an additional $\Delta\pi_2 = \$10$ for the deceitfully acquired $\Delta P = 5$ units of additional power. However, as ΔP will actually be distributed to appliances in class c_3 (whose tariff/utility value is $\mu = 1$) the revenue that LA_2 may actually obtain by selling ΔP is only \$5. Thus, in accordance with the claim made in the above theorem, by using the proposed payoff strategy VCG-EP, LA_2 incurs a loss of \$5 for being deceitful.

Table 3.2: *Categorization of common appliances equipped within households/establishments*

Category	Common appliances with energy consumption (in watts)
Cat-1	lights (100), ceiling fans (100), security cameras (100), projectors (300) and monitors (200)
Cat-2	desktops (300), laptops (100), water pumps (1000), projectors (300) and audio system (200)
Cat-3	air purifiers (300), humidifiers (300), dehumidifiers (300), ACs (1000) and heaters (1000)
Cat-4	printers (500), television (500), rice cookers (200), water purifiers (200), vacuum cleaners (200) and coffee makers (1000)
Cat-5	dishwashers (1000), washing machines (500), microwaves (1000), kettles (1000) and refrigerators (500)

3.3 Experimental Results

We have extensively evaluated the performance of the proposed optimal allocation strategy namely, *Dynamic Programming based Power Allocator* (DPA) and the pricing mechanism namely, *VCG based Equitable Pricing* (VCG-EP), by conducting experiments on empirically generated random microgrid scenarios. These random scenarios are generated by using a data generation framework, which is discussed next.

3.3.1 Data Generation Framework

Following the system model presented in Section 3.1, various random microgrid scenarios have been generated by systematically varying, **a)** the number of load aggregators (N) as 10, 15, 20 and 25, and **b)** the available power (P) as 5MW, 10MW, 15MW, 20MW. The discretizing parameter (pu) that defines the power allocation levels (PL) has been considered to be pu = 10kW. The households/establishments within any mi-

crogrid are classified into five different types and this classification is based on total power consumption. The bounds on total power demand for these five different types are as follows: Type I $\leq$ 2kW, Type II {$>$ 2 and $\leq$ 4}kW, Type III {$>$ 4 and $\leq$ 6}kW, Type IV {$>$ 6 and $\leq$ 8}kW, Type V {$>$ 8 and $\leq$ 10}kW. The number of households within any microgrid is randomly chosen from a uniform distribution within the range 500 to 1000. Each household is randomly assigned one of the types mentioned above. We assume that these households are equipped with a set of commonly used appliances, as shown in table 3.2. This table also shows the empirical categorization of appliances into five different classes (viz. Cat-1, Cat-2, Cat-3, Cat-4 and Cat-5), based on their relative urgency. Cat-1 appliances are of the highest priority in terms of urgency towards uninterrupted power supply. Cat-2 to Cat-5 are of progressively lower priorities. Given the type of a household (lower and upper limit on power consumption), each household is randomly assigned multiple instances of appliances listed in the table, such that the total power consumption of the household lies within the upper and lower limits. The system is assumed to acquire an utility value μ_1=10 per unit of power, when the total demand of Cat-1 appliances is satisfied. Similarly, the utilities corresponding to the remaining categories Cat-2 to Cat-5 are assigned with monotonically decreasing values, μ_2=8, μ_3=6, μ_4=4 and μ_5=2, respectively. The revenue earned by a microgrid for satisfying the aggregate demand of a category is considered to be proportional to its total utility. We have assumed $\rho = 0.5$ as the value of the proportionality constant. Given, the aggregate demands and the associated utility values corresponding to the five categories of appliances, a load aggregator consolidates them into five demand choices (cumulative demands and its associated utility values), which are forwarded to the EDCo.

3.3.2 Results

Experiments have been conducted on random scenarios generated through the data generation framework discussed above, and the results for the proposed algorithms namely, DPA and VCG-EP have been obtained. All the plots shown in the results represent the mean over 50 distinct random scenarios. The performance metrics used for evaluation

of the proposed algorithms are as follows.

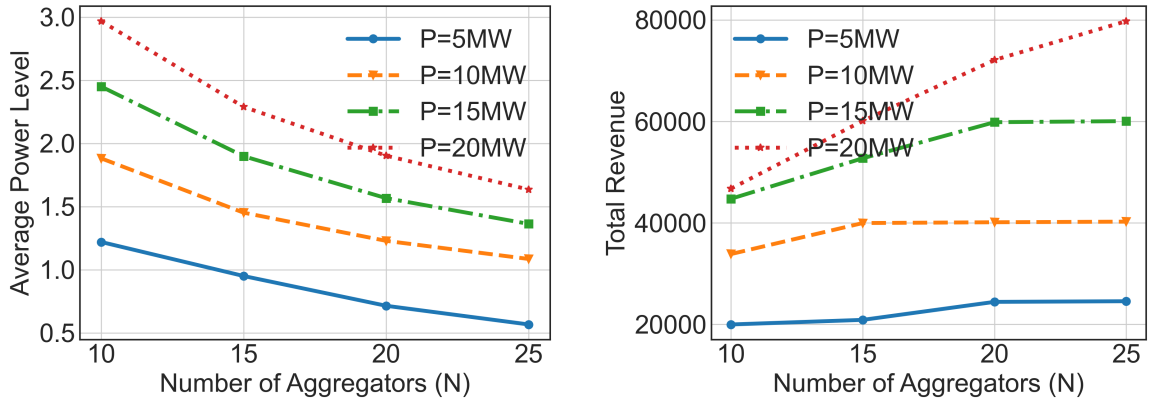

(a) #LAs vs Average Power Level

(b) #LAs vs Total Revenue

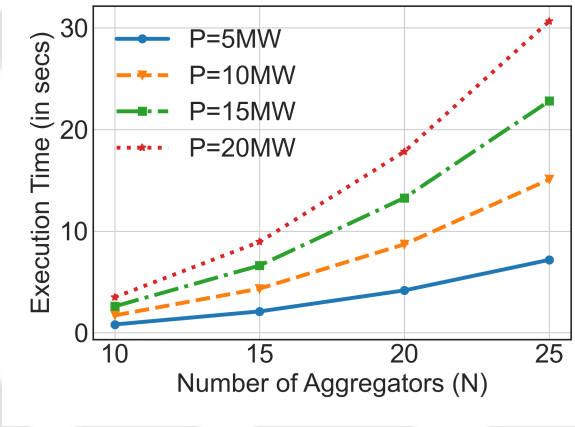

(c) #LAs vs Execution Time

Figure 3.1: *Compilation of the results for different number of aggregators (N) and distinct values of available power (P)*

- the *average power allocation level*, calculated as the mean of the power allocation level (index of the selected demand choice) over all the LAs, selected by DPA.
- the *total revenue* earned by the EDCo, calculated as the sum of the payoffs determined by applying VCG-EP.
- the *execution times* (in seconds), taken by VCG-EP to generate solutions.

Figure 3.1(a) depicts the data points for the average power level allocated to an LA

by the proposed allocation algorithm DPA, as the number of LAs (N) is varied from 10 to 25. The curves shown in this figure correspond to four distinct scenarios of available power P ={5MW, 10MW, 15MW, 20MW}. It may be observed from the figure that, the average power level that may be allocated to an LA decreases with increase in the number of aggregators, for a fixed value of available power (P). This is expected because, with the same amount of power being distributed among a higher number aggregators, it is more likely that the appliance demands corresponding to a fewer number of urgency classes can be satisfied, on average. Again as is obvious, as available power increases, the average power level also increases.

Figure 3.1(b) shows the plots for the total revenue obtained by the EDCo, as the number of LAs (N) is varied from 10 to 25. The plot curves shown in this figure correspond to four distinct values of available power P (={5MW, 10MW, 15MW, 20MW}). It may be observed from the figure that, in all the different scenarios of available power the total revenue increases or atleast remains the same, as the number of aggregators become higher. This is because, with more number of aggregators participating in the power allocation procedure, DPA is more likely to select the demands corresponding to higher urgency classes across all the LAs. This results in an increase in the total utility that is achieved by the system. Since, the utilities are directly proportional to the LAs' payoffs, the total revenue also increases proportionately.

Figure 3.1(c) presents the plots for the execution times taken by the proposed payment mechanism namely VCG-EPC, as the number of LAs (N) is varied from 10 to 25 and the available power P is varied as P ={5MW, 10MW, 15MW and 20MW}. It may be observed from this figure that, the execution time steeply increases with increase in the number of aggregators, for any given value of P. This is mainly because, in order to determine the payoff corresponding to each one of the LAs, VCG-EP must recompute the maximum total utility of the system (h_i in equation 3.3) by barring the LA's demand choices under consideration. This necessitates additional overhead of calling the allocation procedure DPA once for each LA. It may also be observed from this figure that, the execution time also increases abruptly with increase in the available power. With

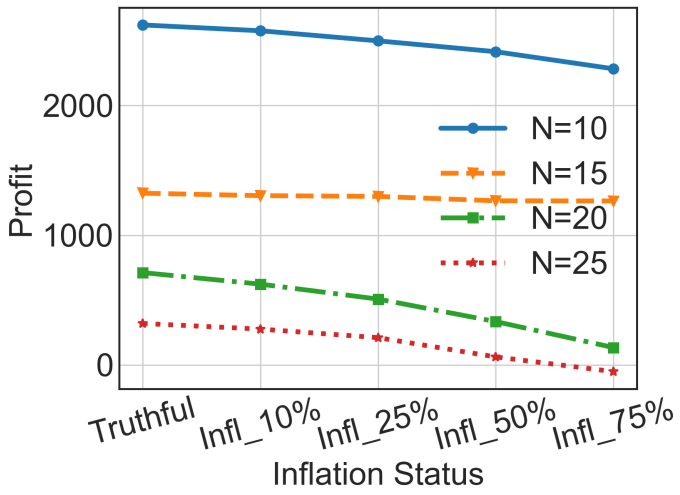

Figure 3.2: *Profits obtained by an LA, for varied inflations*

increase in available power, the number of power allocation levels PL ($=P/pu$) increases. With a higher number of power allocation levels, the number of subproblems that needs to be computed to obtain the optimal solution also increases, leading to higher execution times.

Figure 3.2 portrays the variation in average profits obtained by any given LA, when it report truthfully as well as when it is untruthful with different degrees of deceitful inflations on actual demand choices. For this experiment, we have generated scenarios with varying number of aggregators ($N = 10$, 15, 20 or 25), with the total available power P remaining same ($P = 20$MW) in all of them. For a given scenario with a fixed value of N, the demand choices for all classes of all LAs have been generated from a normal distribution with the same mean and standard deviation. This data set is considered as the true choices of the LAs. Given a data set, an LA is randomly selected (uniformly) and subjected to four different degrees of inflations ("Infl_10%", "Infl_25%", "Infl_50%" and "Infl_75%",) on actual demand choices. For example, a data set for "Infl_10%" is obtained by selecting the actual demand choices of all LAs except one randomly chosen LA. The aggregate demand of a certain class (say, Cat-2) for this LA is enhanced by promoting 10% of the aggregate demand of its immediately lower urgency class (Cat-3)

to Cat-2. In effect, the cumulative demand choices of Cat-3 and all higher urgency classes get transformed.

It may be observed from figure 3.2 that, the average profit obtained by an LA is maximal when it reports its actual choices. Further, the profits decrease as the degree of deceitful inflations become higher. For example when N=20, the average profits (over 50 data sets) obtained by an LA reduces gradually from \$732 (truthful scenario) to \$640 ("Infl_10%"), \$534 ("Infl_25%"), \$351 ("Infl_50%") and \$146.0 ("Infl_75%"). It may be observed that, this trend directly follows Theorem 3.2.2.1, which states that the revenue generated for the additional power untruthfully acquired is always lower than the payoff determined by VCG-EP for that additional power. Moreover as discussed in Section 3.2.2, the LA's payoff (equation 3.2) is determined by the aggregate utility sacrificed by the other LAs, for the amount of power allocated to the LA. Therefore, higher the amount of power untruthfully acquired by an LA, higher becomes the aggregate utility sacrificed by the other LAs. Thus, the LA's payoff proportionally increases with the proportional increase in deceitfully acquired power. Consequently, the profit decreases with higher degrees of inflations.

3.4 Summary

In this chapter, we propose a novel DR framework that allows an EDCo to equitably distribute its available power among microgrids under its purview. Given the consolidated demand information from all the microgrid LAs, we propose an optimal allocation strategy called Dynamic Programming based Equitable Power Allocator (DPA) which attempts to maximize the total utility of the system. Further, to enforce truthful reporting of the consolidated demands by the LAs, we propose a novel pricing mechanism called VCG-based Equitable Pricing (VCG-EP). Results on various empirically generated microgrid scenarios show that, i) the EDCo benefits by achieving a desired system level goal (i.e., maximum total utility) while equitably distributing its available power and ii) the system attains stability as truthfulness becomes the preferred choice of action for a given set of rationally acting LAs. This is because the LAs' payoffs are minimal

(and profits are maximum) when they are truthful. In the next chapter, we deal with the problem of transient power shortage scenarios caused by dynamic power supply imbalances and propose near instantaneous power balancing strategies.

Chapter 4

Brownout-based Real-Time Power Distribution Strategies

In the last chapter, we have proposed a truthful pricing mechanism for equitably distributing an available power among a set of microgrids. Typically, truthful mechanism schemes such as the one proposed in Chapter 3 (VCG-EP together with DPA), involve multiple stakeholders and can be computationally complex. Therefore, they are applied for auctions in electricity markets that are conducted a day-ahead/week-ahead. However, the need for equitable distribution among multiple parties may be necessary in more transient and near real-time scenarios as well. Obviously in such cases, the scheme discussed in the previous chapter is not applicable.

In this chapter, we deal with the design of real-time brownout based power distribution mechanisms for handling power shortages in dynamic scenarios. For example, scenarios where grids may face transient power deficits due to sudden surges in demands and/or forecast errors related to renewable generation. We devise a comprehensive Demand Response (DR) based framework for brownout based electricity distribution/scheduling. The design of this framework is essentially inspired from models proposed for resource allocation strategies typically used for Quality of Service (QoS) oriented scheduling mechanisms for real–time applications. Being an online power allocation strategy that strives to mitigate dynamic imbalances between electricity supply and demand, the framework is guided by the following soft real-time specification, gov-

erned by recommendations of IEEE standards on Power Quality (IEEE Std 1159 [111]): *Brownout based mitigation of imbalances in demand-supply must be conducted quickly and within about* $\sim$0.5 *seconds (for a 50Hz power system) in order to maintain satisfactory power quality.*

The scheduling model considered in this work essentially boils down to a *Multiple Choice Knapsack Problem (MCKP)* formulation similar to [5]. However, the proposed optimal solution namely *Dynamic Programming (DP)* in [5] when applied to our scenario proves to be prohibitively expensive in terms of computational overheads. More specifically, conventional DP violates the above stated soft real-time requirement suggested by IEEE Std 1159. Therefore, we modified the *DP* algorithm and devised a new strategy known as *Streamlined DP-based Priority level Allocator (SDPA)*. It capitalizes on the discrete nature of the power allocation demands to work with a far lower number of non-dominating partial *DP*-solutions and allows the ultimate optimal solution to be generated much faster. In order to mitigate dynamic power imbalances in very large grids (where SDPA may fail to deliver a solution within the specified time bound), a fast and efficient heuristic strategy namely, the *Proportionally Balanced Priority level Allocator (PBPA)*, has been devised.

4.1 Related Work

The formulation of this work is based on resource allocation strategies typically used for QoS sensitive task execution in real-time systems. Brief summary of a few works related to QoS in real-time systems is presented as follows. An analytical model (called Q-RAM) for Quality of Service (QoS) management in large distributed systems was proposed by Rajkumar et al. in [67, 68, 96]. All these Q-RAM based schemes endeavor to meet application specific needs along multiple quality dimensions such as timeliness, reliable delivery schemes, data quality etc. In [5, 11], authors proposed a resource adaptation mechanism for real-time applications with multiple QoS-levels where each service-level has an associated resource demand and QoS based reward. For a system with limited computational resources, the objective is to judiciously multiplex available resources by

choosing an appropriate service-level for each application such that aggregate system level QoS is maximized. In [5], authors model the QoS optimization formulation as a *Multiple Choice Knapsack Problem (MCKP)* and propose a dynamic programming solution (henceforth referred to as *DP*) for the same. This *DP*-based solution although optimal, incurs high computational cost and is not applicable to carry out short term adjustments in resource allocations. Thus, they further propose a greedy heuristic algorithm (*HA*) which attempts to maximize the aggregate reward by locally adjusting the allocated QoS levels for handling handle transient load fluctuations. In this work, we compare the performance of our proposed algorithms viz. *SDPA* and *PBPA*, with the existing strategies namely, *DP* and *HA*.

4.2 System Model and Problem Formulation

The system considered in this work is modeled as a set of $\mathcal{N}$ subareas $S_1, S_2, ..., S_{\mathcal{N}}$, under the purview of a utility/electricity service provider as shown in Figure 4.1. Each subarea S_i in turn consists of a collection of establishments, where establishments may represent households, administrative buildings, business and industrial units, hospitals, schools, etc. Electrical appliances within establishments or the establishments themselves are then partitioned into a set of distinct equivalence priority classes, where the priority of an appliance/establishment is determined by its urgency towards uninterrupted power supply. Household appliances such as lights, fans and other basic conveniences may be considered *essential* and allocated the highest priority. Similarly, business critical establishments, hospitals, schools etc., may also be considered essential and assigned the highest priority. The remaining loads within a subarea fall under the broad class of non-essential loads and may consist of a variety of appliances including air conditioners, water heaters, PCs, TVs, washing machines, dish washers, etc. The utility further provides K_i priority levels $(l_i^1, l_i^2, ..., l_i^j, ..., l_i^{K_i})$ within each subarea S_i at various distinct tariff rates $(tar_i^1, tar_i^2, ..., tar_i^j, ..., tar_i^{K_i})$ for the non-essential loads, such that higher the priority, higher is the corresponding tariff. The priority of a level is inversely proportional to its level-id. That is, lower the level-id, higher is the priority and so, $j < j' \implies tar_i^j > tar_i^{j'}$.

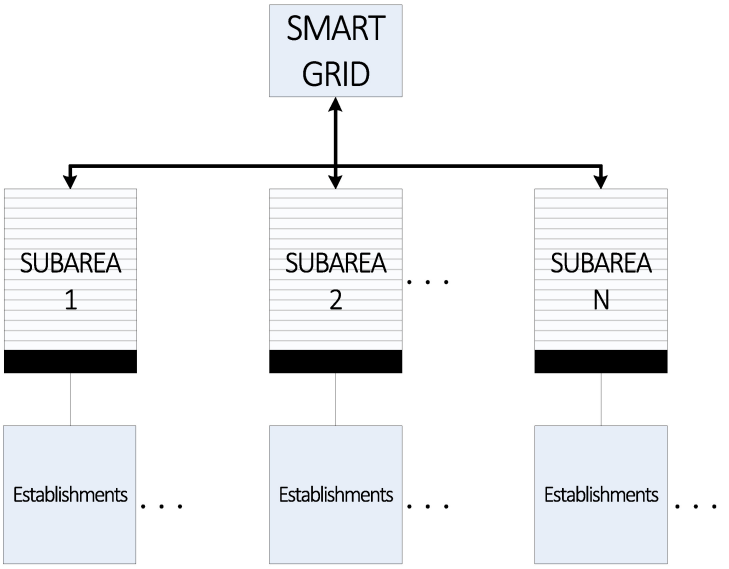

Figure 4.1: *System Model*

Thus, l_i^1 is the highest priority non-essential level and the tariff corresponding to that level is highest, for any subarea S_i. Similarly, $l_i^{K_i}$ denotes the lowest priority non-essential level and its tariff rate is the least among all non-essential levels, for any subarea S_i. A consumer may optionally choose any one of these priority levels for each of his non-essential loads/appliances. Thus essentially, the loads within subarea S_i get divided into $K_i + 1$ disjoint subgroups, one of which (l_i^0) corresponds to the class of essential loads, while the remaining K_i contain all the non-essential loads.

Let, p_i^0 denote the total power demand and r_i^0 denote the overall reward earned (by satisfying the demand p_i^0) corresponding l_i^0 , which comprises of all essential loads in S_i. Corresponding to the non-essential loads, let p_i^j represent the aggregate curtailable/non-essential power demand of all loads/appliances contained in priority levels 1 through j. The total reward value (r_i^j) corresponding to the non-essential loads, at the j^{th} level is then given by:

$$r_i^j = \sum_{j'=1}^{j} tar_i^{j'} \times (p_i^{j'} - p_i^{j'-1}) \tag{4.1}$$

During transient power deficits, the total quantity of power P supplied by the utility

drops below the total demand for power. Obviously, in such a situation, rolling blackouts can be avoided only if P is higher than the total essential/critical power demand ($\sum_{i=1}^{\mathcal{N}} p_i^0$). After satisfying this total essential power demand, a revenue aware allocation/distribution of the residual power P_R ($= P - \sum_{i=1}^{\mathcal{N}} p_i^0$) among the subareas is done, so that reward to the utility is maximized.

$$\text{maximize} \sum_{i=1}^{\mathcal{N}} \sum_{j=1}^{K_i} r_i^j * x_i^j \tag{4.2a}$$

$$\text{subject to} \sum_{i=1}^{\mathcal{N}} \sum_{j=1}^{K_i} p_i^j * x_i^j \leq P_R \tag{4.2b}$$

$$\sum_{j=1}^{K_i} x_i^j \leq 1, \forall i \in [1, \mathcal{N}], x_i^j \in \{0, 1\} \tag{4.2c}$$

Equation 4.2 represents a formal *Integer Linear Programming (ILP)* formulation to the above reward maximization problem. In the equation, x_i^j is a binary decision variable which is set to 1 ($x_i^j = 1$) if subarea S_i is allocated power at level l_i^j. The first constraint in equation 4.2b guarantees that the total amount of power allocated to all subareas do not surpass the total residual power (P_R) available with the utility for non-essential loads. The second constraint as given in equation 4.2c forces each subarea to select at most one priority level.

4.2.1 Example 1

Consider a very small hypothetical smartgrid, where the utility has to distribute an available amount of power $P = 41$ among three subareas S_1, S_2 and S_3. While S_1 and S_2 have 3 priority levels each, S_3 has 2 priority levels. The power and reward values $\langle p_i^j, r_i^j \rangle$ corresponding to each priority level (l_i^j), for all subareas, are given as follows:

$S_1 : \{l_1^0\langle 2, 0\rangle, l_1^1\langle 5, 13\rangle, l_1^2\langle 7, 16\rangle\}$,

$S_2 : \{l_2^0\langle 6, 0\rangle, l_2^1\langle 14, 9\rangle, l_2^2\langle 18, 16\rangle\}$ and

$S_3 : \{l_3^0\langle 7, 0\rangle, l_3^1\langle 19, 19\rangle\}$.

The total essential power demand of all the subareas is 15 (i.e., $2+6+7$). As a socio-

economic fairness measure the system first satisfies the total essential power demand over all subareas. The remaining power P_R $(= 41 - 15 = 26)$ is then used to satisfy the non-essential power demands of the subareas. The number of non-essential priority levels (K_i) of S_1, S_2 and S_3 are $K_1 = 2$, $K_2 = 2$ and $K_3 = 1$. Hence, the optimization problem for the given scenario boils down to:

$$\text{maximize} \sum_{j=1}^{2} r_1^j * x_1^j + \sum_{j=1}^{2} r_2^j * x_2^j + \sum_{j=1}^{1} r_3^j * x_3^j$$

$$\text{subject to} \sum_{j=1}^{2} p_1^j * x_1^j + \sum_{j=1}^{2} p_2^j * x_2^j + \sum_{j=1}^{2} p_3^j * x_3^j \leq 26$$

$$\sum_{j=1}^{2} x_1^j \leq 1, \quad \sum_{j=1}^{2} x_2^j \leq 1, \quad x_3^1 \leq 1, \quad x_i^j \in \{0, 1\}$$

4.3 Dynamic Programming Based Priority level Allocator (DP)

In the above subsection, we formulated the priority level selection/power allocation strategy as an *Integer Linear Programming (ILP)* problem. However, it is well known that although an *ILP* provides optimal solutions, it is inherently exponential in nature and is poor in terms of scalability. A closer look reveals that the scheduling problem has an optimal substructure. Hence, the optimal solution may be obtained as a composition of the optimal solutions to a set of its sub-problems and therefore, *Dynamic Programming (DP)* provides a natural solution mechanism. This makes it possible to obtain optimal solutions with execution times which are pseudo-polynomial in the number of potential power allocation levels (PL). *DP* is essentially an optimization procedure and the problem definition in equation 4.2 can be represented by the following recursive formulation [5]:

$$R(i, \varrho) = \begin{cases} 0, \quad if\ (i = 0)\ or\ (\varrho = 0) \\ \max\limits_{j} \{R(i-1, \varrho), r_i^j + R(i-1, \varrho - p_i^j)\}, \\ \qquad\qquad \forall j \in \{1, K_i\}, \varrho \geq p_i^j \end{cases} \tag{4.3}$$

The description of the variables used in the above equation is given in Table 4.1.

Table 4.1: *Notations*

Variable	Explanation
i	Index for subarea
j	Index for priority level
ϱ	Index for upper bound on power level
$\mathcal{N}$	Number of subareas
P_R	Available residual power
pu	Power allocation step size
PL	Total number of available power allocation levels at power resolution pu
K_i	Number of priority levels available for i^{th} subarea
L	Upper bound on the number of priority levels corresponding to a subarea i.e., $L = \mathbf{max}\{K_1, ..., K_{\mathcal{N}}\}$
p_i^j	Power level for the i^{th} subarea at the j^{th} priority level
r_i^j	Reward obtained by i^{th} subarea at the j^{th} priority level
ψ_i	List of distinct partial optimal solutions considering atmost i subareas
ϕ_{ij}	List of distinct partial solutions considering upto i subareas, but restricting the i^{th} subarea to operate only at its j^{th} priority level
β_{in}	The n^{th} node of ψ_i
δ_{ijn}	The n^{th} node of ϕ_{ij}
$\beta_{in}{\rightarrow}p$	The bound on power level for the n^{th} node in ψ_i
$\beta_{in}{\rightarrow}r$	The reward corresponding to the n^{th} node in ψ_i
$\beta_{in}{\rightarrow}EPL$	List of selected priority levels for the subarea $S_1, S_2, \ldots, S_i$ corresponding to the n^{th} node of solution ψ_i

The solution procedure is typically a multi-step decision process which iterates over all subareas, priority levels and power allocation levels. The power allocation levels are defined as the number of *discretely quantified power allocation units* considered (pu) given the total available power P_R (pu defines the smallest unit of power that can be assigned to any subarea; used to denote the difference between any two consecutive power allocation levels that may be considered in the problem). The total number of power allocation levels (PL) is calculated as: $PL = P_R/pu$

It may be observed from equation 4.3 that the dynamic programming algorithm

returns a reward value $R(i, \varrho)$ in each recursive call which represents the optimal solution to the sub-problem that considers atmost i subareas $(S_1, S_2, \ldots, S_i)$ and atmost ϱ power allocation levels among the total PL available levels. The optimal reward value $R(i, \varrho)$ depends on the priority level selected for the i^{th} subarea. Hence, for each priority level, DP checks the optimal aggregate reward obtained by $i-1$ subareas when the total power allocated to them is upper bounded by $(\varrho - p_i^j)$. To obtain the optimal reward $R(i, \varrho)$, DP selects that priority level $j \in \{1, K_i\}$ for the i^{th} subarea which fetches the highest reward. The performance of the algorithm has been enhanced by using a technique called *memoization*. Memoization is a special kind of caching, where the partial optimal solution obtained for a sub-problem is stored in the memory so that repetitive computation of the solution to the same sub-problem may be avoided. All such partial solutions are memoized as they are used to obtain further partial optimal solutions in later stages and finally, the overall optimal solution is obtained.

The computational complexity of DP is $O(\mathcal{N} * L * PL)$, where $\mathcal{N}$ is number of subareas, L $(=\mathbf{max}\{K_1, K_2, \ldots K_\mathcal{N}\})$ is an upper bound on the number of priority levels corresponding to a subarea and PL denotes the number of *discretely quantified power allocation levels* considered, given the total available power P_R and power resolution pu. Our experimental results show that, given 50 subareas with 10 priority levels per subarea and with 250 MW of available power at power resolution pu $(= 1kW)$, DP takes ∼13 secs on average to generate a solution on a 3.2 GHz computing core. Clearly, this overhead is significantly high to be useful for distributing available power among subareas in real-time.

However, as discussed before, the optimization problem is inherently discrete in nature. Thus, we do not obtain continuous improvements in rewards of a subarea with each incremental power allocation to it. Rather, improvements in reward has a step-wise nature with (K_i) steps corresponding to each subarea S_i. Now typically, $K_i << PL$ and consequently, a majority of the optimal solutions $R(i, \varrho)$ do not return distinct values. As a result, the generic dynamic programming algorithm which memoizes all partial solutions for each distinct value of i and ϱ, may suffer from high and unnecessary com-

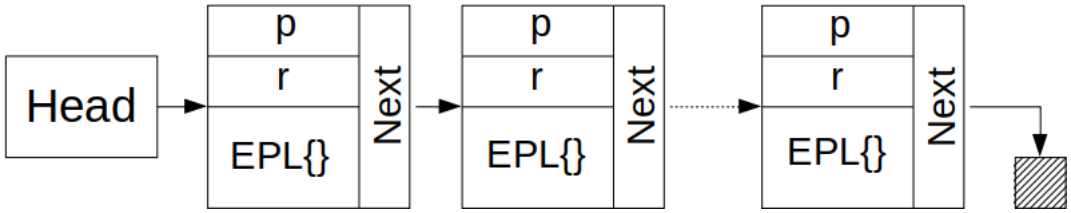

Figure 4.2: *General structure of lists ψ_i or any list in Φ*

putational overheads. This overhead may be reduced (often drastically) through a more efficient implementation which memoizes only those partial optimal solutions which provide distinct enhancements in reward with increment in the bound on power ϱ, for each value of i. Further, it may be observed that this reduced memoization does not cause solution optimality to be compromised. Now we propose such an efficient and optimal solution strategy.

4.4 Streamlined DP-based Priority Level Allocator (SDPA)

In this section, we present the *Streamlined Dynamic Programming based Priority Level Allocator (SDPA)*. Before describing the algorithm in detail, we first discuss the major data structures used by *SDPA*. The textual description of the data structures and the algorithm has been supported by a running example using the scenario presented in Example 1 (Section 4.2.1). Figure 4.3 depicts snapshots of the states of the data structures at a few important stages, as the algorithm is run over this example scenario.

4.4.1 Data Structure

The principal data structure used by the *SDPA* algorithm is a set of linked lists, each of which contains partial optimal solutions. The general structure of these linked lists is shown figure 4.2. Each node within any of the linked lists represents a partial optimal solution and consists of the following fields: **(a)** bound on maximum usable power (p), **(b)** obtained reward (r), **(c)** An enumeration/list of selected priority levels for the subareas in the solution (EPL). Similar to *DP*, the algorithm iterates over the $\mathcal{N}$ subareas

Figure 4.3: *Iterative steps of SDPA*

producing the final optimal solution after all subareas have been considered.

At the beginning of the i^{th} iteration, *SDPA* inherits the linked list ψ_{i-1} from the $(i-1)^{th}$ iteration. ψ_{i-1} contains the list of distinct partial optimal solutions corresponding to the sub-problem considering atmost $(i-1)$ subareas $\{S_1, S_2, \ldots, S_{i-1}\}$. The n^{th} node of ψ_i is denoted by β_{in}. For example, from figure 4.3 we see that for iteration $i = 2$, *SDPA* inherits the linked list ψ_1 containing three partial solutions (β_{10}, β_{11} and β_{12}), from iteration $i = 1$. Further, information corresponding to the 2^{nd} partial solution (β_{12}) of ψ_1 may be read as, '*considering only the* 1^{st} *subarea, when the bound on usable power is* $\beta_{12}{\rightarrow}p = 5$*, a maximum reward of* $\beta_{12}{\rightarrow}r = 13$ *is obtained by selecting subarea* S_1 *at priority level* 1*, as indicated by the array* $\beta_{12}{\rightarrow}EPL = \{1, \_, \_\}$'.

During the i^{th} iteration, *SDPA* builds a set of linked lists $\Phi_i = \{\phi_{ij} \mid j \in \{1 \ldots K_i\}\}$, where K_i is the number of priority levels available for the i^{th} subarea. Any linked list

ϕ_{ij} in Φ_i contains partial solutions considering upto i subareas, but restricting the i^{th} subarea to operate only at its j^{th} priority level. The n^{th} node of ϕ_{ij} is denoted by δ_{ijn}. For example, from figure 4.3 we see that for iteration $i = 2$, *SDPA* builds three linked lists ϕ_{20}, ϕ_{21} and ϕ_{22}. The partial solutions (nodes) within the linked list ϕ_{21} are obtained by considering subareas S_1 and S_2, but restricting the subarea S_2 to operate only at its 1^{st} priority level. Referring figure 4.3 again, the solution corresponding to the 2^{nd} node (δ_{212}) of ϕ_{21} is obtained by combining the solution for the second node (β_{12}) of ψ_1 with the power and reward values for the 1^{st} priority level of subarea S_2. Hence, the solution for this node becomes: ($\delta_{212}{\rightarrow}p = 14 + 5 = 19$, $\delta_{212}{\rightarrow}r = 13 + 9 = 22$, $\delta_{212}{\rightarrow}EPL = \{1, 1, \_\}$). While combining, only those partial solutions (δ_{ijn}) for which the total power (p) consumed by the subareas in the solution is atmost the maximum available power (PL), are considered feasible and retained. The rest of the solutions are discarded and not accommodated in the linked-lists Φ_i.

Finally, at the end of the i^{th} iteration, *SDPA* merges the linked lists within Φ_i and constructs a single linked list ψ_i, which consists of partial optimal solutions considering upto subareas $\{S_1, \ldots S_i\}$. It may be noted that the nodes in any of the linked lists follow a strict ordering based on the values of its attributes $'r'$ and $'p'$. For the linked list ψ_i say, any two consecutive nodes always satisfy the following two constraints: (i) $\beta_{in}{\rightarrow}p < \beta_{i(n+1)}{\rightarrow}p$, (ii) $\beta_{in}{\rightarrow}r < \beta_{i(n+1)}{\rightarrow}r$. That is, all linked lists store only the non-dominating solutions and discard the rest. For example, it may be observed from figure 4.3 that, there are a total of 9 nodes within the linked lists ϕ_{20}, ϕ_{21} and ϕ_{22} corresponding to iteration $i = 2$, but the merged list ψ_2 contains only 7 nodes. Two nodes (δ_{211} in ϕ_{21} and δ_{221} in ϕ_{22}) gets discarded as their inclusion leads to the violation of the above non-dominance constraints.

Definition: A set of partial optimal solutions $\psi_1, \psi_2, \ldots$ chosen from a set of partial solutions $\delta_1, \delta_2, \ldots$ are said to be non-dominating solutions if there does not exist a δ_i for a ψ_j such that, $\delta_i \rightarrow p \leq \psi_i \rightarrow p$ and $\delta_i \rightarrow r > \psi_i \rightarrow r$.

Algorithm 3 Streamlined DP based Priority level Allocator (SDPA)

Input:
Number of Subareas $\mathcal{N}$,
Number of power levels $PL{=}\lfloor \frac{P_R}{pu} \rfloor$,
Number of priority levels K_i in S_i $\forall i$,
Power p_i^j and corresponding reward r_i^j $\forall i \in \mathcal{N},\ j \in K_i$
Output:
Allocated priority level for each Subarea

1: Initial solution list ψ_0 has a single node β_{00} with,
(i) $\beta_{00}{\rightarrow}p = 0$, (ii) $\beta_{00}{\rightarrow}r = 0$ and (iii) $\beta_{00}{\rightarrow}EPL = \{\dots\}$
2: **for** i from 1 to $\mathcal{N}$ **do** ▷ Loop over all Subareas
3: $\phi_{i0}{=}\ \psi_{i-1}$; $G = |\psi_{i-1}|$ ▷ Let G denote #nodes in ψ_{i-1}
4: **for** j from 1 to K_i **do** ▷ Loop over all priority levels of each subarea
5: **for** n from 1 to G **do** ▷ Loop over nodes of ψ_{i-1}
6: $\delta_{ijn}{\rightarrow}p = \beta_{(i-1)n}{\rightarrow}p + p_i^j$
7: **if** $\delta_{ijn}{\rightarrow}p > PL$ **then**
8: **Break** (Go to step 4)
9: $\delta_{ijn}{\rightarrow}r = \psi_{(i-1)n}{\rightarrow}r + r_i^j$
10: $\delta_{ijn}{\rightarrow}EPL = \psi_{(i-1)n}{\rightarrow}EPL \bigcup \{j\}$
11: Enqueue the node δ_{ijn} into ϕ_{ij}
12: ψ_i = **Merge** $\left(\phi_{i0}, \phi_{i1}, \dots, \phi_{iK_i}\right)$

4.4.2 Detailed Algorithm

The *Streamlined Dynamic Programming based Priority Level Allocator (SDPA)* strategy is an iterative algorithm which memoizes only those partial optimal solutions which provide distinct enhancements in reward. A step wise description of the *Streamlined DP-based Priority level Allocator (SDPA)* is presented in Algorithm 3. In step 1, the algorithm initializes the partial solution with a single node (β_{00}) considering zero subareas and zero reward. For example, this initialization step creates the linked list ψ_0 with one node β_{00} as shown in figure 4.3. Then from steps 2 to 12, the *SDPA* strategy iteratively builds the final optimal solution. In the i^{th} iteration (step 2), the algorithm includes one extra subarea S_i to the sub-problem and builds a set of partial optimal solutions $\Phi_i = \left\{\phi_{ij}\ \forall j \in [1, K_i]\right\}$ from ψ_{i-1} (refer steps 3 to 11). In step 3, ϕ_{i0} is obtained by

assigning the linked list ψ_{i-1} and this preserves the solutions obtained in the previous iteration $(i-1)$. The nested for loops in steps 4 to 11 and steps 5 to 11 generates the partial optimal solutions ϕ_{ij} by including the i^{th} subarea at the j^{th} priority level with the partial solution ψ_{i-1}. For example, the second node δ_{212} of ϕ_{21} (refer figure 4.3) is generated by combining the second node β_{12} of ψ_1 with $l_2^1\langle 14, 19\rangle$. The n^{th} iteration of the inner loop (in lines 5 to 11) populates the field $\delta_{ijn}{\rightarrow}p$ with the sum of p_i^j (power level of the i^{th} subarea at the j^{th} priority level) and $\beta_{(i-1)n}{\rightarrow}p$ (step 6). If this aggregate power demand $\delta_{ijn}{\rightarrow}p$ results in an overload ($\delta_{ijp}{\rightarrow}p > PL$), such overloads will also happen for subsequent values of n, as ψ_{i-1} is sorted in strictly increasing order of p and r. Hence in this situation, the control breaks out from the inner loop and goes back to step 4 and no further nodes are enqueued into the solution list ϕ_{ij}. In the example, while attempting to combine the power demand 19 of l_3^1 with the power value 19 of β_{24}, the aggregate utilized power of the node δ_{314} becomes $\delta_{314}{\rightarrow}p = 38$, which is clearly greater than the total available power $PL = 26$. Therefore the control breaks out from the inner loop, making ϕ_{31} a three node list with δ_{313} being the last node. Otherwise (when, $\delta_{ijn}{\rightarrow}p \leq PL$), the algorithm calculates the other two attribute values of node δ_{ijn}, namely, $\delta_{ijn}{\rightarrow}r$ and $\delta_{ijn}{\rightarrow}EPL$ in steps 9 and 10, respectively. δ_{ijn} is then enqueued at the current tail of ϕ_{ij} in step 11. Finally in step 12, the partial optimal solution ψ_i is constructed by using a **Merge()** routine as described in Algorithm 4. All the calculated ϕ_{ij} solutions are given as input to the **Merge()** function.

The **Merge()** procedure merges the linked lists $\phi_{i0}, \phi_{i1}, \ldots, \phi_{iK}$ to generate the partial optimal solutions ψ_i which considers upto i subareas $(S_1, S_2, \ldots, S_i)$. As discussed above, the generated solution is non-dominating with respect to both power p and obtained reward r. The while loop in steps 6 to 19 iterates until Φ_i becomes empty. In step 7, the algorithm determines the subset of partial solutions (k_{ia_1}, k_{ia_2}, $\ldots k_{ia_\lambda}$) with the minimal amount of utilized power among all solutions over all linked lists in Φ_i. It may be noted that as all the linked lists in Φ_i are sorted in increasing order of power levels, this subset is obtained by comparing only the current heads (k_{ij}) of the linked lists in Φ_i. Then, in step 8, the algorithm finds that solution node (pointed by k_{im})

Algorithm 4 Merge $(\phi_{i0}, \phi_{i1}, \ldots, \phi_{iK_i})$

Input: ϕ_{i0}, $\phi_{i1}, \ldots, \phi_{iK_i}$
Output: ψ_i

1: Let $\Phi_i = \{\phi_{i0}, \phi_{i1}, \ldots, \phi_{iK_i}\}$
2: Let k_{ij} be pointers to the heads of the lists ϕ_{ij}
3: Let σ_i be a pointer to the tail of the list ψ_i
4: **for** $j = 0 \ldots K_i$ **do** $k_{ij} = \phi_{ij}.head \rightarrow Next$
5: $\sigma_i = \psi_i.head$; $\psi_i.head \rightarrow r = 0$; $\psi_i.head \rightarrow p = 0$
6: **while** $\Phi_i \neq \{\}$ **do**
7: Find $\{a_0, a_1, \ldots, a_\lambda\}$, such that, $\{\{a_0, \ldots, a_\lambda\} \subseteq \{0, \ldots, K_i\}, k_{ia_0} \rightarrow p == k_{ia_1} \rightarrow p == \ldots == k_{ia_\lambda} \rightarrow p == min_{j=0}^{K_i}\{k_{ij} \rightarrow p\}\}$
8: Find m, such that, $\{m \in \{a_0, a_1, \ldots, a_\lambda\}, k_{im} \rightarrow r == max_{j=a_0}^{a_\lambda}\{k_{ij} \rightarrow r\}\}$
9: **if** $\sigma_i \rightarrow r < k_{im} \rightarrow r$ **then**
10: $\sigma_i \rightarrow Next = new\_node()$
11: $\sigma_i = \sigma_i \rightarrow Next$
12: $\sigma_i \rightarrow r = k_{im} \rightarrow r$
13: $\sigma_i \rightarrow p = k_{im} \rightarrow p$
14: $\sigma_i \rightarrow EPL = k_{im} \rightarrow EPL$
15: $\sigma_i \rightarrow Next = NULL$
16: **for** $l = a_0 \ldots a_\lambda$ **do**
17: $k_{il} = k_{il} \rightarrow Next$
18: **if** $k_{il} \rightarrow Next == NULL$ **then**
19: $\Phi_i = \Phi_i \setminus \phi_{il}$
20: Return ψ_i

which fetches the maximum reward (r) among all nodes in the set $\{k_{ia_1}, k_{ia_2}, \ldots k_{ia_\lambda}\}$. In steps 10 to 15, the solution corresponding to k_{im} is appended at the tail of the partially generated linked list ψ_i, provided this addition preserves the non-dominance properties of ψ_i. This is checked through the condition in step 9. It may be noted that other than k_{im}, no other node provided by the set $\{k_{ia_1}, k_{ia_2}, \ldots k_{ia_\lambda}\}$ can possibly contribute a non-dominating solution in ψ_i. Hence, all these nodes are discarded from further consideration in step 17 of the for-loop in steps 16 to 19. If the removal of a node (in step 17) causes a linked-list (say, ϕ_{ij}) in Φ to become empty, then ϕ_{ij} is removed from Φ_i (step 19). The final partial optimal solution (ψ_i) considering upto i subareas $(S_1, S_2, \ldots, S_i)$ and various power levels, is obtained in step 20.

For example in iteration ($i = 3$) (refer figure 4.3), initially the lists ϕ_{30} and ϕ_{31} start with the nodes δ_{301} and δ_{311}. Hence, pointers k_{30} and k_{31} initially point to δ_{301} and δ_{311}. The nodes δ_{301}, δ_{302} and δ_{303} having lower power values compared to δ_{311}, are successively extracted from ϕ_{30} and appended to ψ_3. At this point, k_{30}, k_{31} and σ_3 point to δ_{304}, δ_{311} and β_{33}, respectively. It may be noted that for both the header nodes, utilized power is 19. Hence, both these nodes become part of the subset of header nodes for which the utilized power is minimal ($k_{3a_0} = k_{30}$ and $k_{3a_1} = k_{31}$). However, among these two nodes, k_{30} delivers a higher reward (22) and hence, $k_{3m} = k_{30}$. Thus, k_{30} is extracted from ϕ_{30} and appended to the tail of ψ_3 as its fourth node (β_{34}). To preserve non-dominance properties, δ_{311} is discarded from ϕ_{31} and k_{31} is now made to point to the new head δ_{312}. Finally, after traversing the both lists ϕ_{30} and ϕ_{31} entirely, the merged list ψ_3 having eight nodes, is obtained.

The complexity of *Streamlined Dynamic Programming based Priority Level Allocator (SDPA)* is primarily governed by the complexity of the nested loop structure which we refer to as (i) the outer loop (lines 2 to 12) which iterates over the set of $\mathcal{N}$ subareas, (ii) the inner loop (lines 4 to 11) which iterates over all priority levels of each subarea (the i^{th} subarea contains K_i priority levels) and (iii) the innermost loop (lines 5 to 11) which iterates over all partial optimal solution nodes (there are $G = |\psi_{i-1}|$ solution nodes considering upto $i-1$ subareas for the i^{th} iteration of the outer loop). The outer loop has two main components, (i) the nested for loops (lines 4 to 11) and, (ii) the Merge() procedure (line 12). The complexity of the innermost loop is governed by the number of nodes (or partial solutions) G in ψ_{i-1}, which is upper bounded by the total number of available power levels PL. However $G << PL$, because ψ_{i-1} only contains non-dominating solutions, i.e., only those partial optimal solutions which provide distinct enhancements in reward for distinct increments in the total power utilized in the solution. For this reason, the actual number of nodes (G) in ψ_{i-1}, for any given value of i, is far less than PL which may assume very high values. For example, the value of PL becomes $500,000$ for a total available residual power $P_R = 500MW$ with power allocation step size $pu = 1kW$ ($\frac{500MW}{1kW}$). As the number of priority levels (K_i) for any given subarea

is upper bounded by L, the complexity of the inner loop may be considered to be O(LG), which is <<O($L*PL$) for all practical scenarios. The complexity of the Merge() function is dominated by the while loop (lines 6 to 19). As the while loop traverses through L lists each having G nodes, the complexity of the loop as well as the Merge() function as a whole, may be considered to be O(LG). Hence, the complexity of the each iteration of the outer loop of *SDPA* becomes O(LG). Thus, the overall complexity of *SDPA* considering $\mathcal{N}$ subareas becomes O($\mathcal{N}LG$), which is far less than O($\mathcal{N} * L * PL$), the complexity of DP, as discussed above. Our experimental results show that, given 50 subareas with 10 priority levels per subarea and with 250 MW of available power at resolution pu (= $1kW$), *SDPA* takes ∼0.5 sec on average to generate a solution on a 3.2 GHz computing core, and thus able to satisfy the stipulated soft real-time constraint recommended by IEEE std 1159. Compared to *DP* which takes ∼13 secs for the same scenario, SDPA provides a speed up of ∼24 times. However, for scenarios with a higher number of subareas (which may become a common phenomenon in future Smart Grids where subareas come to be identified as small-scale Microgrids under a big utility comprised of a hierarchical network of numerous such Microgrids), larger amounts of residual power and/or finer resolutions of the discretization parameter, *SDPA* may take multiple seconds (or even higher) to generate optimal solutions. This makes our optimal strategy *SDPA* unsuitable for real-time power distribution in very large scenarios.

To cope with such situations, we have designed a fast and efficient heuristic algorithm called *Proportionally Balanced Priority level Allocator (PBPA)* which has the ability to deliver quick solutions even for very large scenarios, thus meeting real-time requirements of the problem at hand. In addition, *PBPA* is able to provide effective solutions in almost all practical scenarios, whose qualities do not deviate significantly from that of the optimal.

4.5 Proportionally Balanced Priority level Allocator (PBPA)

The *Proportionally Balanced Priority level Allocator* (*PBPA*) is a fast yet efficient heuristic strategy which allows power balance to be restored quickly through a greedy but elegant approach proceeding level by level, so that a higher overall reward may be obtained by the system. It was observed that, in order to obtain good and acceptable solutions, *PBPA* must be aware of the constraint on the available residual power at any stage of the algorithm. Hence, it must not only consider individual rewards during priority level enhancements, but also account for the amount of incremental power required during such an enhancement process. Therefore, the objective function has been transformed from *reward* to *Reward per unit Power (RpP)*. At any given time during the power allocation (or adjusting) process, the subareas are maintained in a priority queue organized as a max-heap. The urgency of a subarea (towards priority level up-gradation) within the heap is decided on the basis of a *key* which is defined for each subarea S_i as follows:

$$key_i = \max(d[RpP^i_{jK_i}], d[RpP^i_{j(j+1)}]) \tag{4.4}$$

Here, $d[RpP^i_{jK_i}]$ denotes the difference in reward per unit power between its current (j) and highest power level (K_i) and $d[RpP^i_{j(j+1)}]$ represents the reward per unit power between its current and immediately higher ($j+1$) power level.

It was observed that key_i (equation 4.4) is able to provide an appropriate balance between the immediate gain obtained through a priority level shift from j to $(j+1)$ and the overall obtainable gain for the subarea ($d[RpP^i_{jK_i}]$). A situation where the consideration of such overall gains may be useful is as follows: Let us consider the relative urgency of two subareas S_m and S_n currently allocated priority levels j and j' respectively (say), at any arbitrary intermediate stage of the power allocation process using *PBPA*. Assume $d[RpP^m_{j(j+1)}]$ is lower than $d[RpP^n_{j'(j'+1)}]$. However $d[RpP^m_{jK_m}] \gg d[RpP^n_{j'K_n}]$. In such a situation, if overall gain values are not considered as part of the *key*, S_n will be selected for upgradation by one level over S_m, even if its overall gain ($d[RpP^m_{jK_m}]$) is much greater than max ($d[RpP^n_{j'K_n}]$, $d[RpP^n_{j'(j'+1)}]$). A more severe case is that, if S_m's

Algorithm 5 Proportionally Balanced Priority level Allocator (PBPA)

Input:
Number of Subareas $\mathcal{N}$,
Number of priority levels K_i in S_i $\forall i$,
Power p_i^j and corresponding reward r_i^j $\forall i \in \mathcal{N},\ j \in K_i$
Output:
Allocated priority level for each Subarea

1: Determine *Residual Power* $(P_R) = P - \sum_{i=1}^{\mathcal{N}} p_i^0$
2: Compute initial keys, $key_i = \max(d[RpP^i_{0K_i}], d[RpP^i_{01}])$, $\forall S_i$
3: Build *max-heap* H of subarea using initial key values
4: Let cl_i store the current level for each subarea S_i; initially, $cl_i = 0$
5: Incremental Power ip
6: **while** H is not empty **do**
7: Extract subarea S_i from the root of the *max-heap* H
8: **if** $cl_i = 0$ **then** $ip = p_i^{cl_i+1}$ **else** $ip = p_i^{cl_i+1} - p_i^{cl_i}$
9: **if** $(P_R < ip)$ **then**
10: Continue ▷ subarea S_i gets removed from H
11: **else**
12: Update $P_R = P_R - ip$; $cl_i = cl_i + 1$
13: **if** $cl_i == K_i$ **then**
14: Continue ▷ subarea S_i gets removed from H
15: Update $key_i = \max(d[RpP^i_{cl_iK_i}], d[RpP^i_{cl_i(cl_i+1)}])$
16: Re-heapify S_i in H

immediate gain $d[RpP^m_{j(j+1)}]$ is relatively very low, S_m may be indefinitely starved in spite of potentially handsome overall gains. Defining the key as $\max(d[RpP^i_{jK_i}], d[RpP^i_{j(j+1)}])$ appropriately handles the situation.

The step by step working principle of the *PBPA* algorithm is as follows: Step 1 calculates the residual power P_R which needs to be re-distributed among all the subareas. In step 2, the algorithm calculates the initial key values (key_i) for all subareas. Then, based on the calculated keys, *PBPA* builds a max-heap in step 3. Step 4 initializes the current priority level to zero for each subarea. Then, from steps 6 to 16, *PBPA* iteratively increments (updates) the priority level for all subareas till the max-heap (H) is empty. Then algorithm extracts subarea S_i from the root of the heap H in step 7. If the incremental power (ip) is greater than the residual power (P_R) then the subarea S_i is

removed from the max-heap (step 10). Otherwise, the algorithm increments its priority level by 1, updates its *key* value and reheapifies it in steps 11 to 16. If any subarea S_i reaches its highest possible priority level (step 14), then the subarea is removed from the max-heap.

The asymptotic worst case complexity of this heuristic is $O(\mathcal{N}) + O(\sum_i K_i log\mathcal{N})$ where, $\mathcal{N}$ is the total number of subareas. The complexity $O(\mathcal{N})$ is for the formation of the heap data structure. The $O(\sum_i K_i log\mathcal{N})$ overhead is for the reheapify operation and updating the remaining excess capacity at each priority level upgradation. A step by step description of the PBPA algorithm is presented in Algorithm 5.

4.5.1 Example

Here, we elaborate the working principle of *PBPA* using the same example scenario as presented in section 4.2.1 (Example 1). The *PBPA* algorithm distributes the residual power $P_R = 26$ among the three subareas S_1, S_2 and S_3. The initial key values are: $key_1 = \max(\frac{16-0}{7-2}, \frac{13-0}{5-2}) = 4.33$, $key_2 = \max(\frac{16-0}{18-6}, \frac{9-0}{14-6}) = 1.33$ and $key_3 = \max(\frac{19-0}{19-7}, \frac{19-0}{19-7}) = 1.58$. A Max Heap H is built using these initial key values. Subarea S_1 with the highest key value (present at the root of H), is extracted from the heap. P_R and cl_1 are updated to 21 $(26-5)$ and 1, respectively. Now, the key value key_1 for the subarea S_1 is updated as $\max(\frac{16-13}{7-5}, \frac{16-13}{7-5}) = 1.5$. S_1 is inserted back into the Max Heap H. Then, the subarea S_3 with $key_3 = 1.58$ is extracted from the heap. P_R and cl_3 are updated to 2 $(21-19)$ and 1, respectively. Now, S_3 is discarded for further level up-gradation since $cl_3 = K_3 = 1$. Similarly, the next iterations follow and the levels for the subareas are upgraded accordingly. The algorithm terminates when the heap becomes empty. The total reward obtained is 35 and the obtained operating levels for S_1, S_2 and S_3 are 2,0,1, respectively.

4.5.2 Handling Dynamic Demand-Supply Variations

Demand and supply of power is generally time-varying in nature. Such dynamic changes may be handled by our framework through the following mechanism: (1) Divide time

into short length timeframes (of duration say, 15 minutes). (2) Account for changes in the amount of available supply power (P_R) and the requirements of the priority levels in each subarea, at the boundary of each frame. (3) If the overall deficit/surplus power at the current frame boundary is within a stipulated threshold, adjust the amounts power allocated to each subarea such that the disturbance in demand-supply balance can be mitigated. Such adjustments may be conducted through a slight variation of the PBPA algorithm which progressively upgrades/degrades the priority levels allocated to subareas starting from their current levels, instead of starting from level 0 (as mentioned in line 4 of Algorithm 5 (PBPA)). While a max-heap of keys is employed to conduct level enhancements during demand underloads, a min-heap is used for level degradations during overloads. (4) If the total imbalance over all subareas is above the stipulated threshold, a more comprehensive and precise redistribution of power is necessary. Hence in this case, employ SDPA or PBPA (exact version; Algorithm 5) to mitigate such power imbalances (depending on size of the total service-area under a utility). (5) The brownout based power allocation problem considered in this work has an important social perspective. Thus, in addition to always serving essential loads of all subareas, repetitive dynamic reallocations of power through the procedure discussed above must take care that a subset of subareas are not unfairly selected for power allocation over and over again (because they deliver higher rewards) while a few other subareas are unduly starved. We now discuss a strategy for addressing this important social issue of *fairness*.

4.5.3 Fairness

In there endeavor to maximize rewards, both the *SDPA* and *PBPA* strategies may become unfair during repetitive dynamic re-distribution of residual power among subareas. However, fairness can be conveniently incorporated within *SDPA*/*PBPA* by modifying the maximization parameter from *reward* (r) to a *weighted reward* (wr) (in equation 4.2), which takes into account the fraction of the total residual power received in the past (say, the last W time frames), by each subarea. Given the amount of power allocated

to the i^{th} subarea in the w^{th} frame (P_i^w), the total power AP_i allocated to S_i in the previous W frames is given by:

$$AP_i = \sum_{w=1}^{W} P_i^w \tag{4.5}$$

Therefore, total fractional power (FP_i) allocated to S_i in the last W frames become:

$$FP_i = \frac{AP_i}{\sum_{w=1}^{W} P_{RG}^w} \tag{4.6}$$

where, P_R^w represents the total available residual power in the w^{th} time frame. Given FP_i and r_i^j, the reward corresponding to the j^{th} priority level of the i^{th} subarea at the current frame boundary, weighted reward wr_i^j may be obtained as:

$$wr_i^j = \frac{r_i^j}{FP_i} \tag{4.7}$$

From equations 4.6 and 4.7, it may be noted that FP_i appropriately enhances the rewards r_i^j corresponding to different priority levels of a subarea S_i, based on fraction of the total power received by it in the past and thereby imbibes fairness in the dynamic power allocation process.

4.6 Experiments and Results

The performance of the proposed algorithms, namely, *Streamlined DP-based Priority Level Allocator (SDPA)* and *Proportionally Balanced Priority Level Allocator (PBPA)* have been extensively evaluated and compared against the optimal and heuristic strategies DP and HA respectively, proposed in [5]. We have already discussed the *DP* strategy in section 4.3. The *heuristic algorithm (HA)* is similar to *PBPA* but uses a simpler key value *reward* (r_i^j), instead of *Reward per unit Power* (RpR_i^j), as employed by PBPA. Therefore, at any intermediate stage of the algorithm, *HA* chooses that subarea for level increment (by one) which fetches the highest gain in reward among all subareas.

Comparative measures of performance for all the four schemes have been obtained under various scenarios using a data generation framework which we discuss next.

Table 4.2: *Simulation setup*

Number of Subareas ($\mathcal{N}$)	10 to 100
Number of Levels per Subarea (L)	5 to 10
Available Residual Power (P_R)	50 MW to 350 MW
Power Allocation Step Size (pu)	1kW

4.6.1 Data Generation Framework

Following the discussion in Section 4.2, we have designed a data generation framework, in which each scenario consists of $\mathcal{N}$ Subareas under the purview of a single utility provider. Each subarea contains L non-essential priority levels. After supplying power to essential levels, the utility provider has a residual power P_R which must be distributed among the different priority levels of all the subareas. The objective is to maximize the reward obtained through the distribution process. Table 4.2 summarizes the parameters and their variations as considered in the experiments. We have considered systems with varying number of subareas ($\mathcal{N}$ = 10 to 100), where each subarea contains either 5, 8 or 10 non-essential priority levels (L). Experiments have been conducted with different residual power (P_R) values which vary within the range 50MW to 350 MW.

The households/establishments in the utility grid are classified into five types based on minimum (P_{min}) and maximum (P_{max}) power consumption limits. Power consumption intervals $\langle\ P_{min}(kW), P_{max}(kW)\rangle$ for the five types are as follows: Type I $\langle 1.6, 2.0\rangle$, Type II $\langle 3.2, 4.0\rangle$, Type III $\langle 4.8, 6.0\rangle$, Type IV $\langle 6.4, 8.0\rangle$ and Type V $\langle 8.0, 10.0\rangle$. We assume that electric power within a household is consumed by a set of common appliances which we have listed down in table 4.3. Typical rated powers for the appliances have been depicted (within brackets) beside each appliance. Each household is assigned a subset of these appliances (with possibly multiple instances of a given appliance) such that the summation of their rated powers fall within the power consumption interval corresponding to that household's *type*.

Table 4.3: *Various Categories of Appliances; lower an appliance's category, higher is the chance that it gets a high priority level; a priority level with lower index has a higher priority.*

Appliance Category	**Appliances with rated power**
C1	LED Bulb (30 W), Tubelights (60 W), Fans (75 W) etc.
C2	TVs (100 W), Desktops (250 W), Fridge (250 W) etc.
C3	Printers (30 W), Routers (20 W), Water-coolers (75 W) etc.
C4	e-cooker (250 W), Wash Machines (500 W), Microwave (1000 W) etc.
C5	AC (1000 W), Dish Washer (1200 W), Electric Heater (2000 W) etc.

Next, each instance of an appliance allocated to a household is randomly assigned a distinct non-essential priority level (between 1 and L) using a normal distribution. Table 4.3 also shows the appliances classified into five empirically assigned categories ($C1 \ldots C5$). The category of an appliance has been decided based on the notion of an approximate urgency of the appliance towards uninterrupted power supply. Thus, lower an appliance's category, higher becomes the probability that the appliance gets mapped to a high priority level. In any subarea S_i, the number of households (H_i^t) of a particular type (say t), is picked from a uniform random distribution within the range $\langle 800,\ 1000 \rangle$. The total power demand/load (p_i^j) corresponding to subarea S_i's subscription at priority level j, is given by the summation of the rated powers of all appliances which are allocated to priority level j or lower. Subscription at a given priority level (say, j) is also associated with a fixed tariff rate (tar_i^j) per kW. In our experiments, we have assumed this rate for the j^{th} priority level to be equal to $(L - j) + 1$ (i.e., $tar_i^j = (L - j) + 1$). The total reward value (r_i^j) corresponding to the j^{th} level is then given by:

$$r_i^j = \sum_{j'=1}^{j} (L - j + 1) \times (p_i^{j'} - p_i^{j'-1}) \tag{4.8}$$

4.6.2 Simulation Results

A series of simulation based experiments have been conducted to obtain comparative results of the proposed strategies, *SDPA* and *PBPA*, with the existing strategies, *DP* and *HA* [5], using different performance metrics and under varying scenarios. The performance metrics which have been considered for evaluation are: (i) *Mean priority-level allocated to each subarea (average level)*, (ii) *Reward obtained* in percentages, (iii) *Average run time for each algorithm* and (iv) *Speedup*.

Figure 4.4 shows the plots for the average priority levels allocated to each subarea by all the strategies namely, *DP/SDPA*, *PBPA* and *HA*, as the available power (P_R) varies from 50MW to 350MW. This experiment has been conducted with #subareas $\mathcal{N} = 50$ and with #priority levels $L = 10$. Figure 4.4 also presents the mean error of average levels, depicting 95% confidence intervals for all the algorithms. These confidence intervals have been generated for a sample size of 25 (i.e., 25 distinct random scenarios). Both *DP* and *SDPA* algorithms exhibit exactly the same result because of their optimal behavior in the level allocation process. Hence, a single plot has been depicted in Figure 4.4 for both the strategies. It may be observed from the figure that for all the methodologies, the average priority level that may be allocated to the subareas increases in general as P_R increases. This is expected because, with the increase in total available power, the number of priority levels that can be allocated to any subarea on an average, also increases (with a fixed number of subareas). Although the trends for all the strategies are similar, *DP/SDPA* is seen to provide better overall average allocation of levels with respect to *PBPA*, while *PBPA* performs better than HA, over all the scenarios. This may be attributed to the progressively better precision in the distribution of power for the *HA*, *PBPA* and *SDPA* strategies. By taking optimal decisions in power allocation, SDPA allocates highest overall levels in all scenarios. On the other hand, the performance of PBPA is observed to be consistently better than HA. This may

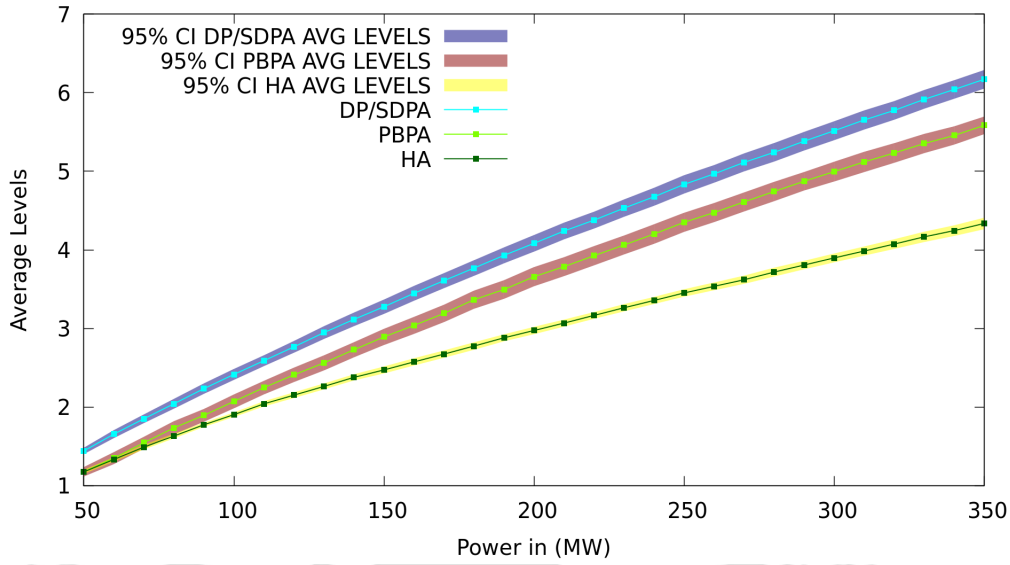

Figure 4.4: *Average allocated Priority level Vs Power*

be attributed to the following two reasons: (i) Instead of directly using *reward* as the objective parameter as done in *HA*, *PBPA* uses *reward per unit power* as its *key* and this allows it to take more elegant decisions balancing both gains (in terms of rewards) and the resource (power) consumption involved in providing such gains and (ii) The definition of the key value in *PBPA* also appropriately takes into account the trade-off between immediate gains (between the current and next levels) and the overall gains (between the current and highest levels) that may be obtained by a subarea.

Figure 4.5 depicts the plots for aggregate rewards (measured in percentages) acquired by all the subareas (a subarea operating at the highest priority-level represents 100% reward) by using the different priority-level allocation strategies, as the available power (P_R) varies from 50MW to 350MW. This experiment has been conducted with #subareas $\mathcal{N} = 50$ and #priority levels $L = 10$. Figure 4.5 also presents mean error of rewards, depicting 95% confidence intervals for all the proposed algorithms. Both *DP* and *SDPA* algorithms exhibit exactly the same result because they both take optimal decisions. Hence, the plot shows the same trend for them. It may be observed from the figure that the aggregate rewards obtained by all the strategies increase with increasing available

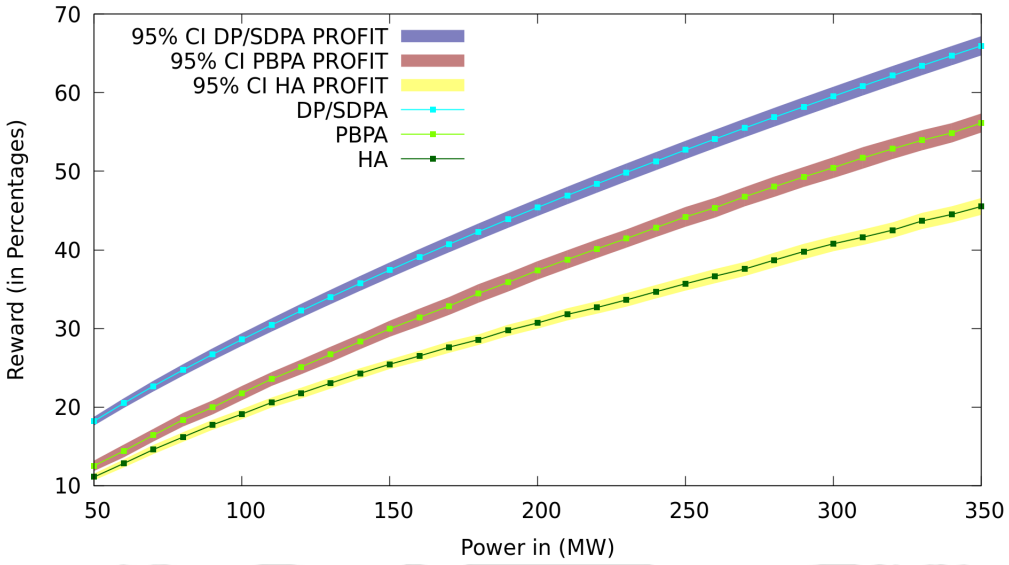

Figure 4.5: *Reward Vs Power*

power. This is because, the reward acquired by an allocation strategy is directly proportional to the allocated levels (refer Figure 4.4). *PBPA* and *HA* are seen to obtain lower rewards than *DP* and *SDPA* in all the scenarios due to their inherent heuristic nature. However, it may be noted that *PBPA* performs better than *HA* due to its level by level consideration of reward obtained per unit power consumption, and this allows it to deliver a more fine grained distribution of available power among subareas.

Figs. 4.6(a) to 4.6(c) show the comparative results for aggregate rewards (in percentage of the maximum achievable rewards) achieved by *SDPA*, *PBPA* and *HA* for three distinct $\#Levels$ ($= 5, 8$ and 10) per subarea, as P_R is varied from 50MW to 350MW. The number of subareas ($\mathcal{N}$) considered in this experiment is 50. As both *DP* and *SDPA* produce optimal results, we have not provided separate results for *DP*. It may be observed from the figures that as the number of levels increases, the *SDPA* algorithm achieves better rewards in all scenarios. This is because, higher number of levels for each subarea provides more flexibility to the algorithm in its allocation strategy. Such flexibility provides better power utilization during distribution and hence, fetches higher rewards. However, it may also be noted that the performance gain obtained by increas-

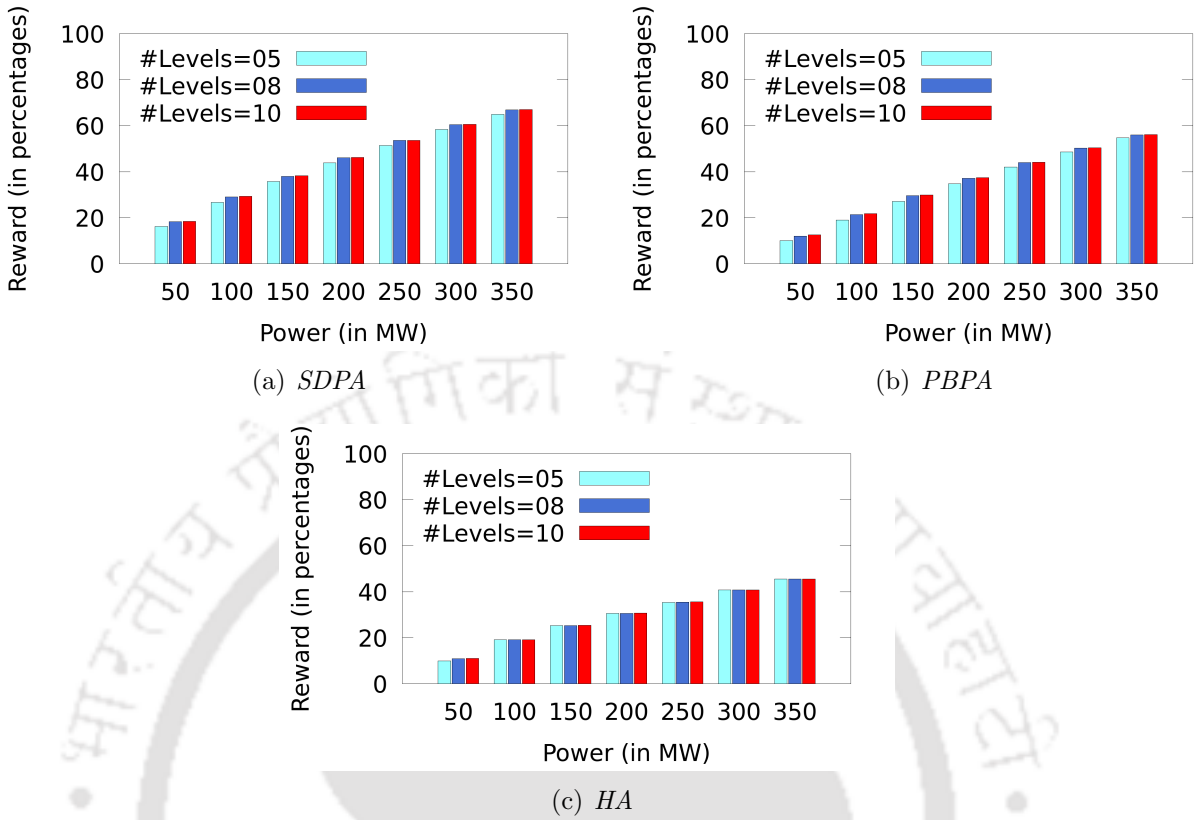

(a) *SDPA* (b) *PBPA*

(c) *HA*

Figure 4.6: *Comparative results of Reward (in Percentages) with varying number of priority levels*

ing the number of levels (L) is not linearly proportional as L increases from 5 to 10. For example, the performance gain obtained by incrementing L from '5 to 8' and '8 to 10' are 2.06% (i.e., 58.39%-60.45%) and .19% (i.e., 60.45%-60.64%), respectively (when the strategy is *SDPA* and when $P_R = 300MW$). Values of L at around 8 has been seen to produce good results in almost all cases.

Table 4.4 shows the average execution time (in ms) taken by *DP*, *SDPA*, *PBPA* and *HA* as P_R varies from 50MW to 350MW. This experiment has been conducted with #subareas $\mathcal{N} = 50$ and #priority levels $L = 10$. It may be observed from the table that the average execution time of *DP* is comparatively much higher than the other strategies. This is because *DP* calculates partial solutions for all possible bounds on number of subareas ($\forall i \in \{0, \mathcal{N}\}$), priority levels ($\forall l \in \{0, L\}$) and power levels

Table 4.4: *Comparison of Execution Times and Speedup between DP, SDPA & PBPA*

Power (in MW)	Time in (ms)				Speed Up		
	DP	SDPA	HA	PBPA	DP vs SDPA	DP vs PBPA	SDPA vs PBPA
50	1337	151	0.013	0.013	9	1.0×10^5	1.1×10^4
100	3472	283	0.018	0.017	12	2.1×10^5	1.7×10^4
150	6208	384	0.021	0.019	16	3.2×10^5	2.0×10^4
200	9355	468	0.024	0.021	20	4.5×10^5	2.2×10^4
250	12942	539	0.026	0.022	24	5.8×10^5	2.4×10^4
300	17233	597	0.029	0.023	29	7.5×10^5	2.6×10^4
350	21387	643	0.032	0.024	33	8.8×10^5	2.6×10^4

($\forall p \in \{0, PL\}$). On the other hand, the *SDPA* scheme memoizes only those partial optimal solutions which provide distinct enhancements in reward with increment in the bound on available residual power p (for each value of the number of subareas considered) and as a result, achieves significant reduction in its computational overhead/run time. It may be observed form the table that *SDPA* is found to be about 9 to 33 times faster than *DP* and thus applicable to real-time brown-out based power distribution in moderate sized grids ($P_R <$ ~250MW). However, for very large grids ($P_R >$ ~250MW), SDPA takes time > ~500 ms which violates the stipulated real-time requirements of dynamic power imbalance mitigation. On the other hand, both the heuristic strategies (*PBPA* and *HA*) are seen to achieve significant speed-ups with respect to the optimal strategies (*DP* and *SDPA*) due to their greedy decisions in the power re-distribution process. Additionally, *PBPA* algorithm is able to generate good and acceptable solutions much quicker and therefore, it may be considered as a suitable strategy to meet the real-time requirements of dynamic power imbalance mitigation in very large grids.

Fig 4.7(a) and fig 4.7(b) shows the comparative results for the average execution time (in ms) taken by *SDPA* and *PBPA* for five different values of P_R, ranging from $100MW$ to $500MW$ (and with $600ms$ mark), as the number of subareas varies from 10 to 100.

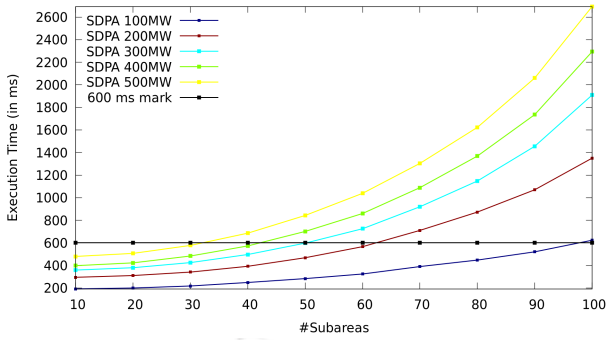

(a) *SDPA*

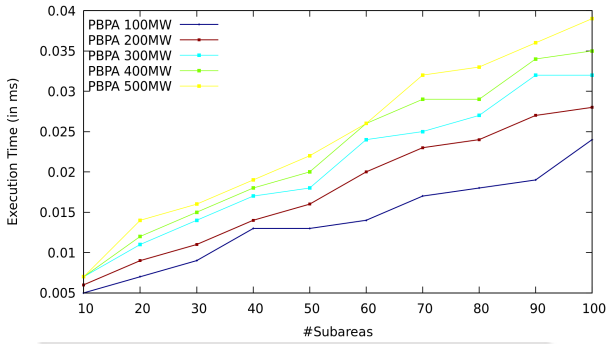

(b) *PBPA*

Figure 4.7: *Comparative results of average execution time (in ms) with varying number of subareas.*

This experiment has been conducted with #priority levels $L = 10$, for all subareas. A horizontal line has been drawn corresponding to the $600ms$ mark to clearly distinguish solutions which take less than and more than $600ms$ to produce outputs. It may be noted that executions which take more than $600ms$ to produce results are infeasible with respect to real-time power distribution as discussed earlier [111]. For example, situations for which *SDPA* can be feasibly applied in real-time scenarios are 100 subareas with atmost $100MW$ of power, 60 subareas with atmost $200MW$ of power and 50 subareas with atmost $300MW$ of power. From fig 4.7(b), it may be seen that execution times for *PBPA* increases monotonically as number of subareas and/or amounts of residual power, becomes higher. Finally, comparing figs 4.7(a) and 4.7(b), we observe that for all experimental scenarios over varying #subareas and amounts of residual power, *PBPA*

is always about 10^4 times faster than *SDPA*.

4.7 Summary

In this chapter, a new methodology for avoiding complete blackouts through brownout based power distribution has been introduced. The brownout based power distribution problem has been formulated as an optimization problem and shown that solution strategies such as conventional dynamic programming (DP) incur substantial overheads. In order to accelerate the *DP*-based solution, an algorithm called *SDPA* has been devised. *SDPA* memoizes only non-dominating intermediate partial solutions and hence, in most practical scenarios, it is able to derive optimal solutions far quicker. However, it was observed that *SDPA* which may even take times upto a few seconds, in scenarios containing a very large number of subareas or significantly high residual power, cannot be used to mitigate sudden imbalances between demand and supply of power in real-time, caused by dynamic switch-on/switch-off of appliances/establishments. Hence, a fast and efficient heuristic known as *Proportionally Balanced Power Allocator (PBPA)* is also proposed. *PBPA* obtains good and acceptable solutions with rewards being atmost 12% lower than optimal. However, *PBPA* can produce results approximately 10^4 times faster compared to *SDPA*. Thus *PBPA* can be used even for very large values of residual power, number of subareas and priority levels with negligible/imperceptible disturbances in grid voltages and frequencies. In the following chapter, we deal with the problem of power deficits in microgrids, especially the ones that are completely disconnected from main grid and operated in islanded mode. We propose a novel brownout based power distribution strategy among consumers, for such grids.

Chapter 5

A Centralized Appliance Scheduling Mechanism for Microgrids

Microgrid power systems are often confined to a small geographical region, for example, a campus, a community or a small town [113]. Structurally, a microgrid consists of multiple components such as the electrical loads corresponding to the households/establishments within its purview, distributed/centralized energy resources along with associated substations, distribution networks, etc [80]. A microgrid operates autonomously (commonly referred as *islanded mode*) if the energy resources within itself are sufficient to satisfy its demands [30]. Otherwise, it switches to *gird–connected mode* and procures electrical power from external grids, as and when needed. However, to avoid loss of power due to long distance transmissions, reduce emissions through enhanced penetration of renewable generation and to contain the effects of faults/disturbances within small localized regions, partial or fully *islanded mode* of operation is being considered increasingly important [9]. Additionally, islanded microgrid designs also provide a mechanism for the electrification of remote geographical regions such as high altitude terrains, deserts, small islands, etc [7].

Power deficit scenarios within such microgrids are typically caused due to a higher percentage of renewable energy penetration into the microgrid system. One way to handle power deficits is by procuring the required amount of power from an external source such as an electricity distribution company. Chapter 3 deals with such a handling

mechanisms. However, such mechanisms may not be a practical choice for some remote microgrids that mostly remain disconnected from any external source and operate autonomously.

In this chapter, we propose a centralized price-based DR scheme for brownout based appliance scheduling. As part of the proposed methodology, we revisit the appliance scheduling problem from the perspective of an entire microgrid instead of standalone establishments, as considered in the related works (refer, Chapter 2, Section 2.4, Task Scheduling based DR Programs and Section 2.4.1). The outline of our proposed work is presented as follows. The microgrid utility defines a fixed number of alternative electricity tariff rates which its consumers can subscribe to, depending on their appliances' urgency towards uninterrupted power supply. For this setting, the proposed work attempts to address the following scheduling problem. Given, (a) the day–ahead estimates on total electrical energy available with the microgrid for different equal length time slots of a day, (b) specifications of appliance requests such as type (either rigid or elastic), subscribed tariff rates and preferred time intervals during which service is required, and (c) the monetary penalty towards allocation of non–preferred slots to appliances, *determine a schedule of appliances for the entire day, such that the total revenue earned by the microgrid is maximized.*

5.1 System Model and Formulation

In this work, the system model is comprised of three crucial entities namely, *Microgrid Energy Manager*, *Load Aggregator* and *Consumers*. A schematic outline of the proposed DR scheme clearly describing the functional entities involved in the scheme as well as their interconnections between them has been depicted in the figure 5.1.

1. *Energy Manager:* A *Microgrid Energy Manager* (usually referred to as a Smart Energy Manager) is responsible for performing tasks such as *unit commitment* [23] and *economic dispatch* [88], to manage electricity generation in a cost–effective fashion. Based on the electricity resource management decisions of the energy manager, it

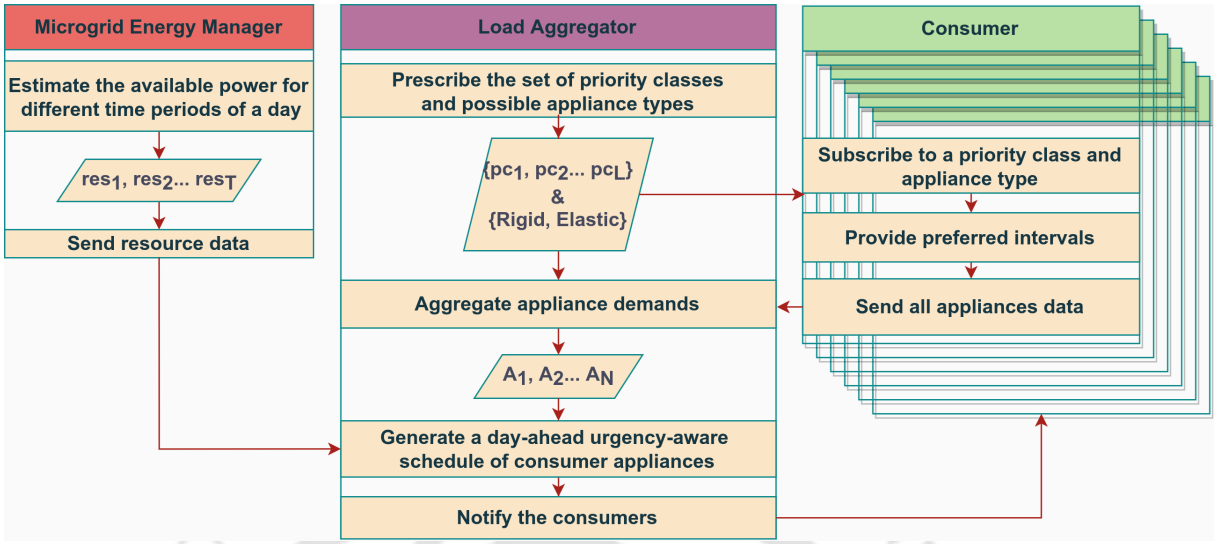

Figure 5.1: *An outline of the proposed scheme*

provides estimates on the total power (comprising renewable/conventional generation as well as externally procured energy, if any) available for distribution within the concerned microgrid, at different timeslots in the next day. Let, the predicted amounts of time slot–wise power resources available with the microgrid utility MU for the next day be denoted as res_1, res_2, ... res_T.

2. *Load Aggregator (LA):* The LA performs scheduling of consumer appliances by taking into consideration their urgency towards uninterrupted power supply and adhering to the power resource bounds estimated by the energy manager for different time slots in a day. The LA offers $\mathcal{L}$ priority classes pc_1, pc_2... $pc_{\mathcal{L}}$, at distinct unit price rates/tariffs tar_1, tar_2... $tar_{\mathcal{L}}$ which the consumer appliances can subscribe to, based on their urgency towards uninterrupted power supply. The priority of a class (say, pc_l) is inversely proportional to its level–id ($l \in [1...\mathcal{L}]$), that is, lower the level–id (say l), the higher is its priority. The priority classes are modeled such that, higher the priority of a class (say pc_l), the higher becomes its price tariff tar_l per unit electricity (1 KiloWatt-Hour) consumed. Hence, $tar_1 < tar_2 <... < tar_{\mathcal{L}}$. Further, the LA provides two choices for appliance types *rigid* (non-deferrable) and *elastic* (deferrable), which a consumer appliance can select

based on requirement. Assuming that, a day to be divided into T equal length non-overlapping time slots, an appliance may require one or more consecutive time slots to accomplish its designated task. For example, assuming a time slot size of 15 minutes, a washing machine may require five consecutive time slots to complete its task. Such electricity demands over multiple time slots are modeled by associating an appliance with an *interval*, which is defined as a 2-tuple entity $PI\langle st, len\rangle$. Here, st denotes the starting time slot of interval $PI\langle st, len\rangle$ and len is the number of consecutive time slots required for successful operation. The LA allows appliances to notify one (rigid) or more (elastic; in decreasing order) preferred intervals at which it requires power supply. Based on choices provided by the consumers, the LA conducts an urgency–aware appliance scheduling for the next day such that acquired revenue is maximized. In the context of time interval allocation to an elastic appliance, a certain discount on tariff (relative to tariffs associated with more preferred intervals) is provided when the most preferred intervals cannot be allocated to a given consumer appliance.

3. *Consumers:* Consumers participate in the DR scheme by recording their appliance specifications (i.e., rated power, subscribed tariff, type, preferred time intervals) through the Home Energy Management (HEMS) devices that are installed at their premises.

Let, A_1, A_2, ... $A_{\mathcal{N}_a}$ be $\mathcal{N}_a$ distinct appliances whose operation must be scheduled by the LA for the next day. The operation request of the i^{th} appliance A_i is characterized by the following attributes,

1. Rated power of the appliance , pow_i (in Kilowatts).

2. Subscribed tariff rate, $pr_i \in \{tar_1 ... tar_{\mathcal{L}}\}$ for its chosen priority class. The unit of any price tariff pr_i is given in terms of *monetary cost per Kilowatt-hour energy consumed over one time slot*. For example, assuming dollar as the unit for monetary cost and one hour to be the time slot size, tariff rate $pr_i = 5$ would mean

that the electricity bill will be 5 dollars for appliance A_i, if one kilowatt power is consumed by the appliance A_i over the time slot interval of one hour.

3. Type of appliance $typ_i \in \{\text{Rigid}, \text{Elastic}\}$.

4. A list of $\mathcal{M}_i$ preferred time intervals PI_{i1}, PI_{i2} ... $PI_{i\mathcal{M}_i}$.

For a rigid appliance A_i, its $\mathcal{M}_i$ preferred intervals must be non–overlapping and denote the set of different time intervals during which service of the appliance is required. Depending on the available energy resource and the scheduling objectives, the LA may either schedule or curtail electricity supply to the entire duration of any such interval (here, an interval is considered to be a non–preemptable entity). On the contrary, the $\mathcal{M}_i$ intervals for an elastic appliance A_i can be partially overlapping and denote the list of alternative interval choices during which A_i's service is demanded, in decreasing order of priority. Therefore, the first interval with respect to an elastic appliance A_i is its most preferred interval and so on, with the last interval being the least preferred one; the utility schedules atmost one of these alternative interval choices.

The revenue R_{ij} corresponding to the operation of a rigid appliance A_i in the j^{th} interval $PI_{ij}\langle st_{ij}, len_{ij}\rangle$ may be calculated as shown in equation 5.1.

$$R_{ij} = pow_i \cdot pr_i \cdot len_{ij} \tag{5.1}$$

As pr_i has a unit of monetary cost per kilowatt-hours, pow_i is represented in kilowatts and len_{ij} is scaled as a time interval in hours. However for an elastic appliance A_i, the revenue also depends on the actual interval selected by the utility. A certain discount on the revenue is provided to the consumer, when A_i is scheduled in any interval other than the most preferred interval. The actual revenue R_{ij} levied by the utility for scheduling A_i at its j^{th} preferred interval (PI_{ij}) is calculated as shown in equation 5.2.

$$R_{ij} = pow_i \cdot pr_i \cdot len_{ij}(1 - Pe(j)) \tag{5.2}$$

Here, $Pe(j)$ is a penalty function which is defined as:

$$Pe(j) = \frac{P^{j-1} - 1}{m} \tag{5.3}$$

Here, P is a penalty factor and m is a moderation constant. It may be observed that, the actual revenue R_{ij} progressively reduces as A_i is scheduled at its less preferred intervals.

The problem of scheduling the operation of appliances can be formally stated as follows. Given the setting with, **a)** the appliance demands A_i $\forall i \in \{1..\mathcal{N}_a\}$, **b)** the revenue values corresponding to all the preferred time intervals of appliances R_{ij} $\forall i \in \{1..\mathcal{N}_a\}$ $\forall j \in \{1..\mathcal{M}_i\}$, and **c)** the available time slot–wise predicted power resources res_t $\forall t \in \{1..T\}$, the LA attempts *to schedule the appliances such that the overall revenue obtained by an MU is maximized*. Since, the priority of appliances is expressed through their subscribed tariff rates, the objective of maximizing the overall revenue obtained by the utility also maximizes the probability of the higher priority appliance being scheduled. Therefore, we formulate the above scheduling problem with the objective of maximizing total revenue obtained by the utility. We now present an *Integer Linear Programming* (ILP) formulation for the proposed appliance scheduling problem.

5.1.1 ILP Formulation

Let us consider a set of binary decision variables: $X = \{x_{ij} : i = 1, 2...\mathcal{N}_a; j = 1, 2...\mathcal{M}_i\}$. The variable $x_{ij} = 1$, when the appliance A_i is scheduled for operation at its j^{th} interval; $x_{ij} = 0$, otherwise. We now present the required constraints on the binary decision variables X, that define the above scheduling problem.

5.1.1.1 Unique interval for elastic appliances

An appliance of type elastic can be scheduled to operate in atmost one of its preferred intervals.

$$\sum_{j=1}^{\mathcal{M}_i} x_{ij} \leq 1 \quad \forall i \in \Big\{ i' | typ_{i'} = \text{“Elastic”} \ \& \ i' \in \{1..\mathcal{N}_a\} \Big\} \tag{5.4}$$

5.1.1.2 Power resource constraints

For any time slot $t \in \{1...T\}$, the aggregate rated powers of all appliances whose preferred interval contains time slot t, must not exceed the total power resource available res_t.

$$\sum_{i=1}^{\mathcal{N}_a} \sum_{j \in W_{it}} pow_i \cdot x_{ij} \leq res_t \quad \forall t \in \{1..T\} \tag{5.5}$$

where,

$$W_{it} = \Big\{ j' | j' \in \{1..\mathcal{M}_i\} \ \& \ t \in \{st_{ij'}, st_{ij'} + 1, \ ... \ (st_{ij'} + len_{ij'})\} \Big\}$$

Here, W_{it} is the set consisting of the indices of those intervals of appliance A_i which contain time slot t within them.

5.1.1.3 Objective function

The objective is to maximize the total revenue obtained by the microgrid utility over all interval choices of the appliances. This is given as shown in the following equation.

$$\text{Maximize} \quad \sum_{i=1}^{\mathcal{N}_a} \sum_{j=1}^{\mathcal{M}_i} R_{ij} \cdot x_{ij} \tag{5.6}$$

5.1.2 A Running Example

In this section, we discuss the system model and formulation presented above using an illustrative example of a hypothetical microgrid. Consider the appliance scheduling problem over a time period of four hours where, this duration is divided into four equal length time slots. The available power resources with the microgrid utility for the respective time slots are given as 5, 5, 8 and 5. Let the number of priority classes be 2. The corresponding price tariffs are tar_1=2 and tar_2=1. The microgrid utility receives five appliance demands as shown in table 5.1. Assuming P=1.15 and m=1.4, the appliances' revenue values for different intervals may be calculated as shown in table 5.2. Given the above scenario, the ILP formulation becomes as follows.

Table 5.1: *An example of appliance demands*

Appl	pow	pr	typ	PIs
A_1	1	1	Rigid	{(1,2), (4,1)}
A_2	5	2	Elastic	{(1,1), (3,1)}
A_3	2	1	Elastic	{(1,2), (2,2), (3,2)}
A_4	3	2	Rigid	{(1,2), (3,1)}
A_5	4	1	Elastic	{(4,1), (3,1), (2,1)}

The unique interval constraint corresponding to the elastic appliances A_2, A_3 and A_5 can be derived from equation 5.4. For example, the constraint for A_2 takes the form: $x_{21} + x_{22} \leq 1$.

As shown in equation 5.5, the power resource constraint must be applied to all time slots t ($\in \{1..4\}$). As example, for $t = 3$, the available power resource is $res_3 = 8$ and the following sets represent those interval indices of the appliances that contain time slot $t = 3$: $W_{23} = \{2\}$, $W_{33} = \{2, 3\}$, $W_{43} = \{2\}$ and $W_{53} = \{2\}$. Given the above sets, the resource constraint for $t = 3$ can be formed as follow: $5x_{22} + 2x_{32} + 2x_{33} + 3x_{42} + 4x_{52} \leq 8$. In the optimal solution obtained through the formulation, decision variables x_{12}=x_{22}=x_{31}=x_{41}=x_{42}=x_{53}=1. Rest of the decision variables take the value 0. The optimal aggregate revenue delivered by the objective function is 35.9. The optimal solution to the above example has been obtained by using a standard ILP solver called IBM CPLEX [49]. In the following section, we present our proposed algorithmic strategy that addresses the above scheduling problem.

5.2 Revenue–aware Appliance Scheduler (RaAS)

The appliance scheduling problem, as formally discussed in the previous section, is an NP-Hard problem and thus, optimal solution strategies as the one provided above are exponential in nature. Hence, the optimal solutions become prohibitively expensive in terms of computational demands and are poor in terms of scalability. For example, it takes ∼2 hours to generate optimal solutions for a moderate sized microgrid scenario

Table 5.2: *Revenue values*

Appl	Revenue values of preferred intervals
A1	R_{11} =1*1*2 = 2; R_{12} =1*1*1=1
A2	R_{21} =5*2*1=10; R_{22} =5*2*1(1-0.11)=8.9
A3	R_{31} =2*1*2= 4; R_{32} =2*1*2(1-0.11)= 3.56; R_{33} =2*1*2(1-0.23)=3.08
A4	R_{41} =3*2*2=12; R_{42} =3*2*1=6
A5	R_{51} =4*1*1=4; R_{52} =4*1*1(1-0.11)=3.56; R_{53} =4*1*1(1-0.23)=3.08

with ∼1 lakh appliances, with a day is divided into 96 time slots (i.e., 15 minutes each). It may be noted that such time overheads may often not be affordable, especially when multiple quick design iterations are needed during design space exploration. Such exploration may be needed, for example, in scenarios where, a regional grid must equitably distribute its pool of resources across time slots in a day, among a set of its component microgrids. Therefore, we have resorted to the design of an efficient heuristic algorithm namely, *Revenue–aware Appliance Scheduler* (RaAS) which has the ability to quickly generate results (say, within a few seconds) while simultaneously delivering close to optimal performance. *RaAS* is an iterative algorithm for scheduling a given set of appliances. At any iteration, RaAS schedules the highest priority interval of an appliance, which is currently unallocated. Before we delve into the detailed description of *RaAS*, we discuss the principal data structures used.

5.2.1 Data Structures

The algorithm uses the following two important list data structures.

i) A list of linked–lists called *Bin* having size $\mathcal{K}$, where $\mathcal{K}$ is a design constant. Each element Bin_c of *Bin* points to a linked–list consisting of a distinct subset of the currently

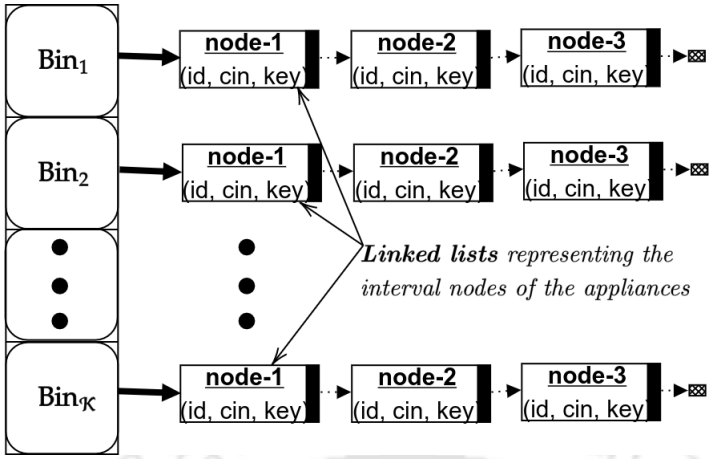

Figure 5.2: *A pictorial representation of the data structure*

unscheduled appliance requests. Each such request node (say, a) contains an appliance *id* ($a.id$), *id* of the specific interval requested for ($a.cin$) and a *key* ($a.key$) whose value denotes the scheduling priority for the node. Values of the parameter *key* are bounded within the range $[k^{min}, k^{max}]$. This range is partitioned into $\mathcal{K}$ equal sized intervals such that the c^{th} *Bin* (Bin_c) points to the linked–list of request nodes whose key values are within the range $\left[k^{min} + c * \Delta k,\ k^{min} + (c+1)\Delta k\right)$ where, $\Delta k = (k^{max} - k^{min})/\mathcal{K}$.

ii) The output schedule is represented as a list–of–lists S of size T. Each element S_t of S contains the list of appliances whose service starts at timeslot $t \in \{1..T\}$.

5.2.2 Detailed Description of RaAS

The pseudocode of the proposed algorithm namely *RaAS*, is shown in Algorithm 6. In steps 1 and 2, the algorithm initializes the total revenue t_rev to 0 and Bin_1, Bin_2... $Bin_{\mathcal{K}}$ with empty linked–lists, respectively. From steps 3 to 10, the algorithm iterates over all $\mathcal{N}_a$ appliances and builds the *Bin* data structure by appending each appliance request node at the head of an appropriate *Bin*, based on its *key* value. The *key* value of a node represents the *effective price tariff* for the appliance's service at the requested interval. *key* is calculated as the ratio of the actual revenue earned by scheduling the appliance, and the corresponding total power demand. Thus,

$$key = R_{ij}/(pow_i * len_{ij}) \tag{5.7}$$

Algorithm 6 Revenue–aware Appliance Scheduler (RaAS)

Input:
a) List of $\mathcal{N}_a$ appliance demands, A_1, A_2... $A_{\mathcal{N}_a}$
b) Number of time slots T
c) Estimated energy resources, res_1, res_2...res_T
d) Penalty function $Pe()$
e) A Bin of size $\mathcal{K}$
Output:
Generated schedule list, S_1...S_T and total revenue t_rev.

1: Initialize $t\_rev := 0$
2: Initialize Bin_1=Bin_2=...$Bin_{\mathcal{K}}$=NULL
3: **for** $i := 1$ **to** $\mathcal{N}_a$ **do**
4: **if** typ_i= "Rigid" **then**
5: **for** j := 1 **to** $\mathcal{M}_i$ **do**
6: Create a new request node a with values, $a.id = i$, $a.cin = j$ and $a.key = pr_i$
7: Append node a to linked–list pointed to by Bin_c, where $c = \lceil (key - k^{min})/\Delta k \rceil$
8: **else**
9: Create a new request node a with values, $a.id = i$, $a.cin = 1$ and $a.key = pr_i$
10: Append node a to linked–list pointed to by Bin_c, where $c = \lceil (key - k^{min})/\Delta k \rceil$
11: Let, mb=c, where Bin_c denotes the highest indexed Bin which is currently non-empty
12: **while** Bin is not empty **do**
13: Extract a, the first node from the linked–list Bin_{mb}
14: Let, $i := a.id$ and $j := a.cin$
15: **if** $res_t \geq pow_i$, $\forall$t := st_{ij} **to** $st_{ij} + len_{ij}$ **then**
16: Append i to $S_{t'}$, where $t' = st_{ij}$
17: $res_t := res_t$ - pow_i, $\forall$t := st_{ij} **to** $st_{ij} + len_{ij}$
18: Increment $t\_rev := t\_rev + a.key \cdot pow_i \cdot len_{ij}$
19: **elseif**
20: **if** typ_i ="Elastic" **and** $j < \mathcal{M}_i$ **then**
21: Update $a.cin := j + 1$
22: Update $a.key := pr_i\Big(1 - Pe(a.cin)\Big)$
23: Reinsert a into linked list of Bin_c, here, $c = \lceil (key - k^{min})/\Delta k \rceil$
24: **else**
25: Discard node a from any further consideration
26: **while** $Bin_{mb} == NULL$ **and** $mb > 0$ **do**
27: $mb := mb$ - 1

From equations 5.1 and 5.2, it may be observed that the RHS of equation 5.7 can be re–written as pr_i and $pr_i(1 - Pe(j))$, for *rigid* and *elastic* appliances, respectively. The index c of the Bin in which the appliance request node is inserted (Bin_c) is given by: $c = \lceil (key - k^{min})/\Delta k \rceil$. Through this process, the appliance request nodes are effectively bucket sorted into the $\mathcal{K}$ available $Bins$. It may be observed that as *all* intervals of a *rigid* appliance are separately considered for scheduling, the algorithm inserts *all* the $\mathcal{M}_i$ nodes of a rigid appliance A_i into the $Bins$ (as shown in steps 5 to 7). In contrast, only *one* node which corresponds to the first (highest priority) interval, is inserted for an *elastic* appliance (refer steps 8 to 10). After building the linked–lists, the algorithm iterates over all the nodes in Bin, and terminates when Bin becomes empty.

At each iteration, the algorithm extracts the node (say, a) at the head of Bin_{mb} where, mb denotes the highest index for which Bin_{mb} is non–empty. The algorithm then attempts to schedule the interval PI_{ij} pointed to by the extracted node a ($i = a.id$ and $j = a.cin$). An appliance A_i can be successfully scheduled for the interval PI_{ij} only if sufficient resources are available at all time slots (st_{ij}, st_{ij}+1,... $st_{ij} + len_{ij}$) encompassing PI_{ij}. This condition is checked in step 15. If the condition holds: i) index i of the i^{th} appliance is appended to the list for the st_{ij}^{th} time slot of the partial schedule S (step 16), ii) the resource demand pow_i of A_i is deducted from the total available resource res_t at each time slot t in the interval PI_{ij} (step17) and, iii) the total revenue t_rev is incremented the revenue earned through the allocation of A_i atPI_{ij} (step 18). If the condition in step 15 fails, node a is removed from further consideration if either i) node a is associated with a rigid appliance, or ii) a corresponds to the last interval of an elastic appliance. When node a corresponds to other intervals of an elastic appliance, its attributes $a.cin$ and $a.key$ are updated according to the appliance's next preferred interval before reinserting back a into an appropriate Bin (refer steps 21, 22 and 23).

The worst case time complexity of the algorithm is given as $\mathcal{O}(\sum_i^{\mathcal{N}_a} \mathcal{M}_i)$, which denotes the sum of the interval choices over all the appliances. This is because, the algorithm attempts to schedule each interval of an appliance atmost once. Considering $\mathcal{M}_i$ to be a constant, the worst case complexity of $RaAS$ becomes $\mathcal{O}(\mathcal{N}_a)$. Our exper-

Table 5.3: *Iterations of RaAS*

Itr	Bins with Linked Lists	Resources	Remarks
–	bin-1 (1,1,1) (1,2,1) (3,1,1) (5,1,1) bin-2 (2,1,2) (4,1,2) (4,2,2)	(5,5,8,5)	Initial Linked–list of Bins and, $mb = 2$
1	bin-1 (1,1,1) (1,2,1) (3,1,1) (5,1,1) bin-2 (4,1,2) (4,2,2)	(0,5,8,5)	Extracted (2,1, 2), S_1={2} Revenue t_rev=10
2	bin-1 (1,1,1) (1,2,1) (3,1,1) (5,1,1) bin-2 (4,2,2)	(0,5,8,5)	Extracted (4,1,2) Resource unavailable Discard node
...	...	...	...
8	bin-1	(0,0,0,0)	Extracted (3,2,.89), S_2= {3}, t_rev = 22.12, Bin is empty

imental results show that for ∼5 lakh appliance requests, the average execution times of *RaAS*, taken over 30 different sample microgrid scenarios, is ∼25 seconds for $\mathcal{K}$=10. Before we discuss the experiments and results in detail, we illustrate the working of the *RaAS* algorithm by considering the same hypothetical microgrid as used for the running example in Section 5.1.2.

5.2.3 Illustrative Example

Table 5.3 shows a few iterations of the RaAS algorithm, in which each row portrays the updated elements of the Bin data structure, the updated resource list and a brief description of the important steps involved within an iteration. Each 3–tuple ($a.id$, $a.cin$, $a.key$) associated with a Bin within any row of the table represents a node. As example, for the first node (1,1,1) in Bin_1 of row 1, $a.id$=1, $a.cin$=1 and $a.key$=1. In this example, we assume $\mathcal{K}$=2 $Bins$; k^{min}=.77 and k^{max}=2. Nodes with key values in the range $[.77, 1.385)$ and $[1.385, 2]$ are inserted into Bin_1 and Bin_2, respectively. Row 1 of

the table depicts, i) the Bin data structure at the beginning of iteration 1, ii) the amount of power resources currently available at each of the four time slots under consideration. During iteration 1, the first interval $PI_{21}\langle 1,1\rangle$ of appliance A_2 (node 1 (2,1,2) of Bin_2, the highest indexed non empty bin) is scheduled at the first time slot, as the amount of available resource (res_1=5) is sufficient to satisfy its power demand pow_i=5. Row 2 of the table shows the updated Bin data structure and updated resource availability list after the allocation of A_2 in iteration 1. The *Remarks* column for row 2 mentions the node extracted from Bin_2, the updated partial schedule S in which, appliance A_2 has been inserted in the list for slot 1 and, the updated obtainable revenue. However in the second iteration, there is no residual resource for scheduling PI_{41}, which corresponds to the node (4,1,2), currently having the highest priority. This node is therefore discarded from further consideration. In a similar fashion, the algorithm proceeds by attempting to schedule intervals of all the other nodes in Bin, until Bin becomes empty. The schedule list S that gets finally generated after all iterations is given as: $S_1 = \{2\}$, $S_2 = \{3\}$, $S_3 = \{4\}$ and $S_4 = \{1, 5\}$. The total revenue obtained by applying our heuristic *RaAS* is 22.12.

5.3 Experiments and Results

The performance of the proposed heuristic algorithm namely, *Revenue–aware Appliance Scheduler* (RaAS) has been extensively evaluated through empirically generated random microgrid scenarios and compared against optimal solutions obtained by solving the *ILP* formulation as given in Section 5.1.1. The *ILP* solver used in the experiments is *IBM ILOG CPLEX Optimization Studio* [49]. Random microgrid scenarios are generated using a data generation framework that we discuss next. Values of various framework parameters such as number of timeslots, types of households/establishments, tariff alternatives etc, have been carefully chosen to represent diverse realistic microgrid scenarios which may possibly occur in practice. The experimental results show that RaAS is very effective towards revenue maximization while at the same time delivering priority and urgency aware appliance schedules. In addition, RaAS is fast and scalable with its so-

Table 5.4: *Categorization of common appliances equipped within households/establishments*

Category	Common appliances with energy consumption (in watts)
Cat-1	lights (100), ceiling fans (100), security cameras (100), projectors (300) and monitors (200)
Cat-2	desktops (300), laptops (100), water pumps (1000), projectors (300) and audio system (200)
Cat-3	air purifiers (300), humidifiers (300), dehumidifiers (300), ACs (1000) and heaters (1000)
Cat-4	printers (500), television (500), rice cookers (200), water purifiers (200), vacuum cleaners (200) and coffee makers (1000)
Cat-5	dishwashers (1000), washing machines (500), microwaves (1000), kettles (1000) and refrigerators (500)

lution generation speeds being about 2^8 times quicker than optimal solutions generated using CPLEX.

5.3.1 Data Generation Framework

Following the description in Section 5.1, various random scenarios that resemble practical appliance demands of a microgrid, have been generated. A flow diagram describing the data generation framework has been presented in figure 5.3. This data generation framework takes into consideration the following inputs (grey boxes in figure 5.3): i) Number of timeslots, ii) Price tariff alternatives, iii) Possible household/establishment types and their consumption bounds, iv) Lower and upper bounds on the number of households for each type, v) An empirical categorization of commonly used appliances, vi) Penalty factor and moderation constant and, vii) Lower and upper bound on available power at different timeslots for the next day. The following outputs are generated (blue

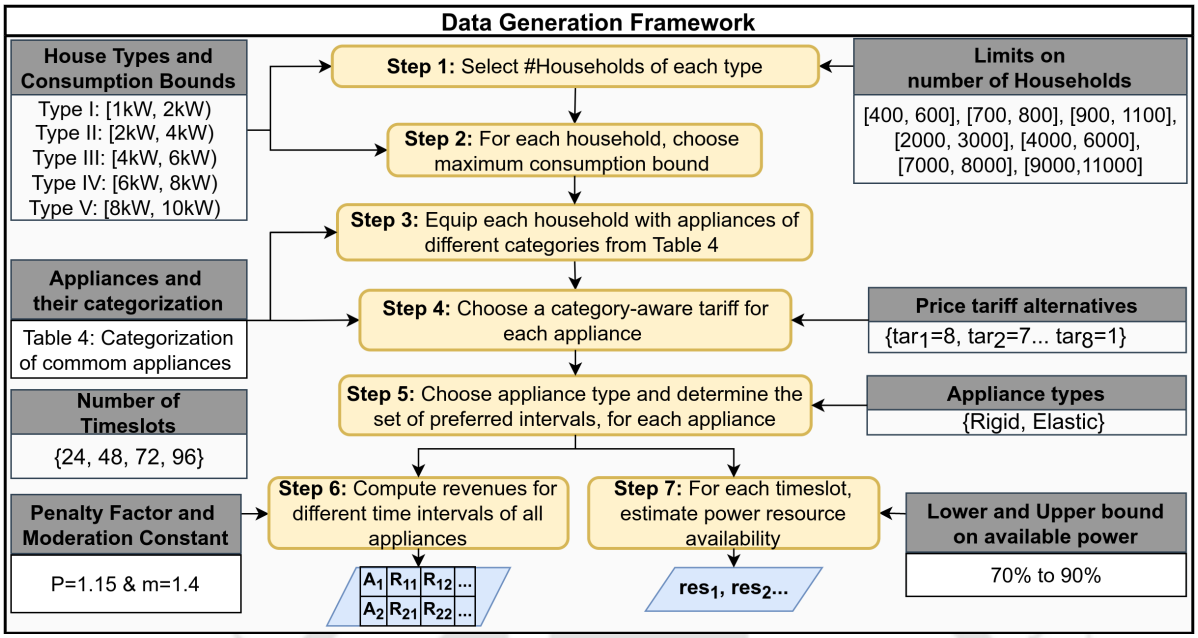

Figure 5.3: *Data Generation Framework- Flow Diagram*

data blocks in figure 5.3): i) Set of appliances ($A_1, A_2, A_3 \ldots$) and ii) resource estimates at different timeslots for the next day ($res_1, res_2 \ldots$). The data for each appliance say $A_i$to consists of the following pieces of information, i) rated power, ii) subscribed tariff, iii) appliance type, iv) a list of preferred intervals (each interval is represented as a 2-tuple ⟨start timeslot, interval length⟩) and, v) the revenue values associated with each preferred interval. We now present a step–wise description of the data generation framework.

Step 1: The objective of the first step is to generate the number of households / establishments in the microgrid, from a given range, [lower limit (ll), upper bounds (ul)]. In this context we have observed that, households/establishments in a developing nation like India may have diverse consumption patterns, depending on socio-economic status, size, purpose of usage (residential/commercial) etc. Accordingly, we have categorized households into five possible types based on their total demand for power. The bounds on total demand for these five types are as follows: Type I: [1kW, 2kW), Type II: [2kW, 4kW), Type III: [4kW, 6kW), Type IV: [6kW, 8kW) and Type V: (8kW, 10kW]. A Type

I household is intended to represent a small lower/middle class establishment having say, a few lights, a couple of fans, a television, a cooking appliance etc., whose total consumption would typically be between 1kW and 2kW. The other types have been designed with a similar philosophy and represent bigger sized establishments having larger power demands. For each of these five household types, step 1 takes as input $[ll, ul]$, and generates the number of households from a normal distribution having mean $\mu = ll + (ul - ll)/2$ and standard deviation $\sigma = (ul - \mu)/3$. We have considered the following options for $[ll, ul]$ viz., [400, 600], [700, 800], [900, 1100], [2000, 3000], [4000, 6000], [7000, 8000], [9000, 11000].

Step 2: Given the number of households of each type (as obtained in step 1), each household is randomly assigned a total consumption value from a uniform distribution within the consumption bounds associated with its type (as discussed in step 1). For example, we select a number uniformly from the range [2000W, 4000W) for a household of Type II.

Step 3: After obtaining the number of households of each type (step 1) along with their individual total consumption values (step 2), we select a set of appliances from five different categories (Cat-1 to Cat-5) as shown in table 5.4 (typical rated powers (measured in watts) depicted within brackets) for each household. This categorization is such that, lower the category id, the higher is the criticality towards uninterrupted power supply. For example, a domestic appliance such as a washing machine can be considered to have lower urgency compared to an essential lighting appliance or even a cooking appliance. Similarly, an office equipment such as a projector or a desktop computer may be assumed to be more urgent than a television set. Therefore, Cat-1 appliances are assumed to be the most critical, while Cat-5 appliances are assumed to be the least important ones.

Step 4: At this step, we assign price tariffs to the selected appliances for each household. The alternative price tariff values considered are, tar_1=8, tar_2=7, tar_3=6, tar_4=5, tar_5=4 and tar_6=3. The selection of one of these six price tariff alternatives is done from normal distributions whose means are weighted by appliance category. The

tariff rates have been selected by taking into account the Indian context, especially the capital city of India, Delhi, where tariffs for different domestic and non–domestic establishments range from 3 to 8 rupees [2].

Step 5: Given, i) the number of timeslots in a day and ii) the appliances equipped within the households of each type (as generated in step 3), this step randomly selects a type, either *rigid* or *elastic*, with equal probability, and determines a set of preferred intervals, for each appliance. Four distinct alternatives for the number of timeslots viz., 24 (1 hour slots), 48 (half hour slots), 72 (20 minute slots) and 96 (15 minute slots), have been considered.

Step 6: After generating the appliance requests (steps 3) along with their associated tariffs (step 4), types and preferred intervals (step 5), the revenue associated with each preferred interval of all appliances is calculated by using equations 5.1 and 5.2. The *penalty factor (P)* and *moderation constant (m)* of the penalty function (refer equation 5.2 in Section 5.1) are taken as 1.15 and 1.4, respectively. These parameters show a typical scenario where consumers are provided progressively increasing monetary incentives when the consumption associated with a certain appliance gets shifted to lower preferred intervals. However, these parameters may be tuned by a microgrid utility so that more consumers are encouraged to participate within the proposed DR scheme while also ensuring a targeted profit return.

Step 7: At this step, we generate random estimates on the power resource available at different timeslots of a day. This step takes as input i) the number of timeslots in a day, ii) the power demand requests of all appliances (steps 3, 4 and 5) and, iii) the lower and upper bound on the available power (70% to 90%). For a given timeslot say t, res_t is considered to be a random value between 70% to 90% of the total power demand at timeslot t. Such random estimates on the available power takes into account challenging scenarios where the resources vary significantly over different time slots of a day.

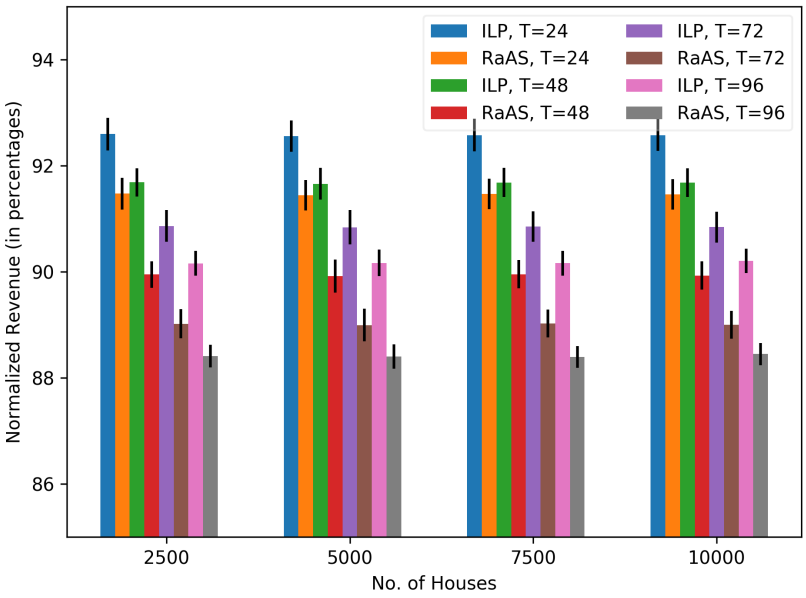

Figure 5.4: *Comparison of the normalized revenues corresponding to the ILP and RaAS, as the #Houses and #Time slots are varied*

5.3.2 Detailed Results

A series of experiments have been conducted to evaluate the RaAS heuristic algorithm and also compare its performance against optimal solutions derived by implementing the proposed ILP (refer Section 5.1.1) with IBM's CPLEX Optimization tool. Experiments have been performed using different performance metrics, under varying microgrid scenarios. The performance metrics which have been considered for evaluation are:

- *Normalized Revenue (NR)*, measured as percentage of the maximum total revenue that may be achieved by scheduling all appliances (with elastic appliances scheduled at their most preferred intervals).
- *Average execution time (ET)*, for the solution generation strategies, measured in seconds.
- *Speedup* $= \frac{\text{Execution time } ILP}{\text{Execution time } RaAS}$

Figure 5.4 shows the comparative results for normalized revenue (NR) corresponding

to solutions delivered by the *ILP* and *RaAS*, for four different variations (24, 48, 72 and 96) in the number of time slots, as the number of houses in a microgrid is varied from 2500 to 10000 (500 to 2000 houses for each of the 5 types). Figure 5.4 also shows the mean error in the obtained NR values (represented as a vertical line on top of the bar plots), depicting 95% confidence intervals for both the strategies. These confidence intervals have been generated for a sample size of 10 (i.e., 10 distinct random scenarios). For *RaAS*, we have used $\mathcal{K}$=10 as the number of *Bin*s. It may be observed from the figure that, performance of both strategies namely, *ILP* and *RaAS* do not significantly vary with increase in the number of households from 2500 to 10000. This shows that both the algorithms scale efficiently in terms of performance, with increase in the number of input appliances. For both strategies, delivered NR values may be seen to steadily decrease as the number of time slots become higher, for any given number of houses. This is because, with the appliances' average service demand durations remaining same, higher number of time slots (T) leads to corresponding increase in the average number of time slots within an appliance's intervals. For example an interval, corresponding to a washing machine having a service demand duration of 2hours, will consist of 2, 4, 6 and 8 time slots, respectively, as the time slot size is decreased from 1hour (T=24) to 15 minutes (T=96). Although, a higher number of time slots allows more accurate allocation of appliances over time, the scheduling problem becomes harder, as the available energy resources get distributed over a larger number of time slots. Because energy resources cannot be shared across time slots, performance degrades with increase in the value of T. Finally, it may be observed that the proposed heuristic algorithm *RaAS* performs appreciably well across various test case scenarios, producing results which are only about 2% poorer than the optimal *ILP* solutions, in most cases.

Table 5.5 presents and compares the solution generation times taken by the *ILP* based optimal solution and the proposed heuristic algorithm *RaAS* (with $\mathcal{K}$=10), as the number of houses is varied from 2500 to 10000 (500 to 2000 houses for each of the 5 types), and four different variations for the number of time slots (T=$\{$24, 48, 72, 96$\}$). This table also depicts comparative results by showing the *speedups* obtained by *RaAS*

Table 5.5: *Average Execution times of ILP and RaAS, as #Houses and #Time slots are varied*

				No. of Households			
				2500	**5000**	**7500**	**10000**
No. of Time slots	**T=24**	**Exec. Times (in sec)**	**ILP**	236.72	1102.48	2034.86	3662.57
			RaAS	0.90	1.99	3.04	4.05
		Speedups		264.1	553.2	670.3	905.4
	T=48	**Exec. Times (in sec)**	**ILP**	294.48	1131.93	2818.95	5042.03
			RaAS	0.93	2.04	3.08	4.07
		Speedups		315.6	554.7	915.0	1239.3
	T=72	**Exec. Times (in sec)**	**ILP**	438.40	1526.62	3215.16	6057.16
			RaAS	0.95	2.09	3.18	4.19
		Speedups		459.4	731.1	1011.8	1444.3
	T=96	**Exec. Times (in sec)**	**ILP**	536.94	1862.51	4365.06	7506.27
			RaAS	0.99	2.18	3.24	4.30
		Speedups		543.3	855.7	1345.4	1745.1

over *ILP*. It may observed from the table that execution times of RaAS are significantly less than ILP for all cases with speedups varying between $\sim 2^8$ to $\sim 2^{11}$. For any fixed number of time slots, execution times corresponding to the *ILP* increase steeply as the number of houses within a microgrid becomes higher. This is because, the total number of appliances to be scheduled is proportional to the number of houses. With its exhaustive state space enumeration, the *ILP* is very sensitive to the number of appliances and hence, execution times drastically increase when the number of appliances grows. The optimal ILP strategy is also sensitive to the number of time slots to be scheduled. Hence, solution generation times are seen to increase at a high rate as the number of time slots into which a day is partitioned, increases. In comparison, RaAS incurs much lower execution times ($<\sim$5 seconds, in all cases) pointing to its scalability and thus its applicability, in large problem scenarios.

Figures 5.5 and 5.6 depict respectively the plots for the normalized revenues and average execution times of *RaAS*, for four different values of the number of *Bins* ($\mathcal{K}$={1,

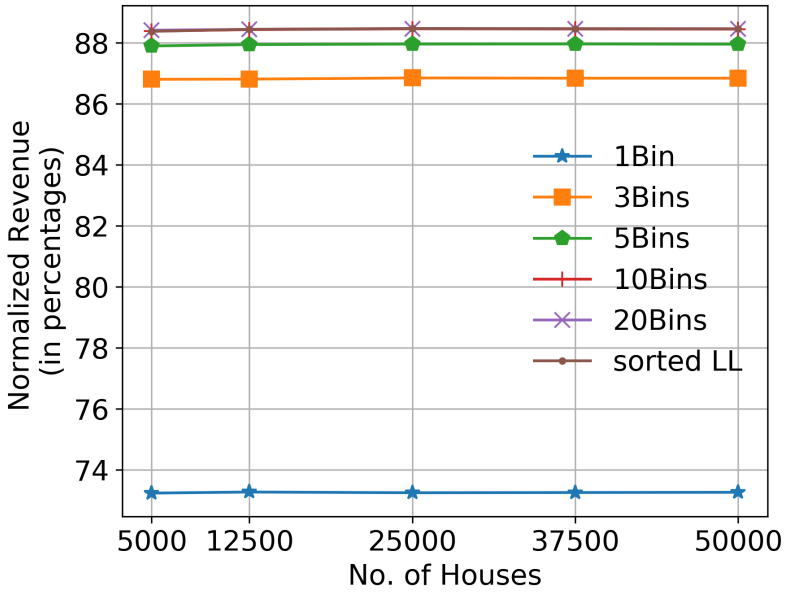

Figure 5.5: *Normalized revenues of RaAS, as the #Houses and #Bins are varied*

3, 5, 10}) and with the number of houses varying from 5000 to 50000 (1000 to 10000 houses for each of the 5 types). With this variation in the number of houses, the number of appliances to be scheduled ranges from ∼50000 to ∼500000. Figure 5.5 also shows the plot for a case ("sorted LL") where we consider a single linked–list or *Bin* in which all nodes are always maintained in non-increasing order of their key values. It may be noted that, when a single sorted linked–list is used, *RaAS* always finds and extracts the highest priority appliance node at the head of the linked–list. In comparison, any individual linked–list within a bucket sorted set of *Bin*s (as proposed in Algorithm 6), is unsorted. By extracting the node at the head of the highest indexed non–empty *Bin*, *RaAS* actually chooses a high priority node (which fall within the range of key values of this *Bin*); however, this node is not guaranteed to be the one with the largest key value. As the total revenue delivered by *RaAS* critically hinges on the selection of appliance nodes in non–increasing order of key values, performance of the algorithm improves as the number of *Bin*s considered, increases. From figure 5.5 it may be observed that, *RaAS* performs poorly when it has to work with a single unsorted *Bin*. However,

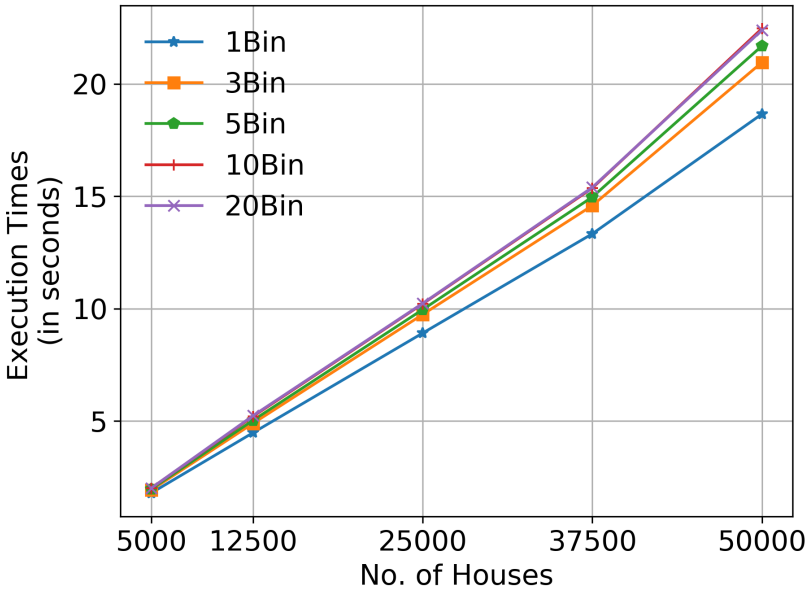

Figure 5.6: *Average execution times of RaAS, as the #Houses and #Bins are varied*

the performance significantly improves as the appliance nodes become more and more ordered (w.r.t key values) with increase in the number of *Bin*s from 3 to 20. Further we see that, performance achieved with 20 *Bin*s is same as that achieved using 10 *Bin*s. Additionally, the performance with 10 or 20 *Bin*s coincides with the normalized revenues achieved when a single sorted linked–list is used. This indicates that, approximately bucket sorting the appliance nodes into 10 *Bin*s is sufficient for RaAS to achieve peak performance, and there is no need to further increase the number of *Bin*s. On the other hand, we observe that there is hardly any change in obtained revenues when the number of houses are varied.

We experimentally evaluated that *RaAS*, when designed with a single sorted linked–linked, becomes computationally very expensive. For example, even for 5000 households (50000 appliances approx.), it takes 30 minutes on average to generate solutions. Analysis reveled that such high computation times are incurred primarily due to the overhead associated with the need to always maintain a very large number of appliance nodes in the form of an ordered linked–list. On the other hand, through a bucket sort based

design the appliance nodes are effectively sorted (approximately) in $\mathcal{O}(n)$ time (where n denotes the number of nodes). Moreover, all insertions and extractions on this *Bin* data structure can be performed in $\mathcal{O}(1)$ time. From figure 5.5 we saw that this "bucket sort" based design with 10 *Bin*s, performs equally well as a "single sorted linked–list" based design. From figure 5.6 we see that, even when the number appliances is of the order of 500000 (50000 households) execution time taken by *RaAS* is less than 25 seconds when 10 *Bin*s are used. Further, the execution times may be observed to increase linearly with increase in the number of houses. Furthermore, the execution times also increase with the increase in the number of bins, but the increase can be considered negligible. Collectively, execution times for all the data points is observed to be less than 20 odd secs, which demonstrates the scalable nature of the proposed algorithm.

5.4 Summary

In this chapter, a new price–based Demand Response scheme for scheduling appliances (*rigid* and *elastic*) within microgrids has been proposed. The appliance scheduling problem has been formulated as an Integer Linear Programming (ILP) problem and shown that optimal benchmark strategy (using a standard ILP solver called CPLEX) incurs high overheads in terms of solution generation times which may be inapplicable in many scenarios. Therefore, a fast but efficient heuristic algorithm named *Revenue–aware Appliance Scheduler* (RaAS) has been proposed. RaAS is able to produce appreciably good solutions with delivered revenues only about 2% lower on average, than the optimal *ILP* solutions. On the other hand, solution generation times of *RaAS* have been found to be 2^8 to 2^{11} times lower compared to the solutions obtained by the optimal strategy. Thus, *RaAS* is applicable even in big microgrids with a large number of appliance demands. In the next chapter, we deal with the problem of obtaining cost effective DER sizing decisions for designing a new microgrid.

Chapter 6

Sizing and Unit Commitment for Cost-Optimal Microgrid Designs

In the earlier chapters, we have considered different methodologies for scheduling and distribution of a limited amount of available power among the consumers within a single microgrid or among a group of peer microgrids. *In this chapter, we attempt to determine both, the optimal number of installations and the generation schedule of different types of distributed generators and the battery units together, such that overall generation related costs are minimized, while ensuring that the demand for power is satisfied at all times.*

Most essential microgrid components include, i) microsources/distributed generators (DGs) such as solar photovoltaics (PVs), wind turbines (WTs), microturbines (MT) and fuel cells (FC), ii) energy storage systems (ESS) like batteries, flywheels, pumped hydro-electricity etc, and iii) local flexible loads like electric vehicles, ACs, dish washers, etc. An appropriate mix of installations of DGs and batteries can mitigate overall emissions while ensuring a reliable power supply within a microgrid. Renewable DGs are widely available and are popular because of their clean/emission-less generations. However, these renewable DGs incur a high investment cost and thus, decisions on their installations have to be cost efficient. The optimal number of renewable DG installations is influenced by many parameters. A few critical parameters include, the unit's capital costs, the seasonal load profiles of a region, climatic conditions like the availability of solar irradiance and wind speeds within the region etc. The power generation from these renewable DGs

are volatile (rapidly changing) and intermittent (irregular) in nature. Such intermittent generations which cause demand and supply imbalances can be partially handled with the support of dispatchable DGs. The dispatchable units like microturbines (MTs) and fuelcells (FCs) are characterized by various specifications like minimum and maximum generation capacities, limits on ramp up and down rates, minimum on/off times, etc. Based on the amount of renewable generation these dispatchable generators need to be scheduled so that a given load is satisfied as well as spinning reserves are maintained for emergency purposes. Due to operational limitations and carbon emission bounds, it may not always be possible to economically schedule the dispatchable generators due to extreme peaks and valleys caused by intermittent renewable generations. Energy storage systems are a viable solution to this problem, where such storage mechanisms allow peak shaving of the load profiles with the ability to store surplus power generations from the renewable generators. *In this chapter, we model the mentioned sizing and unit commitment problem as a Mixed Integer Linear Programming (MILP) formulation. This formulation attempts to determine the optimal number of unit installations as well as the generation schedule of different DGs and batteries, such that, the total capital expenditure associated with DG installations as well as their operational costs at chosen generation levels, is minimized.*

It may be noted from the above literature that, the state-of-the art in microgrid design starting from appropriate unit commitment (UC) along with microgrid planning on optimal sizing and generation mix of PVs, wind turbines, microturbines, and batteries, may still be considered to be in its nascent stages. *In this work, we propose a generic model for systematic design space exploration which enables designers to determine microgrid sizing that converges to a cost minimal design point.*

6.1 The Models

Microgrids enable rapid integration and large scale penetration of renewable sources, therefore the wildly popular Photovoltaics (PV) and Wind Turbines (WT) are chosen as the prime components while designing a microgrid. The highly volatile, intermittent and

uncontrollable power from the renewables exhibit various challenges in grid operation. Controllable DGs like Microturbines (MT), Fuel Cells (FC) and energy storage systems like batteries are considered as an integral part of the system model, so that feasible grid operation can be ensured. We now present empirical models corresponding to each of the considered DGs as well as batteries.

6.1.1 Photovoltaic (PV) Power

Photovoltaic/Solar power is produced by a semiconductor device known as Photovoltaic (PV) cell, that directly transforms sunlight into electricity. These cells are connected in a series-parallel configuration to form a PV array and thereby scale to generate requisite energy level. The operation of a PV array depends on various factors which include electrical (PV efficiency, output power, temperature etc), environmental (solar irradiation, direction, rain, air temperature, etc.), physical (cell type, array size, etc.) and mechanical (position, incline angle, etc.) [27, 109]. Out of these, the most influential factors that effect the power output are array size, temperature and irradiance. Certain electronic circuits called Maximum Power Point Trackers (MPPT) are often used to ensure operation of the PV source at the maximum power point during different environmental conditions. There are several MPPT techniques that automatically find the voltage or current at which a PV array should operate to obtain the maximum power point [35,110,116]. The empirical model of a PV panel as used in [21] and [112] is shown by equation 6.1.

$$P_{PV}(A, I, Te) = \eta AI(1 - 0.005(Te - 25)) \tag{6.1}$$

Here, η is the conversion efficiency the solar cell array (%); A is the array area (m^2); I is the solar irradiance (kW/m^2); and Te is the ambient air temperature (° C).

In this work, we have used a software tool called System Advisor Model (SAM) to simulate a unit of solar pv system with the following specifications. The SunPower SPR-E19-310-COM module which has a maximum rated power 310 Wdc, nominal efficiency of about 19% and panel area 1.63 m^2, has been used. Yasakawa Solectria Solar SGI

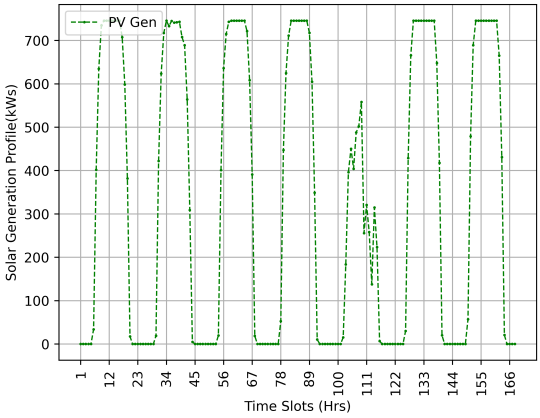

Figure 6.1: *Hourly Solar Generation for a typical week*

750XTM inverter with maximum output AC power of about 750 kW is selected for the simulation. Using the above components, an array of size 1000kWdc has been obtained. The modeled unit of pv system consists of 3228 modules, having 12 modules per string and 269 such strings in parallel, as the design configuration. The weather data from National Renewable Energy Laboratory (NREL) for the location Arizona (Lat 34.29, Long -111.66) has been used. The simulated solar generation for a typical week i.e., June 1 to June 7, can be seen in the figure 6.1.

6.1.2 Wind Turbines

Wind power is generated from wind turbines by the converting mechanical energy produced by the rotation of blades, into electrical energy. Wind Turbines are constructed near locations with strong and sustained winds. The power generation from wind turbines solely depends on the availability of the wind. Thus, wind speed predictions play an important role in anticipating the wind power. The empirical WT model based on the power curve of the turbine is given in equation 6.2 [21, 79].

$$P_{WT}(v) = \begin{cases} 0 & v \leq v_c \text{ or } v \geq v_f \\ p_r * \frac{v^k k - v_c^k}{v_r^k - v_c^k} & v_c \leq v \leq v_r \\ p & v_r \leq v \leq v_f \end{cases} \tag{6.2}$$

Here, p_r is the rated electrical power, v_c is the cut-in wind speed, v_r is the rated wind

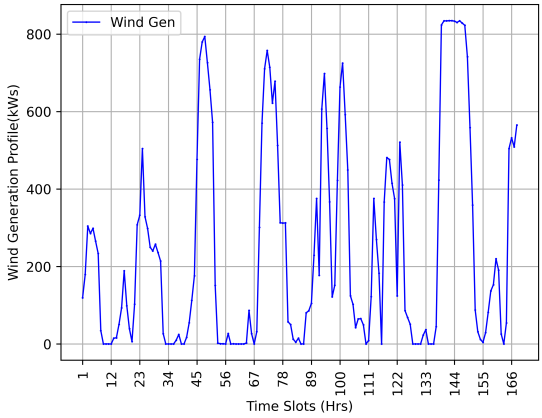

Figure 6.2: *Hourly Wind Generation for a typical week*

speed and v_f is the cut-off wind speed.

Similar to the PV system as simulated above, we have used SAM to simulate a unit of wind turbine system. Mitsubishi MWT 1000A wind turbine with 1000 kW rated power, $v_c = 3$ m/s, $v_r = 12$ m/s and $v_f = 25$ m/s has been modelled. The weather data from National Renewable Energy Laboratory (NREL) for the location Arizona (Lat 34.29, Long -111.66) has been used. The simulated wind generation for the design week i.e., June 1 to June 7, is shown in the figure 6.2.

6.1.3 Microturbines and Fuel Cells

Microturbine generators are based on the principle of micro-combustion and can generate powers ranging from few kWs to few hundred kWs. Microturbines harness fuels like natural gas, diesel, biogas etc., to generate power. The primary usage of microturbines is to provide back up and to compensate the intermittent and volatile power outputs from renewable sources. The quadratic fuel cost characteristic of a microturbine can be seen in equation 6.3 [21].

Fuel cells are the futuristic and innovative technologies that turn hydrogen and oxygen into electrical energy without emitting any harmful gases. The fuel cost equation for a fuel cell is similar to that of microturbine and is shown in equation 6.4.

Table 6.1: *Functional properties of microturbines and fuel cells*

Props	MT1	MT2	MT3	MT4	MT5	FC1	FC2	FC3	FC4	FC5
a($/h)	30	50	30	50	30	30	80	80	80	80
b($/kwh)	0.13	0.35	0.13	0.35	0.13	0.13	0.5	0.5	0.5	0.5
c($/kw2h)	1E-04	1E-04	1E-06	1E-04	1E-04	1E-06	1E-04	1E-04	1E-04	1E-06
P_(kW)	100	100	100	100	100	100	100	100	100	100
P^(kW)	2000	1000	2000	1000	2000	2000	1000	1000	1000	1000
C($/start)	150	30	150	30	150	150	30	30	30	30
RU(kW)	500	450	500	450	500	500	450	450	450	450
RD(kW)	500	450	500	450	500	500	450	450	450	450

$$F_{MT} = a_{MT} + b_{MT} \times p_{MT} + c_{MT} \times p_{MT}^2 \tag{6.3}$$

$$F_{FC} = a_{FC} + b_{FC} \times p_{FC} + c_{FC} \times p_{FC}^2 \tag{6.4}$$

where, a_{MT}, b_{MT} and c_{MT} are the cost coefficients of microturbine and a_{FC}, b_{FC} and c_{FC} are the cost coefficients of fuel cell. Because of the mechanics involved in these fuel based generators, they power output is constrained by other properties like, minimum and maximum rated power output, start up costs, ramp up and down limits. The table 6.1 shows the properties of 10 different generators that are considered in this work.

6.1.4 Energy Storage Systems (ESS)

Storage systems can used in microgrids to compensate the fluctuations caused by the renewable sources. The excess energy stored in the ESS can be utilized during periods when the renewable power is insufficient, thus ensure cost cutting caused by operating fuel based generators. Different types of storage technologies that exist are, electro-chemical batteries, super-capacitors and flywheel energy storage. Among them Lithium-ion (Li-ion) batteries are the most popular and are widely available. Because of their high

energy densities and long lifetimes, they are used in electric vehicles, space and avionics and power systems [41] and therefore are better suitable for portable microgrids as well.

Batteries capacities are normally expressed in two forms: Coulometric capacities (Ah) and Energy capacities (Wh). We follow the energy capacity notation. The battery specifications are typically attributed with C-rates and E-rates. A 1C rate battery with specified charge current will charge the whole battery in one hour and similarly, 1E rate battery with specified discharge power will discharge the entire battery in one hour. For example, 1E-rate 1 kWh battery with 1kW discharge power, discharges the entire battery in one hour and 1/2 E-rate 1 kWh battery with 500 watt discharge power will discharge the entire battery in two hours [1]. The charge and discharge equations for a battery are shown in equation 6.5. Where P_t^d and P_t^c are the discharge and charge powers at a time slot t. Δt is the charging and discharging duration unit (one hour as considered in this work). η_c and η_d are the charging and discharging efficiencies of the battery, respectively. Further, the operation of a system is constrained by the operating limits such as, maximum allowable power while charging and discharging 6.7, energy capacity limits 6.8, etc.

$$\text{Discharge:} \quad E(t+1) = E(t) - \frac{\Delta t P_t^d}{\eta_d} \tag{6.5}$$

$$\text{Charge:} \quad E(t+1) = E(t) + \Delta t P_t^c \eta_c \tag{6.6}$$

$$0 \leq P_t^d, P_t^c \leq P^{max} \quad \forall t \tag{6.7}$$

$$E^{min} \leq E(t) \leq E^{max} \tag{6.8}$$

Given the empirical models of the DGs and batteries, the next section presents a *Mixed Integer Linear Programming* (MILP) based problem formulation for designing a cost optimal microgrid that attempts to determine the optimal sizing of the DGs and batteries.

6.2 Proposed Mixed Integer Linear Program (MILP)-Optimal Sizing Problem Formulation

In this section, we first formulate the cost minimizing objective function and discuss various necessary constraints that define the feasible search space for the decision variables. We also provide description of the modeled decision variables that define the problem state space, as and when needed. The objective function is formulated as follows.

6.2.1 Cost minimizing objective function

The objective of designing a cost-effective microgrid is to minimize the total investment cost along with the operational cost of the microgrid. Investment cost may primarily include cost of buying and installation of the individual type of DGs and batteries, and the operational cost includes the cost for operating the DGs and batteries. Typically, the operation costs for the batteries and the renewable DGs are negligible and thus, are not considered in the formulations. The minimizing objective is shown in the equation 6.9

$$\textbf{Minimize} \quad \big(OC + IC\big) \tag{6.9}$$

where,

$$OC = \sum_{t}^{T} \sum_{i}^{N_{DG}=N_{mt}+N_{fc}} \Big[c_{t,i}^{pr} + c_{t,i}^{st}\Big] \tag{6.10}$$

and

$$IC = \Big[\sum_{i}^{N_{DG}=N_{mt}+N_{fc}} C_i^{inv} w_i\Big] + \Big[\sum_{j}^{N_{NDG}=N_{pv}+N_{wt}} C_j^{inv} w_j\Big] + \Big[\sum_{k}^{N_{BAT}} C_k^{inv} w_k\Big] \tag{6.11}$$

OC represents the total operational cost that is calculated for every nonrenewable DG unit (i.e., both microturbines and fuel cells) over T time slots. The operational cost of the non-dispatchable generators is negligible, therefore, the cost related to the operation of non-dispatchable generators is not considered in the objective. We introduce two sets of continuous decision variables: production cost (c^{pr}) and start up cost (c^{st}). $c_{t,i}^{pr}$ and $c_{t,i}^{st}$ refers to the cost of production and the start up cost, respectively, by the i^{th} non-dispatchable generator at the t^{th} time slot.

IC represents the total investment cost of the microgrid and is calculated as sum of three product terms, (i)the sum product of unit cost (C_i^{inv}) of N_{DG} number of nonrenewable DGs and its installation status w_i, (ii) the sum product of unit cost (C_j^{inv}) of N_{NDG} number of renewable DGs and its installation status w_j and, (iii) the sum product of unit cost (C_k^{inv}) of N_{BAT} number of batteries and its installation status w_k . For any given generator (including batteries), the installation status decision variable (say, w_i for the i^{th} nonrenewable DG) is set to 1 ($w_i = 1$), if the corresponding generator is chosen to be installed; otherwise it is set to 0 (i.e., w_i=0).

The minimizing objective is subject to various technical constraints that ensures reliable and secure operation of the microgrid. The necessary constraints are formulated as follows.

6.2.2 Constraints:

Production Cost ($c_{t,i}^{pr}$): The fuel cost incurred by the i^{th} non-renewable DG for generating $p_{t,i}$ amount of power at any given time slot t, is expressed as given in equation 6.12.

$$c_{t,i}^{pr} = a_i v_{t,i} + b_i p_{t,i} + c_i p_{t,i}^2 \quad \forall t \in T, \forall i \in N_{DG} \tag{6.12}$$

Here, a_i, b_i and c_i are the constant quadratic coefficients of the i^{th} generator, whose values are given in table 6.1. $v_{t,i}$ is the binary decision variable that is equal to 1 if the unit i is ON at time slot t, otherwise $v_{t,i} = 0$. A linear approximation to the above quadratic equation is represented using a piece-wise linear form which is shown in the equations 6.13-6.18, along with a graphical example shown in figure 6.3.

$$c_{t,i}^{pr} = A_i v_{t,i} + \sum_{l}^{NL_i} G_i^l \delta_{t,i}^l \quad \forall t \in T, \forall i \in N_{DG} \tag{6.13}$$

$$p_{t,i} = \underline{P}_i v_{t,i} + \sum_{l}^{NL_i} \delta_{t,i}^l \quad \forall t \in T, \forall i \in N_{DG} \tag{6.14}$$

$$\delta_{t,i}^1 \leq \left(UL_i^1 - \underline{P}_i\right) v_{t,i} \quad \forall t \in T, \forall i \in N_{DG} \tag{6.15}$$

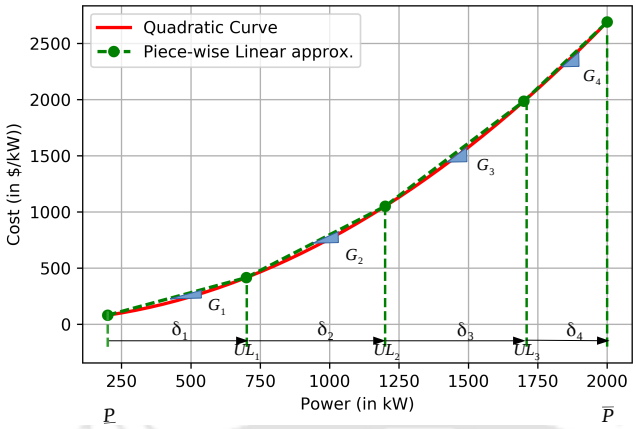

Figure 6.3: *Linearization of a Quadratic Curve* $c^{pr}(p) = 30 + 0.13 * p + 0.0006 * p^2$

$$\delta_{t,i}^{l} \leq \left(UL_i^l - UL_i^{l-1}\right) v_{t,i} \qquad \forall t \in T, \forall i \in N_{DG}, \forall l \in \left(2 \ldots NL_i - 1\right) \quad (6.16)$$

$$\delta_{t,i}^{NL_i} \leq \left(\overline{P}_i - UL_i^{NL_i-1}\right) v_{t,i} \qquad \forall t \in T, \forall i \in N_{DG} \quad (6.17)$$

$$\delta_{t,i}^{l} \geq 0 \quad \forall t \in T, \forall i \in N_{DG}, l \in \{1 \ldots NL_i\} \quad (6.18)$$

where, $A_i = a_i + b_i\underline{P} + c_i\underline{P}^2$.

Start up cost ($c_{t,i}^{st}$): When a dispatchable generator is brought back to *ON* state in the current time slot which was in the *OFF* state previously, significant start up cost is incurred. The equations 6.19 and 6.20 determine the start up cost incurred by the i^{th} generator at time slot t.

$$c_{t,i}^{st} = SC_i \left[v_{t,i} - v_{t-1,i}\right] \; \forall t \in T, \forall i \in N_{DG} \quad (6.19)$$

$$c_{t,i}^{st} \geq 0 \quad \forall t \in T, \forall i \in N_{DG} \quad (6.20)$$

Here, SC_i is the start up cost of i^{th} generator (refer, table 6.1) and $v_{t,i}$ is the binary decision variable which represents the operating status, (i.e., $v_{t,i} = 1$ if the i^{th} generator is ON at time slot t and $v_{t,i} = 0$ otherwise).

Investment cost: Equation 6.21 ensures that, a generator i can be scheduled to *ON* or *OFF* states only when it is installed (ie., $w_i = 1$).

$$v_{t,i} \leq w_i \quad \forall t \in T, \forall i \in N_{DG} \tag{6.21}$$

Real power balance: The aggregate power produced by the generators, i.e., non-renewable generation ($\sum_i^{N_{DG}} p_{t,i}$) and renewable generation ($\sum_j^{N_{NDG}} P_{t,j} * w_j$) along with the battery discharge and/or charge power at any given timeslot t must be at least that it satisfies the total load/demand at time slot t. A battery unit k can be assumed as a generator when it is discharging and can be assumed as a load when it is charging. Therefore, we introduce two sets of decision variables $p^c_{t,k}$ and $p^d_{t,k}$ to represent the charging and discharging power the battery unit k, respectively. The real power balance constraint is given by the equation 6.22.

$$\sum_{i}^{N_{DG}} p_{t,i} + \sum_{j}^{N_{NDG}} P_{t,j} * w_j + \sum_{k}^{N_{BAT}} v^d_{t,k}\, p^d_{t,k} \sum_{k}^{N_{BAT}} v^c_{t,k}\, p^c_{t,k} \geq D_t \quad \forall t \in T \tag{6.22}$$

Here, D_t represent the aggregate real power load at time slot t of the considered microgrid region.

Spinning reserves requirement: A microgrid operator need to maintain enough generation capacities (to compensate certain unexpected contingent situations like a generator failure or any disruption to the supply), so that within a short duration (say 10 min) the demand is met. Equation 6.23 ensures the spinning reserves requirement by the operator.

$$\sum_{i}^{N_{DG}} \overline{P}_{t,i} v_{t,i} + \sum_{j}^{N_{NDG}} P_{t,j} * w_j + \sum_{k}^{N_{BAT}} v^d_{t,k}\, p^d_{t,k} \sum_{k}^{N_{BAT}} v^c_{t,k}\, p^c_{t,k} \geq D_t + R_t \quad \forall t \in T \tag{6.23}$$

Ramp UP and Down Limits: With respect to a consequent pair of time slots, the rate of increase or decrease in the output of fuel based generators is constrained to ramp up (RU) and ramp down (RD) limits which is shown in equations 6.24 and 6.25.

$$p_{t,i} - p_{t-1,i} \leq RU_i \quad \forall t \in T, \forall i \in NG \tag{6.24}$$

$$p_{t-1,i} - p_{t,i} \leq RD_i \quad \forall t \in T, \forall i \in NG \tag{6.25}$$

Charge or discharge constraint: At any time slot t, a battery unit k can be either be charged or discharged but not both. The following equation 6.26 ensures this constraint.

$$v^c_{t,k} + v^d_{t,k} = 1 \qquad \forall k \in N_{BAT}, \forall t \in T \tag{6.26}$$

Battery capacity update: While charging or discharging power, the energy capacities of the batteries has to be updated. Therefore, the amount of energy charged ($v^c_{t,k} p^c_{t,k} \Delta t \eta_c$) is added to the capacity at time slot $t+1$, while the amount of energy discharged ($\frac{v^d_{t,k} p^d_{t,k} \Delta t}{\eta_d}$) is subtracted from the capacity at time slot $t+1$. Because of the above constraint 6.26, either energy is added/subtracted to the battery at a given time slot, but not both.

$$c_{t+1,k} = c_{t,k} + v^c_{t,k} p^c_{t,k} \Delta t \eta_c - \frac{v^d_{t,k} p^d_{t,k} \Delta t}{\eta_d} \quad \forall k \in N_{BAT}, \forall t \in T \tag{6.27}$$

Power charge and discharged limits: The amount of power charge ($p^c_{t,k}$) / discharge ($p^d_{t,k}$) given to a battery unit is bounded by the upper and lower limits, shown in the equation 6.28

$$P^{Min}_{BAT} \leq p^c_{t,k}, p^d_{t,k} \leq P^{Max}_{BAT} \qquad \forall k \in N_{BAT}, \forall t \in T \tag{6.28}$$

Battery capacity limits: The energy capacity ($c_{t,k}$) of a battery has a maximum and minimum limit as shown in the equation 6.29

$$C^{Min}_{BAT} \leq c_{t,k} \leq C^{Max}_{BAT} \qquad \forall k \in N_{BAT}, \forall t \in T \tag{6.29}$$

6.3 Experiments and Results

In this work, we consider three different microgrid scenarios and perform cost analysis on the optimized sizing results. In the first scenario, renewable generators and batteries are neglected i.e., a microgrid with only fuel based generators (microtubines and fuelcells) has been designed. In the second scenario, results for both renewable generators (solar and wind) as well as with the dispatchable fuel based generators (microturbines and fuelcells) has been obtained. In the last scenario, we add battery systems to the previous scenario and perform optimization. All the case studies are performed by tak-

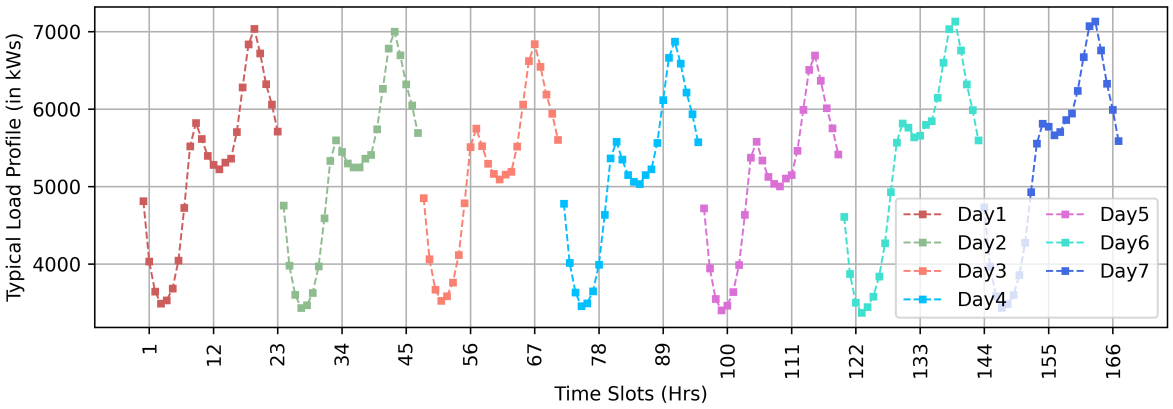

Figure 6.4: *Typical Loads during summer*

ing into consideration weather data and load profile for the region Arizona, US (Lat. 34.29, Long. -111.66). The required weather data and load profiles has been obtained through the National Renewable Energy Laboratory web portal. Precisely, the hourly data corresponding to a particular week of the month June (June 1 to June 7 of a typical meteorological year (TMY3)) has been taken as input. The input data consists of 168 entries (i.e., the number of times slots $T = 168$), each corresponding to a particular hour of a typical week. The load profiles for the considered region are shown in figure 6.4. The design space exploration of the MILP sizing optimization problem, as formulated in Section 6.2, has been performed using an industry standard ILP solver called IBM CPLEX on a 3.2 GHz quad core computing system.

6.3.1 Case 1: Sizing Microturbines and Fuel cells

The cost of a single Microturbine/Fuel cell unit is approximately $\$650,000$, for a rated power of 1000kW system. With a 10 year life time, the normalized cost (C_i^{inv}, $\forall i \in \{1..N_{DG}\}$) for one week design period can be calculated as $(650000*7)/(10*365) = \$1246$. Given the hourly load profiles over a week, the solution prescribes the installation of five microturbines, and four fuel cells are needed to be installed. The obtained total cost of this system is 331015. Thus, the total fuel cost can be calculated as $331015 - 1246*9 = 319801$. With the aggregate load for the entire week being 874688kW, the per unit cost

becomes, \$331015/874688kW = \$.37. Given, the approximate CO_2 emissions for 1kW of power generated using a microturbine to be 720g, the total emissions can be calculated as $319801 * 720 = 230256$ kilo grams.

6.3.2 Case 2: Sizing fossil fuel generators with renewable generators

In this case study, we take into consideration both the renewable generators, solar photovoltaics and wind turbines. The total cost for a 1000kWdc PV system and 1000kW wind turbine, as designed using SAM tool, is approximately \$1028, 838 and \$1303, 000, respectively. Assuming a typical life time of about 25 years for both the renewable generators, the normalized cost of one PV system is approximately $C_j^{inv} = \$780$, $\forall j \in \{1..N_pv\}$ and one wind turbine is $C_j^{inv} = \$994$, $\forall j \in \{1..N_wt\}$. The optimal sizing obtained for this system is as follows, four microturbines, one fuel cell, eight PVs and sixteen wind turbines. The total cost of the system is \$98044.

6.3.3 Case 3: Sizing Distributed Generators with batteries

The last case study deals with the optimal sizing problem including battery system. One unit of Lithium Ion Nickel Manganese Cobalt oxide battery system with a 4000kWh capacity and 1000kW rated power has been considered. The other specifications of the battery system are, maximum C-rate discharge and maximum C-rate charge is 0.25 per/hr, maximum depth of discharge is upto 75%, charging efficiency $\eta_c = 0.9$ and discharging efficiency $\eta_d = 1.11$. The total cost of the battery unit is about \$1310676. With a 25 year life time, the normalized cost $C_k^{inv} = \$1005$. Given the hourly load profiles over a week, the optimal sizing is obtained as follows, four microturbines, one fuel cell, seven PVs, sixteen wind turbines and five battery systems. The total cost of the system is obtained as \$78870. It may be observed, that a significant cost savings can be achieved by including appropriate sized battery system. The load, generation and battery profiles for this scenario can be seen in figure 6.5. Further it may be observed from this figure that, the combined generation (green bars in figure 6.5) from the installed

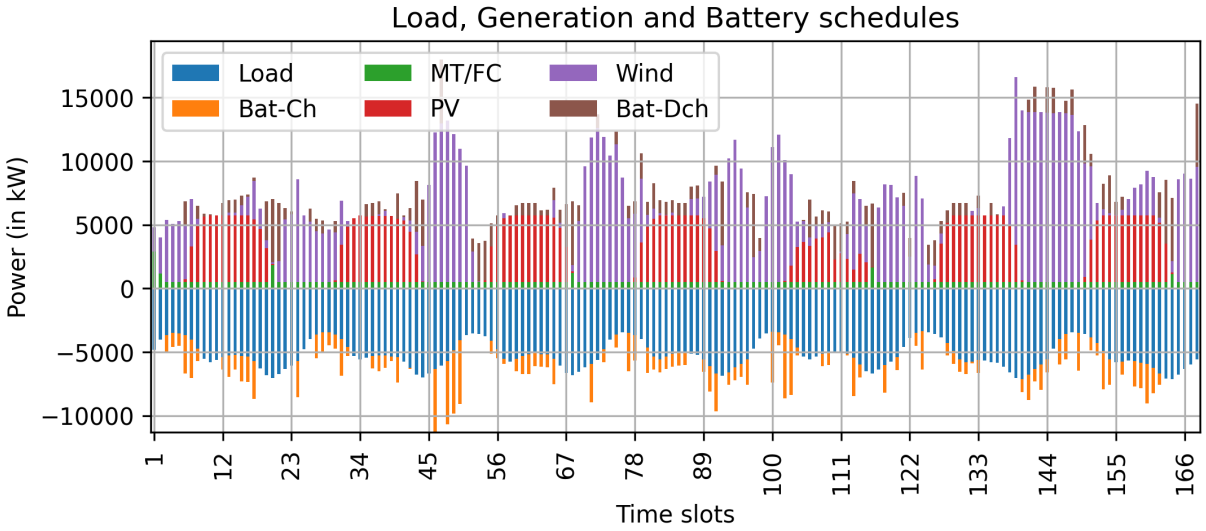

Figure 6.5: *Load, Generation and Battery schedules*

microturbines and fuel cells is only about ∼600kW of power at any given timeslot in the schedule week.

6.4 Summary

This work presents a generic methodology for obtaining optimal sizing of the distributed energy resources viz., PVs, wind turbines, microturbines, fuel cells and batteries such that the total cost of investment as well as the operational cost is minimized. The optimization problem has been formulated as a mixed integer linear programming (MILP) and the design space exploration has been conducted using an industry standard ILP solver called IBM CPLEX. Different case studies have been analyzed by taking into consideration weather and load profile data for the specific state region Arizona, US. The obtained results specify that significant cost can be reduced by investing on the renewable generations along with the fossil fuel based generators. Results also show that the incurred cost can be further reduced with the inclusion of battery systems into the system.

Chapter 7

Conclusions and Future Perspectives

7.1 Summarization

Next generation smart grids are expected to transform into a distributed network of small scale power systems called Microgrids. A microgrid may be defined as a collection of heterogeneous distributed generation systems, storage devices and electric loads, which operate in a coordinated manner and is spread over a small geographical region. Therefore, these girds are relatively small scale power systems which can incorporate everything starting from generation and transmission to distribution as well as consumption, within the confine of the small region of its purview. Microgrids can sometimes be self-sufficient if the demand–supply balance can be maintained by its own resources. Otherwise, in general, a microgrid connects to an external grid so that it can import the deficit power (net requirement) to meet its demand. Being smaller in size, microgrids allow rapid integration of renewable distributed energy resources (DERs) within its distribution systems. However, the variable nature of these renewable DERs pose significant challenges to the system operators in maintaining precise balance between supply and demand. In this context, microgrid design and operations planning are important, yet challenging problems. This is because, a microgrid must be able to manage generation from heterogeneous DERs such as renewables, micro-generators, batteries, occasional buying and selling etc., as well as control consumption (if necessary), so that the system is operated in a reliable and economic fashion. Due to inherent complexity in

managing these resources and rising generation capacities from renewables, occurrence of frequent power shortage scenarios can be a harsh reality even to grids of the future. In this dissertation, we have proposed efficient methodologies for power distribution, appliance scheduling and real–time power balancing, especially to cope with power shortage scenarios. Design of a microgrid deals with the determination of appropriate sizes of suitable DERs that are able to reliably satisfy the loads of a region in a cost effective manner. As a spin–off, this thesis has addressed a few problems related to appropriate sizing of DERs that can satisfactorily balance loads in a cost effective manner. Effective sizing solutions are critical in the planning/design of a new microgrid.

In recent years, researchers have dealt with various electricity distribution and appliance scheduling problems. We have observed that, most of these problems are typically oriented towards reducing peak load consumption. However, due to increasing penetration of variable generation by renewables, especially in microgrids and networks of microgrids, the system is expected to face a significant number of transient power shortage scenarios. This is especially true for grids in developing nations like India, which face severe intermittent power deficits. Power shortages are typically handled by a mechanism called rolling blackouts. Blackouts can cause severe problems as electricity is cutoff to even essential loads which may include business critical establishments as well as basic conveniences like lights and fans. Therefore, there is a dire need for schemes which have benign side-effects and at the same time are efficient in achieving precise control over power distribution during power shortages. Improved smart grid technologies such as smart meters and information and communication systems that enable near real-time bi-direction flow of power generation and usage information, have increased practical applicability of such efficient schemes. These schemes are called Demand Response programs which attempt to alter consumers' demand profiles so that demand-supply balance can be achieved when grid reliability is jeopardized. Brownout is one such important DR scheme which allows selective provisioning of power supply to support essential loads while curtailing supply to less critical ones. The first three contributory chapters (Chapters 3, 4 and 5) deal with the design of efficient brownout based

electricity distribution and allocation strategies especially when grids (a microgrid or a network of microgrids) are facing power shortages. More specifically, Chapter 3 deals with the problem of equitably distributing a limited amount of power available with an electricity distribution company (EDCo) among a set of microgrids under its purview, based on demands advertised by them. The system is modeled as follows. The EDCo uniformly grades appliances into a discrete set of urgency classes. Here, urgency refers to the priority towards uninterrupted power supply. Each of these classes is assigned a utility value, so that higher the urgency, higher is the utility value. The EDCo also prescribes a uniform tariff policy, where a consumer appliance is charged/levied a tariff which is proportional to the utility value of the urgency class to which the appliance is graded. Given this setup, microgrid aggregators are expected to advertise consolidated demands of their consumers as a discrete set of class–wise cumulative choices. Here, choice refers to a pair consisting of a class's cumulative demand and its utility value. Based on the choices reported by a set of microgrid aggregators, the EDCo attempts to disburse its available power among the microgrids, such that aggregate system level utility is maximized.The problem takes into consideration that, the microgrids can be self-centered and may untruthfully advertise inflated demands in order to maximize their own profit. To prevent such activities by selfish microgrids, we propose a truthful mechanism for fairly allocating power against bids made by a set of rationally acting microgrids. The proposed mechanism consists of an optimal allocation strategy called Dynamic Programming based Allocator (DPA) and a pricing policy called VCG based Equitable Pricing (VCG–EP). DPA delivers an optimal distribution strategy for the available power to the microgrids. On the other hand, an aggregator's payment computed by VCG-EP is determined by the maximum total sacrifice in the utility suffered by the other aggregators for the amount of power allocated to the aggregator. Such a mechanism ensures that the payment made by a microgrid aggregator (for the amount of power allocated to it) is minimum when he is truthful.

A truthful mechanism scheme as the one mentioned above involves multiple stakeholders and in general is computationally elaborate. Hence, they are typically applied

for day-ahead/week-ahead electricity auction markets. However, the need for equitable distribution among multiple parties may be necessary in more transient near real-time scenarios as well. Obviously in such cases, the scheme discussed above is not applicable. For example, grids may face transient power deficit scenarios due to sudden surges in demands and/or forecast errors related to renewable generation. IEEE Standards on Power Quality (IEEE std. 1159) recommends that, such dynamic imbalances must be mitigated within about 0.5 seconds, in order to maintain satisfactory power quality. In Chapter 4, we deal with the design of real-time brownout based power distribution mechanisms for handling power shortages in such dynamic scenarios. To perform such controlled distribution, the utility provides a set of priority classes where each class is associated a tariff value such that higher the priority, higher becomes the associated tariff value. Here, priority refers to the urgency towards uninterrupted power supply. A consumer is free to choose any one of the priority classes for his appliance (non-essential). Based on the consumer's choices, the demands within any given subarea can be consolidated into a discrete set of cumulative choices. Given these choices, the electric utility conducts a revenue aware electricity distribution of limited available power, so that the total revenue earned by the utility is maximized. The problem has been formulated as an Integer Linear Programming (ILP). We have shown that, conventional Dynamic Programming (DP) based approaches are computationally expensive and cannot satisfy the real-time requirement presented above, even for grids having moderate sizes. Therefore, we have proposed a streamlined version of DP (called SDPA) which is optimal and yet applicable to moderate sized grids. SDPA is found to be about 9 to 33 times faster than DP. As example, given 50 subareas under the purview of an EDCo, 10 urgency classes and 250 MW of available power, SDPA takes $\sim$0.5 sec to generate a solution. Thus, SDPA can be suitable for scenarios having a few number of subareas. However, even SDPA fails to deliver a solution for scenarios having higher number of subareas and/or higher amounts of available power, within the time bound. Therefore, we have proposed a fast and efficient heuristic algorithm (called PBPA) which is able to generate solutions in upto 4 orders of magnitude faster than SDPA. Although, the quality of these solutions

are found to be less effective of only upto 12%, due to its ability to quickly restore power balance, PBPA can be deployed for real–time power distribution.

Power deficit scenarios within a microgrid mainly occur due its significant dependence on renewable generation. One way to handle power deficits is by procuring the required amount of power from an external source such as an EDCo. Chapter 3 and chapter 4 deals with such handling mechanisms. Oftentimes, it may not be a feasible choice especially for some remote microgrids which are mostly independent/disconnected. In the fifth chapter, we study the problem of appliance scheduling from the perspective of an islanded microgrid. Consumer appliances can be of rigid or elastic types. In addition, appliances can have varying urgency (towards uninterrupted power supply) as well as preferred time intervals for successfully completing a designated task. Chapter 5 focuses on the following scheduling problem. Given, time slot wise predicted amounts of available power with a microgrids, determine a tentative schedule of consumer appliances by taking into consideration the priority of consumer appliances, the type (rigid or elastic) as well as preferred time intervals during which appliance operations are requested. The scheduling problem is observed to be computationally hard and optimal solution generation strategies can lead to substantial overheads. Thus, we proposed a heuristic algorithm called *Revenue–aware Appliance Scheduler* (RaAS) for generating appliance schedules. RaAS performs appreciably well in terms of solution quality with only about 2% lower on average, than optimal solutions. Contrarily, RaAS was found to be 2^8 to 2^{11} times faster when compared to optimal solution generation times.

In addition to the power distribution (Chapter 3), real time power balancing (Chapter 4) and appliance scheduling (Chapter 5) problems, we have also dealt with the microgrid sizing problem in Chapter 6. In the last contributory chapter (Chapter 6), we have attempted to address the problem of determining optimal number of installations of distributed energy resources which include PVs, wind turbines, microturbines as well as batteries. The objective of this sizing problem is to minimize the sum of installation expenditure and operating costs so that the demand for a designated time period is reliably met in a cost effective manner. We model this problem as a Mixed Integer

Linear Programming (MILP) and perform a systematic state space exploration using an industry standard ILP solver called CPLEX. The procedure delivers an optimal solution to the combined problem of the sizing and unit commitment, by taking into account location specific demand and weather data as well as technical properties of DERs and batteries. Experiments have been conducted by taking into consideration the load profiles and weather data for a specific state region namely Arizona, US. Results show that optimal DER sizing for the chosen region exists and significant amounts of total system cost can be reduced by selecting appropriate number of renewable units and batteries.

In summary, the work presented in this thesis focuses on designing efficient policies for microgrid sizing, equitable power distribution, appliance scheduling as well as real–time power balancing. Scheduling algorithms both optimal and heuristic, have been proposed for different power allocation/distribution problems especially in microgrids. Extensive experiments on various microgrid scenarios have been conducted to validate the efficacy of the proposed scheduling strategies.

7.2 Future works

The works presented in this thesis leaves several open directions and there is ample scope for future research in this area. The following are a few future research directions that can be explored.

- **Combined scheduling of preemptive and non-preemptive rigid/elastic appliances in a Microgrid.**

  In Chapter 5, we have dealt with the appliance scheduling problem from the perspective of a islanded microgrid. There, the appliances within a microgrid were considered to be either of rigid and elastic type. While the power consumption of elastic appliances can be deferred/shifted, the supply to rigid appliances cannot be shifted, but can be curtailed if so needed. All appliance requests were considered to be non-preemptive in nature. That is, if an appliance has been scheduled to

start its operation, the supply must be maintained till it finishes its designated task, without any interruption. However, there are practical scenarios where appliance operation may be interrupted provided the designated operation/task is finished within a deadline. For example, charge scheduling of an electric vehicle can be performed in a preemptive manner (with possible intermittent interruptions) provided it is fully charged before the stipulated start hour of its usage. Yet another example is an electric dish washer whose requirement is to finish washing before lunch/dinner times. The overall duration of washing may however include intermediate ideal times when no washing is performed. A few other appliances which may allow preemption are vacuum cleaners, cloth washers and water pumps.

It may be noted that, for a given a set of rigid and elastic appliances, inclusion of preemptive appliance requests within the mix lends more flexibility in the generation of appliance schedules and can allow improved utilization of a given amount of energy resource. However, handling a diverse mix of rigid and elastic appliances which can either be preemptive or non-preemptive, can significantly increase the problem complexity. In recent years, researchers have proposed various appliance scheduling problems which are primarily oriented towards minimization of electricity cost, peak to average load ratio minimization, maximization of user satisfaction [108] etc. Considering only non-preemptive appliances, authors in [14] have modeled the appliance scheduling problem as a variation of *strip packing* whose objective is to minimize overall peak loads. The problem has then been further extended with the inclusion of preemptive appliances, in [17]. However, these problems do not take into consideration possible variation in total available power over time, appliance requests having different priorities and time slot preferences of appliances etc.

Considering the above mentioned factors, we plan to solve the following appliance scheduling problem. Each appliance request (provided by consumers) consists of the following information: i) priority towards uninterrupted supply (expressed by subscribing to one among a set of alternative price tariff offered by an EDCo), ii)

rated power, iii) type (rigid or elastic), iv) preemptability (whether preemption is allowed), v) execution times (in time slots) along with a list of preferred start times and associated deadlines for completion. Given, a) time slot wise estimates of available power with an EDCo, b) the consumer appliance requests, and c) a monetary penalty policy for deferring appliance to non-preferred time intervals, the objective is to determine a schedule for the appliances such that the EDCo's revenue is maximized. We would like to formally model the above scenario as a constraint optimization problem and design search based, heuristic and learning oriented strategies for the same.

- **Criticality aware peak load constrained scheduling of thermostatically controllable appliances**

  HVAC (Heating, Ventilation and Air Conditioning) devices generally contribute to a significant chunk of a power system's overall energy demand. A study in [70] suggests that HVAC systems may account for more than 50% of the total energy consumption in residential and commercial buildings. These devices are usually used to maintain temperature of a stipulated confined space/area (called thermal zone) within a desired range. For HVACs devices in general and ACs in particular, this temperature band is often referred to as the Thermal Comfort Band (TCB). The operation of HVAC devices is controlled by thermostats which maintain the thermal zone under consideration at the desired temperature band by enforcing a stipulated pattern of device ON-OFF cycles. It may be noted that, uncoordinated operation of the huge number of HVAC devices in today's power systems can lead to an unduly stressed system, when the ON cycles of a large fraction of these devices are in phase, thereby resulting in high peak loads. With limited generation capabilities which may also often be intermittent due to the presence of renewables, handling such peak surges becomes critically important especially for microgrids.

  Researchers have traditionally dealt with this problem by designing scheduling strategies for intelligently multiplexing the ON-OFF cycles of a given set of HVAC devices such that peak loads are either minimized or remain capped below an upper

bound [15, 16, 54, 57, 106]. Jindal et at. proposed a HVAC scheduling mechanism to minimize the total energy consumption of university buildings [54]. An efficient strategy for controlling water heaters has been proposed by Shah et al., specifically for time-of-usage based electricity pricing scenarios [106]. Authors in [15, 57] proposed efficient energy management solutions for maintaining comfort bands (TCBs) of a set of thermal zones (controlled by a set of air conditioning devices), under peak load constraints.

As a future work, we would like to extend the above scheduling problem for thermal zones with varying criticality. In addition, each thermal zone may have multiple alternative TCBs with different QoS (Quality-of-Service) values. Here, QoS associated with the TCB of a thermal zone (along with the thermal zone's criticality) determines the reward that the system acquires by maintaining temperatures at that TCB. Let us consider a hypothetical campus microgrid scenario consisting of different establishments such as server rooms, offices, health centers, class rooms, residences, business establishments, laboratories, etc. Different thermal zones within these establishments can have varying criticality. For example, adhering to specific TCBs may be considered to be relatively more critical for thermal zones such as say server rooms or hospital rooms compared to rooms within household establishments. In addition, a thermal zone may allow service at different alternative TCBs, although preferences (QoS values) towards these TCBs may vary. As example, a patient's room within a hospital may have a most preferred TCB say 22-24°C. This TCB may be considered to deliver the highest comfort level; measured by assigning highest QoS value to this TCB. However, the room may allow other alternative TCBs with lower associated QoS values such as 23-25°C and 24-27°C. A criticality weighted QoS value may be considered as the reward for serving as thermal zone at a specific TCB. The objective of the problem could be to maximize aggregate reward when a given set of thermal zones needs to be serviced with a limited total power budget.

- **Generalized microgrid sizing problem**

  In Chapter 6, we have studied the problem of determining appropriate sizes of DERs like microturbines, fuel cells, wind turbines, PVs as well as storage systems like batteries. The objective is to minimize total cost (investment and operational costs) incurred to reliably satisfy demands of a region over a time interval, taking into consideration variations in solar irradiances and wind speeds. The problem has been modeled as a mixed integer linear program (MILP) and we have proposed a generic methodology for systematic design state space exploration using an industry standard ILP solver called IBM CPLEX. ILP based solution strategies are generally NP-Hard and thus perform poorly with increasing input sizes. It may be noted that, this microgrid sizing problem consists of a master problem which deals with sizing aspects of DERs and a sub-problem which determines the commitment schedules of DERs. Although, the master problem can be thought of as a static problem which deals with the binary decisions on whether to choose a unit or not, generating commitment schedules of DERs are sensitive to the dynamic variations associated with renewables based generation, seasonal load profiles, fossil fuel prices, etc. As a future work, we would like to extend the work in chapter 6 by proposing an efficient heuristic strategy for the sub-problem i.e., a microgrid's unit commitment problem. This heuristic strategy is intended to be fast but efficient and should take the output of the static part as its input. We expect this solution to not only to be lighter in weight (in terms of computational overheads) compared to methodology proposed in Chapter 6, but also more efficient as it will be aware of dynamic variations of many important system parameters.

- **DER Sizing with Demand Response** Certain demands corresponding to deferrable appliances within a microgrid can be elastic and sensitive to the tariff set by the microgrid utility. The *Law of Demand* states that, if price for a good is set higher than usual, then the demand for the good decreases. This applies even to electricity demands. In this context, price elasticity is defined as the ratio of the percentage change in load to the percentage change in the price [123]. For example,

if a 50% price hike leads to 50% reduction in load, then the price elasticity is said to be unity. On the other hand, if this 50% price hike leads to only a 10% drop in load, then the price elasticity is 0.2. In addition, in most practical scenarios, price elasticity of electricity loads can be different for different time periods. For example, the loads during peak periods are in general less elastic. In comparison, the demands during off peak periods and mid peak periods can be considered to be more elastic. Here, we intend to solve the following problem. Given the price/demand elasticity values at different time slots of a day, the problem is to determine the dynamic hourly prices for a given load such that a microgrid utility obtains a targeted profit at the end of the day while reliably satisfying the load.

Disseminations out of this Work

Journal Papers

- **Basina Deepak**, Satish Kumar, Sambit Padhi, Arnab Sarkar, Arijit Mondal, Krithi Ramamritham, "Brownout based Blackout Avoidance Strategies in Smart Grids", *IEEE Transactions on Sustainable Computing*, 2020. [Published]
- **Basina Deepak**, Arnab Sarkar, Diganta Goswami, "An Efficient Framework for Brownout Based Appliance Scheduling in Microgrids", *Sustainable Cities and Society, Elsevier*, 2021. [Published]
- **Basina Deepak**, Arnab Sarkar, Diganta Goswami, "Equitable Electricity Distribution and Pricing for a Network of Microgrids", *Sustainable Cities and Society, Elsevier*, 2022. [Submitted]
- **Basina Deepak**, Arnab Sarkar, Diganta Goswami, "A Generic Framework for Designing a Cost–Optimal Microgrid". [To be communicated]

Conference Papers

- **Basina Deepak**, Satish Kumar, Sambit Padhi, Arnab Sarkar, Arijit Mondal, Krithi Ramamritham, "Brownout based Blackout Avoidance Stragtegies in Smart Grids", *Proceedings of the Ninth International Conference on Future Energy Systems (e–energy)*, 2018. [Published]

References

[1] A Guide to Understanding Battery Specifications. [Online]. Available: http://web.mit.edu/evt/summary_battery_specifications.pdf [Pg.127]

[2] "Delhi electricity regulatory commission tariffs." [Online]. Available: http://www.derc.gov.in/sites/default/files/Tariff[space]20Schedule[space]202020-21.pdf [Pg.114]

[3] "Load Generation Balance report, Central Electricity Authority, India," http://www.cea.nic.in/reports/annual/lgbr/lgbr-2016.pdf. [Pg.31]

[4] H. Aalami, M. P. Moghaddam, and G. Yousefi, "Modeling and prioritizing demand response programs in power markets," *Electric Power Systems Research*, vol. 80, no. 4, pp. 426–435, 2010. [Pg.36]

[5] T. Abdelzaher and K. G. Shin, "End-host architecture for qos-adaptive communication," in *Real-Time Technology and Applications Symposium, 1998. Proceedings. Fourth IEEE.* IEEE, 1998, pp. 121–130. [Pg.68], [Pg.69], [Pg.72], [Pg.87], [Pg.90]

[6] J. Aghaei and M.-I. Alizadeh, "Demand response in smart electricity grids equipped with renewable energy sources: A review," *Renewable and Sustainable Energy Reviews*, vol. 18, pp. 64–72, 2013. [Pg.34]

[7] D. Akinyele, J. Belikov, and Y. Levron, "Challenges of microgrids in remote communities: A steep model application," *Energies*, vol. 11, no. 2, p. 432, 2018. [Pg.15], [Pg.97]

[8] S. Bahramirad, W. Reder, and A. Khodaei, "Reliability-constrained optimal sizing of energy storage system in a microgrid," *perspectives*, vol. 1, p. 3, 2012. [Pg.42]

[9] N. N. A. Bakar, M. Y. Hassan, M. F. Sulaima, M. Na'im Mohd Nasir, and A. Khamis, "Microgrid and load shedding scheme during islanded mode: A review," *Renewable and Sustainable Energy Reviews*, vol. 71, pp. 161–169, 2017. [Pg.16], [Pg.97]

[10] D. R. Basina, S. Kumar, S. Padhi, A. Sarkar, A. Mondal, and R. Krithi, "Brownout based blackout avoidance strategies in smart grids," *IEEE Transactions on Sustainable Computing*, 2020. [Pg.8]

[11] E. Bini, G. Buttazzo, J. Eker, S. Schorr, R. Guerra, G. Fohler, K.-E. Arzen, V. Romero, and C. Scordino, "Resource management on multicore systems: The actors approach," *IEEE Micro*, vol. 31, no. 3, pp. 72–81, 2011. [Pg.68]

[12] G. Cau, D. Cocco, M. Petrollese, S. K. Kær, and C. Milan, "Energy management strategy based on short-term generation scheduling for a renewable microgrid using a hydrogen storage system," *Energy Conversion and Management*, vol. 87, pp. 820–831, 2014. [Pg.41]

[13] I. Central Electricity Authority, *Load Generation Balance Report*, 2020, https://cea.nic.in/l-g-b-r-report/?lang=en. [Pg.7], [Pg.13], [Pg.31]

[14] N. Chakraborty, A. Mondal, and S. Mondal, "Efficient scheduling of nonpreemptive appliances for peak load optimization in smart grid," *IEEE Transactions on Industrial Informatics*, vol. 14, no. 8, pp. 3447–3458, 2017. [Pg.9], [Pg.16], [Pg.38], [Pg.143]

[15] N. Chakraborty, A. Mondal, and S. Mondal, "Intelligent scheduling of thermostatic devices for efficient energy management in smart grid," *IEEE Transactions on Industrial Informatics*, vol. 13, no. 6, pp. 2899–2910, 2017. [Pg.37], [Pg.145]

[16] N. Chakraborty, A. Mondal, and S. Mondal, "Multiobjective optimal scheduling framework for hvac devices in energy-efficient buildings," *IEEE Systems Journal*, vol. 13, no. 4, pp. 4398–4409, 2019. [Pg.9], [Pg.38], [Pg.145]

[17] N. Chakraborty, A. Mondal, and S. Mondal, "Efficient load control based demand side management schemes towards a smart energy grid system," *Sustainable Cities and Society*, vol. 59, p. 102175, 2020. [Pg.37], [Pg.143]

[18] C. Chen, S. Kishore, and L. V. Snyder, "An innovative rtp-based residential power scheduling scheme for smart grids," in *2011 IEEE International Conference on Acoustics, Speech and Signal Processing (ICASSP)*. IEEE, 2011, pp. 5956–5959. [Pg.35]

[19] C. Chen, J. Wang, and S. Kishore, "A distributed direct load control approach for large-scale residential demand response," *IEEE Transactions on Power Systems*, vol. 29, no. 5, pp. 2219–2228, 2014. [Pg.8]

[20] S. Chen, Q. Chen, and Y. Xu, "Strategic bidding and compensation mechanism for a load aggregator with direct thermostat control capabilities," *IEEE Transactions on Smart Grid*, vol. 9, no. 3, pp. 2327–2336, 2016. [Pg.45]

[21] S. Chen, H. B. Gooi, and M. Wang, "Sizing of energy storage for microgrids," *IEEE Transactions on Smart Grid*, vol. 3, no. 1, pp. 142–151, 2012. [Pg.6], [Pg.42], [Pg.123], [Pg.124], [Pg.125]

[22] C. Clastres, "Smart grids: Another step towards competition, energy security and climate change objectives," *Energy Policy*, vol. 39, no. 9, pp. 5399–5408, 2011. [Pg.32]

[23] C. Deckmyn, J. Van de Vyver, T. L. Vandoorn, B. Meersman, J. Desmet, and L. Vandevelde, "Day-ahead unit commitment model for microgrids," *IET Generation, Transmission & Distribution*, vol. 11, no. 1, pp. 1–9, 2017. [Pg.98]

[24] R. Deng, Z. Yang, M.-Y. Chow, and J. Chen, "A survey on demand response in smart grids: Mathematical models and approaches," *IEEE Transactions on Industrial Informatics*, vol. 11, no. 3, pp. 570–582, 2015. [Pg.33]

[25] M. A. Deppert, K. Jansen, A. Khan, M. Rau, and M. Tutas, "Peak demand minimization via sliced strip packing," *arXiv preprint arXiv:2105.07219*, 2021. [Pg.38]

[26] K. P. Detroja, "Optimal autonomous microgrid operation: A holistic view," *Applied energy*, vol. 173, pp. 320–330, 2016. [Pg.41]

[27] V. Devabhaktuni, M. Alam, S. S. S. R. Depuru, R. C. Green, D. Nims, and C. Near, "Solar energy: Trends and enabling technologies," *Renewable and Sustainable Energy Reviews*, vol. 19, pp. 555–564, 2013. [Pg.123]

[28] M. Diekerhof, S. Schwarz, F. Martin, and A. Monti, "Distributed optimization for scheduling electrical demand in complex city districts," *IEEE Systems Journal*, vol. 12, no. 4, pp. 3226–3237, 2017. [Pg.9], [Pg.38]

[29] M. Doostizadeh and H. Ghasemi, "A day-ahead electricity pricing model based on smart metering and demand-side management," *Energy*, vol. 46, no. 1, pp. 221–230, 2012. [Pg.34], [Pg.35]

[30] U. N. Ekanayake and U. S. Navaratne, "A survey on microgrid control techniques in islanded mode," *Journal of Electrical and Computer Engineering*, vol. 2020, 2020. [Pg.97]

[31] F. Elghitani and W. Zhuang, "Aggregating a large number of residential appliances for demand response applications," *IEEE Transactions on Smart Grid*, vol. 9, no. 5, pp. 5092–5100, 2017. [Pg.39]

[32] D. Emad, M. El-Hameed, M. Yousef, and A. El-Fergany, "Computational methods for optimal planning of hybrid renewable microgrids: a comprehensive review and challenges," *Archives of Computational Methods in Engineering*, vol. 27, no. 4, pp. 1297–1319, 2020. [Pg.40]

[33] O. Erdinc and M. Uzunoglu, "Optimum design of hybrid renewable energy systems: Overview of different approaches," *Renewable and Sustainable Energy Reviews*, vol. 16, no. 3, pp. 1412–1425, 2012. [Pg.6]

[34] T. Ericson, "Direct load control of residential water heaters," *Energy Policy*, vol. 37, no. 9, pp. 3502–3512, 2009. [Pg.36]

[35] T. Esram and P. L. Chapman, "Comparison of photovoltaic array maximum power point tracking techniques," *IEEE Transactions on energy conversion*, vol. 22, no. 2, pp. 439–449, 2007. [Pg.123]

[36] F. Fanitabasi and E. Pournaras, "Appliance-level flexible scheduling for socio-technical smart grid optimization," *IEEE Access*, 2020. [Pg.39]

[37] H. Farhangi, "The path of the smart grid," *IEEE power and energy magazine*, vol. 8, no. 1, pp. 18–28, 2009. [Pg.1]

[38] M. Farrokhifar, F. Momayyezi, N. Sadoogi, and A. Safari, "Real-time based approach for intelligent building energy management using dynamic price policies," *Sustainable cities and society*, vol. 37, pp. 85–92, 2018. [Pg.38]

[39] D. Feroldi and D. Zumoffen, "Sizing methodology for hybrid systems based on multiple renewable power sources integrated to the energy management strategy," *International journal of hydrogen energy*, vol. 39, no. 16, pp. 8609–8620, 2014. [Pg.42]

[40] C. Gamarra and J. M. Guerrero, "Computational optimization techniques applied to microgrids planning: a review," *Renewable and Sustainable Energy Reviews*, vol. 48, pp. 413–424, 2015. [Pg.40]

[41] L. Gao, S. Liu, and R. A. Dougal, "Dynamic lithium-ion battery model for system simulation," *IEEE transactions on components and packaging technologies*, vol. 25, no. 3, pp. 495–505, 2002. [Pg.127]

[42] M. A. F. Ghazvini, J. Soares, O. Abrishambaf, R. Castro, and Z. Vale, "Demand response implementation in smart households," *Energy and Buildings*, vol. 143, pp. 129–148, 2017. [Pg.38]

[43] X. Guan, Z. Xu, and Q.-S. Jia, "Energy-efficient buildings facilitated by microgrid," *IEEE Transactions on smart grid*, vol. 1, no. 3, pp. 243–252, 2010. [Pg.7]

[44] H. T. Haider, O. H. See, and W. Elmenreich, "A review of residential demand response of smart grid," *Renewable and Sustainable Energy Reviews*, vol. 59, pp. 166–178, 2016. [Pg.7]

[45] R. Hemmati and H. Saboori, "Short-term bulk energy storage system scheduling for load leveling in unit commitment: modeling, optimization, and sensitivity analysis," *Journal of advanced research*, vol. 7, no. 3, pp. 360–372, 2016. [Pg.41]

[46] H. Hermanns and H. Wiechmann, "Demand-response management for dependable power grids," in *Embedded Systems for Smart Appliances and Energy Management*. Springer, 2013, pp. 1–22. [Pg.34]

[47] K. Herter, "Residential implementation of critical-peak pricing of electricity," *Energy policy*, vol. 35, no. 4, pp. 2121–2130, 2007. [Pg.34]

[48] Y. Huang, S. Mao, and R. M. Nelms, "Adaptive electricity scheduling in microgrids," *IEEE Transactions on Smart Grid*, vol. 5, no. 1, pp. 270–281, 2014. [Pg.7]

[49] IBM ILOG CPLEX Optimization Studio. [Online]. Available: https://www.ibm.com/in-en/products/ilog-cplex-optimization-studio [Pg.104], [Pg.110]

[50] M. Iqbal, M. Azam, M. Naeem, A. Khwaja, and A. Anpalagan, "Optimization classification, algorithms and tools for renewable energy: A review," *Renewable and sustainable energy reviews*, vol. 39, pp. 640–654, 2014. [Pg.43]

[51] M. S. Javadi, A. E. Nezhad, P. H. Nardelli, M. Gough, M. Lotfi, S. Santos, and J. P. Catalão, "Self-scheduling model for home energy management systems considering the end-users discomfort index within price-based demand response programs," *Sustainable Cities and Society*, vol. 68, p. 102792, 2021. [Pg.9], [Pg.16], [Pg.38]

[52] N. Javaid, F. Ahmed, I. Ullah, S. Abid, W. Abdul, A. Alamri, and A. S. Almogren, "Towards cost and comfort based hybrid optimization for residential load scheduling in a smart grid," *Energies*, vol. 10, no. 10, p. 1546, 2017. [Pg.38]

[53] H. Jiayi, J. Chuanwen, and X. Rong, "A review on distributed energy resources and microgrid," *Renewable and Sustainable Energy Reviews*, vol. 12, no. 9, pp. 2472–2483, 2008. [Pg.3]

[54] A. Jindal, M. Singh, and N. Kumar, "Consumption-aware data analytical demand response scheme for peak load reduction in smart grid," *IEEE Transactions on Industrial Electronics*, vol. 65, no. 11, pp. 8993–9004, 2018. [Pg.8], [Pg.145]

[55] H. Kanchev, D. Lu, F. Colas, V. Lazarov, and B. Francois, "Energy management and operational planning of a microgrid with a pv-based active generator for smart grid applications," *IEEE transactions on industrial electronics*, vol. 58, no. 10, pp. 4583–4592, 2011. [Pg.41]

[56] M. M. Karbasioun, G. Shaikhet, E. Kranakis, and I. Lambadaris, "Power strip packing of malleable demands in smart grid," in *2013 IEEE International Conference on Communications (ICC)*, 2013, pp. 4261–4265. [Pg.38]

[57] G. Karmakar, A. Kabra, and K. Ramamritham, "Coordinated scheduling of thermostatically controlled real-time systems under peak power constraint," in *2013 IEEE 19th Real-Time and Embedded Technology and Applications Symposium (RTAS)*. IEEE, 2013, pp. 33–42. [Pg.145]

[58] Y. A. Katsigiannis, P. S. Georgilakis, and E. S. Karapidakis, "Hybrid simulated annealing–tabu search method for optimal sizing of autonomous power systems with renewables," *IEEE Transactions on Sustainable Energy*, vol. 3, no. 3, pp. 330–338, 2012. [Pg.40]

[59] S. Kelkar, N. Kothari, and K. Ramamritham, "Brownout energy distribution scheme for mitigating rolling blackouts," in *Proceedings of the 2015 ACM Sixth International Conference on Future Energy Systems*, 2015, pp. 193–194. [Pg.8], [Pg.33]

[60] P. Khajavi, H. Abniki, and A. Arani, "The role of incentive based demand response programs in smart grid," in *2011 10th international conference on environment and electrical engineering*. Ieee, 2011, pp. 1–4. [Pg.36]

[61] A. Khan, N. Javaid, and M. I. Khan, "Time and device based priority induced comfort management in smart home within the consumer budget limitation," *Sustainable cities and society*, vol. 41, pp. 538–555, 2018. [Pg.9], [Pg.16], [Pg.38]

[62] A. Khodaei, "Microgrid optimal scheduling with multi-period islanding constraints," *IEEE Transactions on Power Systems*, vol. 29, no. 3, pp. 1383–1392, 2014. [Pg.42]

[63] A. Khodaei, "Resiliency-oriented microgrid optimal scheduling," *IEEE Transactions on Smart Grid*, vol. 5, no. 4, pp. 1584–1591, 2014. [Pg.42]

[64] M. E. Khodayar, M. Barati, and M. Shahidehpour, "Integration of high reliability distribution system in microgrid operation," *IEEE Transactions on Smart Grid*, vol. 3, no. 4, pp. 1997–2006, 2012. [Pg.7]

[65] N. Kumaraguruparan, H. Sivaramakrishnan, and S. S. Sapatnekar, "Residential task scheduling under dynamic pricing using the multiple knapsack method," in *2012 IEEE PES Innovative Smart Grid Technologies (ISGT)*. IEEE, 2012, pp. 1–6. [Pg.9], [Pg.16], [Pg.38]

[66] R. H. Lasseter, "Microgrids," in *2002 IEEE power engineering society winter meeting. Conference proceedings (Cat. No. 02CH37309)*, vol. 1. IEEE, 2002, pp. 305–308. [Pg.3]

[67] C. Lee, J. Lehoczky, D. Siewiorek, R. Rajkumar, and J. Hansen, "A scalable solution to the multi-resource qos problem," in *Real-Time Systems Symposium, 1999. Proceedings. The 20th IEEE.* IEEE, 1999, pp. 315–326. [Pg.68]

[68] C. Lee, J. Lehoezky, R. Rajkumar, and D. Siewiorek, "On quality of service optimization with discrete qos options," in *Real-Time Technology and Applications Symposium, 1999. Proceedings of the Fifth IEEE.* IEEE, 1999, pp. 276–286. [Pg.68]

[69] J. Lee, G.-L. Park, S.-W. Kim, H.-J. Kim, and C. O. Sung, "Power consumption scheduling for peak load reduction in smart grid homes," in *Proceedings of the 2011 ACM Symposium on Applied Computing*, 2011, pp. 584–588. [Pg.37]

[70] Y. M. Lee, R. Horesh, and L. Liberti, "Optimal hvac control as demand response with on-site energy storage and generation system," *Energy Procedia*, vol. 78, pp. 2106–2111, 2015. [Pg.144]

[71] F. Lezama, J. Soares, B. Canizes, and Z. Vale, "Flexibility management model of home appliances to support dso requests in smart grids," *Sustainable Cities and Society*, vol. 55, p. 102048, 2020. [Pg.39]

[72] B. Li, R. Roche, and A. Miraoui, "Microgrid sizing with combined evolutionary algorithm and milp unit commitment," *Applied energy*, vol. 188, pp. 547–562, 2017. [Pg.42]

[73] H. Liang, B. J. Choi, W. Zhuang, and X. Shen, "Towards optimal energy store-carry-and-deliver for phevs via v2g system," in *2012 Proceedings IEEE INFOCOM*. IEEE, 2012, pp. 1674–1682. [Pg.5]

[74] H. Liang and W. Zhuang, "Stochastic modeling and optimization in a microgrid: A survey," *Energies*, vol. 7, no. 4, pp. 2027–2050, 2014. [Pg.2]

[75] Y. Liang, L. He, X. Cao, and Z.-J. Shen, "Stochastic control for smart grid users with flexible demand," *IEEE Transactions on Smart Grid*, vol. 4, no. 4, pp. 2296–2308, 2013. [Pg.34]

[76] N. Lidula and A. Rajapakse, "Microgrids research: A review of experimental microgrids and test systems," *Renewable and Sustainable Energy Reviews*, vol. 15, no. 1, pp. 186–202, 2011. [Pg.40]

[77] T. Logenthiran, D. Srinivasan, A. Khambadkone, and T. S. Raj, "Optimal sizing of an islanded microgrid using evolutionary strategy," in *Probabilistic Methods Applied to Power Systems (PMAPS), 2010 IEEE 11th International Conference on.* IEEE, 2010, pp. 12–17. [Pg.6], [Pg.42]

[78] S. Lu, N. Samaan, R. Diao, M. Elizondo, C. Jin, E. Mayhorn, Y. Zhang, and H. Kirkham, "Centralized and decentralized control for demand response," in *ISGT 2011.* Ieee, 2011, pp. 1–8. [Pg.34]

[79] M. Lydia, S. S. Kumar, A. I. Selvakumar, and G. E. P. Kumar, "A comprehensive review on wind turbine power curve modeling techniques," *Renewable and Sustainable Energy Reviews*, vol. 30, pp. 452–460, 2014. [Pg.124]

[80] C. Marnay, S. Chatzivasileiadis, C. Abbey, R. Iravani, G. Joos, P. Lombardi, P. Mancarella, and J. von Appen, "Microgrid evolution roadmap," in *2015 international symposium on smart electric distribution systems and technologies (EDST).* IEEE, 2015, pp. 139–144. [Pg.2], [Pg.97]

[81] E. Mayhorn, K. Kalsi, M. Elizondo, W. Zhang, S. Lu, N. Samaan, and K. Butler-Purry, "Optimal control of distributed energy resources using model predictive control," in *Power and Energy Society General Meeting, 2012 IEEE.* IEEE, 2012, pp. 1–8. [Pg.41]

[82] S. Moon and J.-W. Lee, "Multi-residential demand response scheduling with multi-class appliances in smart grid," *IEEE transactions on smart grid*, vol. 9, no. 4, pp. 2518–2528, 2016. [Pg.9], [Pg.38]

[83] H. Morais, P. Kádár, P. Faria, Z. A. Vale, and H. Khodr, "Optimal scheduling of a renewable micro-grid in an isolated load area using mixed-integer linear programming," *Renewable Energy*, vol. 35, no. 1, pp. 151–156, 2010. [Pg.6], [Pg.41]

[84] H. Mortaji, S. H. Ow, M. Moghavvemi, and H. A. F. Almurib, "Load shedding and smart-direct load control using internet of things in smart grid demand response management," *IEEE Transactions on Industry Applications*, vol. 53, no. 6, pp. 5155–5163, 2017. [Pg.8]

[85] K. Moslehi and R. Kumar, "A reliability perspective of the smart grid," *IEEE transactions on smart grid*, vol. 1, no. 1, pp. 57–64, 2010. [Pg.6]

[86] D. Muthirayan, D. Kalathil, K. Poolla, and P. Varaiya, "Mechanism design for demand response programs," *IEEE Transactions on Smart Grid*, vol. 11, no. 1, pp. 61–73, 2019. [Pg.35]

[87] E. Nekouei, T. Alpcan, and D. Chattopadhyay, "Game-theoretic frameworks for demand response in electricity markets," *IEEE Transactions on Smart Grid*, vol. 6, no. 2, pp. 748–758, 2014. [Pg.35]

[88] M. Nemati, M. Braun, and S. Tenbohlen, "Optimization of unit commitment and economic dispatch in microgrids based on genetic algorithm and mixed integer linear programming," *Applied energy*, vol. 210, pp. 944–963, 2018. [Pg.98]

[89] N. Nissan, T. Roughgarden, E. Tardos, and V. V. Vazirani, "Algorithmic game theory." [Online]. Available: https://www.cs.cmu.edu/~sandholm/cs15-892F13/algorithmic-game-theory.pdf [Pg.52]

[90] U. D. of Energy, "The smart grid: an introduction," *Prepared by Litos Strategic Communication*, 2008. [Pg.1]

[91] P. Palensky and D. Dietrich, "Demand side management: Demand response, intelligent energy systems, and smart loads," *IEEE transactions on industrial informatics*, vol. 7, no. 3, pp. 381–388, 2011. [Pg.36]

[92] A. Parisio and L. Glielmo, "A mixed integer linear formulation for microgrid economic scheduling," in *Smart Grid Communications (SmartGridComm), 2011 IEEE International Conference on*. IEEE, 2011, pp. 505–510. [Pg.6], [Pg.41]

[93] E. S. Parizy, H. R. Bahrami, and S. Choi, "A low complexity and secure demand response technique for peak load reduction," *IEEE Transactions on Smart Grid*, vol. 10, no. 3, pp. 3259–3268, 2018. [Pg.8]

[94] B. D. Raj, S. Kumar, S. Padhi, A. Sarkar, A. Mondal, and K. Ramamritham, "Brownout based blackout avoidance strategies in smart grids," in *Proceedings of the Ninth International Conference on Future Energy Systems*, 2018, pp. 456–458. [Pg.8]

[95] B. D. Raj, A. Sarkar, and D. Goswami, "An efficient framework for brownout based appliance scheduling in microgrids," *Sustainable Cities and Society*, p. 103936, 2022. [Pg.34]

[96] R. Rajkumar, C. Lee, J. Lehoczky, and D. Siewiorek, "A resource allocation model for qos management," in *Real-Time Systems Symposium, 1997. Proceedings., The 18th IEEE*. IEEE, 1997, pp. 298–307. [Pg.68]

[97] B. Ramanathan and V. Vittal, "A framework for evaluation of advanced direct load control with minimum disruption," *IEEE Transactions on Power Systems*, vol. 23, no. 4, pp. 1681–1688, 2008. [Pg.36]

[98] M. Rastegar, M. Fotuhi-Firuzabad, and F. Aminifar, "Load commitment in a smart home," *Applied Energy*, vol. 96, pp. 45–54, 2012. [Pg.9], [Pg.16], [Pg.37], [Pg.38]

[99] A. Ravichandran, P. Malysz, S. Sirouspour, and A. Emadi, "The critical role of microgrids in transition to a smarter grid: A technical review," in *2013 IEEE Transportation Electrification Conference and Expo (ITEC)*. IEEE, 2013, pp. 1–7. [Pg.45]

[100] M. Ross, R. Hidalgo, C. Abbey, and G. Joós, "Energy storage system scheduling for an isolated microgrid," *IET renewable power generation*, vol. 5, no. 2, pp. 117–123, 2011. [Pg.41]

[101] T. Roughgarden, *Twenty lectures on algorithmic game theory*. Cambridge University Press, 2016. [Pg.55]

[102] T. Samad and S. Kiliccote, "Smart grid technologies and applications for the industrial sector," *Computers & Chemical Engineering*, vol. 47, pp. 76–84, 2012. [Pg.36]

[103] P. Samadi, H. Mohsenian-Rad, R. Schober, and V. W. Wong, "Advanced demand side management for the future smart grid using mechanism design," *IEEE Transactions on Smart Grid*, vol. 3, no. 3, pp. 1170–1180, 2012. [Pg.35]

[104] P. Samadi, R. Schober, and V. W. Wong, "Optimal energy consumption scheduling using mechanism design for the future smart grid," in *2011 IEEE International Conference on Smart Grid Communications (SmartGridComm)*. IEEE, 2011, pp. 369–374. [Pg.35]

[105] P. G. Sessa, N. Walton, and M. Kamgarpour, "Exploring the vickrey-clarke-groves mechanism for electricity markets," *IFAC-PapersOnLine*, vol. 50, no. 1, pp. 189–194, 2017. [Pg.35]

[106] J. J. Shah, M. C. Nielsen, T. S. Shaffer, and R. L. Fittro, "Cost-optimal consumption-aware electric water heating via thermal storage under time-of-use pricing," *IEEE Transactions on Smart Grid*, vol. 7, no. 2, pp. 592–599, 2015. [Pg.145]

[107] H. Shakouri and A. Kazemi, "Multi-objective cost-load optimization for demand side management of a residential area in smart grids," *Sustainable cities and society*, vol. 32, pp. 171–180, 2017. [Pg.8]

[108] A. Shewale, A. Mokhade, N. Funde, and N. D. Bokde, "An overview of demand response in smart grid and optimization techniques for efficient residential appliance scheduling problem," *Energies*, vol. 13, no. 16, p. 4266, 2020. [Pg.143]

[109] G. K. Singh, "Solar power generation by pv (photovoltaic) technology: A review," *Energy*, vol. 53, pp. 1–13, 2013. [Pg.123]

[110] P. Singh, D. Palwalia, A. Gupta, and P. Kumar, "Comparison of photovoltaic array maximum power point tracking techniques," *Int. Adv. Res. J. Sci. Eng. Technol*, vol. 2, p. 138, 2015. [Pg.123]

[111] J. C. Smith, G. Hensley, and L. Ray, "IEEE Recommended Practice for Monitoring Electric Power Quality," *IEEE Std*, pp. 1159–1995, 1995. [Pg.4], [Pg.7], [Pg.14], [Pg.68], [Pg.95]

[112] C. Tao, D. Shanxu, and C. Changsong, "Forecasting power output for grid-connected photovoltaic power system without using solar radiation measurement," in *Power Electronics for Distributed Generation Systems (PEDG), 2010 2nd IEEE International Symposium on*. IEEE, 2010, pp. 773–777. [Pg.123]

[113] D. Thomas, O. Deblecker, and C. S. Ioakimidis, "Optimal design and techno-economic analysis of an autonomous small isolated microgrid aiming at high res penetration," *Energy*, vol. 116, pp. 364–379, 2016. [Pg.97]

[114] R. Urgaonkar, B. Urgaonkar, M. J. Neely, and A. Sivasubramaniam, "Optimal power cost management using stored energy in data centers," in *Proceedings of the ACM SIGMETRICS joint international conference on Measurement and modeling of computer systems*, 2011, pp. 221–232. [Pg.5]

[115] J. S. Vardakas, N. Zorba, and C. V. Verikoukis, "A survey on demand response programs in smart grids: pricing methods and optimization algorithms," *IEEE Communications Surveys & Tutorials*, vol. 17, no. 1, pp. 152–178, 2015. [Pg.8], [Pg.29], [Pg.32]

[116] D. Verma, S. Nema, A. Shandilya, and S. K. Dash, "Maximum power point tracking (mppt) techniques: Recapitulation in solar photovoltaic systems," *Renewable and Sustainable Energy Reviews*, vol. 54, pp. 1018–1034, 2016. [Pg.123]

[117] F. Viani and M. Salucci, "A user perspective optimization scheme for demand-side energy management," *IEEE Systems Journal*, vol. 12, no. 4, pp. 3857–3860, 2017. [Pg.9], [Pg.16], [Pg.38]

[118] E. I. Vrettos and S. A. Papathanassiou, "Operating policy and optimal sizing of a high penetration res-bess system for small isolated grids," *IEEE Transactions on Energy Conversion*, vol. 26, no. 3, pp. 744–756, 2011. [Pg.39]

[119] I. WEO, "International energy agency, world energy outlook 2012," *Paris Google Scholar*, 2012. [Pg.2]

[120] Y. Xu and S. H. Low, "An efficient and incentive compatible mechanism for wholesale electricity markets," *IEEE Transactions on Smart Grid*, vol. 8, no. 1, pp. 128–138, 2015. [Pg.35]

[121] Z. Yahia and A. Pradhan, "Multi-objective optimization of household appliance scheduling problem considering consumer preference and peak load reduction," *Sustainable Cities and Society*, vol. 55, p. 102058, 2020. [Pg.9], [Pg.16], [Pg.38]

[122] S. Yaw, B. Mumey, E. McDonald, and J. Lemke, "Peak demand scheduling in the smart grid," in *2014 IEEE international conference on smart grid communications (SmartGridComm)*. IEEE, 2014, pp. 770–775. [Pg.38]

[123] N. Zhou, N. Liu, J. Zhang, and J. Lei, "Multi-objective optimal sizing for battery storage of pv-based microgrid with demand response," *Energies*, vol. 9, no. 8, p. 591, 2016. [Pg.146]

[124] Q. Zhou, W. Guan, and W. Sun, "Impact of demand response contracts on load forecasting in a smart grid environment," in *2012 IEEE Power and Energy Society General Meeting*. IEEE, 2012, pp. 1–4. [Pg.34]